THE MOLECULAR INVESTIGATION OF THE EFFECTS OF SIMVASTATIN, A CHOLESTEROL REDUCING DRUG, ON DIFFERENT RAT SKELETAL MUSCLE TISSUES

A THESIS SUBMITTED TO
THE GRADUATE SCHOOL OF NATURAL AND APPLIED SCIENCES
OF
MIDDLE EAST TECHNICAL UNIVERSITY

BY

NİHAL ŞİMŞEK ÖZEK

IN PARTIAL FULFILLMENT OF THE REQUIREMENTS
FOR
THE DEGREE OF MASTER OF SCIENCE
IN
BIOLOGY

SEPTEMBER 2007

Approval of the Thesis:

THE MOLECULAR INVESTIGATION OF THE EFFECTS OF SIMVASTATIN, A CHOLESTEROL REDUCING DRUG, ON DIFFERENT RAT SKELETAL MUSCLE TISSUES

submitted by **NİHAL ŞİMŞEK ÖZEK** in partial fulfillment of the requirements for the degree of **Master of Science in Biological Sciences Department, Middle East Technical University** by,

Prof. Dr. Canan Özgen
Dean, Graduate School of **Natural and Applied Sciences** _____

Prof. Dr. Zeki Kaya
Head of Department, **Biological Sciences** _____

Prof. Dr. Feride SEVERCAN
Supervisor, **Biological Sciences Dept., METU** _____

Examining Committee Members:

Assoc. Prof. Dr. Ewa Jakubowska Doğru _____
Biological Sciences Dept., METU

Prof. Dr. Feride Severcan _____
Biological Sciences Dept., METU

Assoc. Prof. Dr. Mehmet Dinçer Bilgin _____
Biophysics Dept., ADU

Assoc. Prof. Dr. Yıldırım Sara _____
Medical Pharmacology Dept.,HU

Dr. Sreeparna Banerjee _____
Biological Sciences Dept., METU

Date: 07.09.2007

I hereby declare that all information in this document has been obtained and presented in accordance with academic rules and ethical conduct. I also declare that, as required by these rules and conduct, I have fully cited and referenced all material and results that are not original to this work.

Name, Last name : Nihal Şimşek Özek
Signature :

ABSTRACT

THE MOLECULAR INVESTIGATION OF THE EFFECTS OF SIMVASTATIN, A CHOLESTEROL REDUCING DRUG, ON DIFFERENT RAT SKELETAL MUSCLE TISSUES

ŞİMŞEK ÖZEK, Nihal

M.Sc., Department of Biology

Supervisor: Prof. Dr. Feride SEVERCAN

September 2007,125 pages

In the present study Fourier Transform Infrared (FTIR) and Attenuated Total Reflectance FTIR (ATR-FTIR) Spectroscopy were used to examine the effects of simvastatin on structure, composition and function of macromolecules of three different rat skeletal muscles EDL (Extensor Digitorium Longus), DIA (Diaphragm) and SOL (Soleus) containing different amount of slow and fast twitch fibers, at molecular level.

Simvastatin, a lipophilic statin, is widely used in the treatment of hypercholesterolemia and cardiovascular diseases due to its higher efficacy. However, long term usage of statins give rise to many adverse effects on different tissues and organs. Skeletal muscle accounts for around 45 % of the total body weight and has a high metabolic rate and blood flow. As a consequence, it is highly exposed to drugs within the circulation. Therefore, it is one of the target tissues of statins. The two main types of muscle fibers are type I (slow-twitch) and type II (fast-twitch) fibers; having different structural

organization and metabolic features. EDL is a fast twitch muscle while SOL is slow twitch muscle. On the other hand, DIA shows intermediate properties between slow and fast twitch muscle.

The results of ATR-FTIR and FTIR spectra revealed a considerable decrease in protein and lipid content of simvastatin treated skeletal muscles, indicating protein breakdown or decreased protein synthesis and increased lipolysis. Moreover changes in protein structure and conformation were observed. In simvastatin treatment, muscle membrane lipids were more ordered and the amount of unsaturated lipids was decreased possibly due to lipid peroxidation. The drug treatment caused a decrease in the content of nucleic acids, especially RNA, and hydrogen and non-hydrogen bonded phospholipids in the membrane structures of skeletal muscles.

In all of the spectral parameters investigated EDL muscle was more severely affected from statin treatments while SOL was less affected from the drug treatments. Thus, FTIR and ATR-FTIR spectroscopy appear to be useful methods to evaluate the effects of statin on skeletal muscle tissues at molecular level.

Key words**:** ATR-FTIR spectroscopy, FTIR spectroscopy, statin, skeletal muscle, skeletal muscle fiber types

ÖZ

KOLESTEROL DÜŞÜRÜCÜ SİMVASTATİNİN FARKLI SIÇAN İSKELET KAS DOKULARI ÜZERİNDEKİ ETKİLERİNİN MOLEKÜLER DÜZEYDE İNCELENMESİ

ŞİMŞEK ÖZEK, Nihal

Yüksek Lisans, Biyoloji Bölümü

Tez Yöneticisi: Prof. Dr. Feride Severcan

Eylül 2007, 125 sayfa

Bu çalışmada simvastatinin farklı oranlarda hızlı ve yavaş tipte iskelet kası lifleri içeren sıçan EDL, DIA ve SOL kasları üzerindeki etkisi Fourier Dönüşüm Kızılötesi ve Attenuated Total Reflektans Spektroskopisi (FTIR) ile moleküler düzeyde incelenmiştir.

Lipofilik karakterde olan simvastatin efikasitesinin yüksek olmasından dolayı hiperkolesterominin ve kardiyovasküler hastalıkların tedavisinde kullanılır. Uzun süreli kullanımlarında birçok dokuda ve organda yan etkileri meydana gelmektedir. Vücut ağırlığının % 45'ini oluşturan iskelet kası yüksek metabolik hıza ve kan akışına sahiptir. Bunun sonucunda dolaşımda yer alan ilaçlardan yüksek oranda etkilenir. Bu nedenden dolayı statinlerden en fazla etkilenen dokulardandır. Yapısal organizasyonu ve matabolik özellikleri birbirinden farklı iki ana kas lifi çeşidi vardır: tip I (yavaş kasılan) ve tip II (hızlı kasılan). Extensor digitorum longus (EDL) hızlı kasılan bir kas iken, soleus (SOL) yavaş kasılan bir kastır. Diğer taraftan diyafragma (DIA) EDL ve SOL arasında özelliklere sahip bir kastır.

ATR-FTIR ve FTIR sonuçlarısimvastatin verilmiş iskelet kaslarında artmış lipoliz ve protein yıkımı ya da azalmış protein sentezini gösteren lipid ve protein içeriğinde önemli bir azalma olduğunu göstermektedir. Ayrıca protein yapısı ve konformasyonunda değişiklikler gözlenmiştir. Simvastatin tedavisinde kas membrane lipidlerinin daha düzenli olduğu ve doymamış lipid miktarında, muhtemelen lipid peroksidasyonundan kaynaklanan, bir azalış olduğu gösterilmiştir. İlaç tedavisi iskelet kaslarında nükleik asit miktarında, özellikle RNA miktarında ve membran yapısındaki hidrojen-bağlı ve hidrojen bağlı olmayan fosfolipidlerin miktarında azalmaya neden olmuştur.

İncelenen bütün spektral parametrelerden EDL kasının simvastatin tedavisinden daha çok etkilendiği, SOL kasının ise söz konusu ilaç tedavisinden minimum düzeyde etkilendiği bulunmuştur. Sonuç olarak, ATR-FTIR ve FTIR spektroskopi teknikleri statinlerin iskelet kas dokuları üzerindeki etkilerini moleküler düzeyde incelemek için kullanışlı birer araç olarak görünmektedir.

Anahtar Kelimeler: ATR-FTIR spektroskopisi, FTIR spektroskopisi, statin, iskelet kası, iskelet kas lifi çeşitleri

To , my father , Yaşar, my daughter, Bilge and my husband, Ersin

ACKNOWLEDGEMENTS

I would like to thank to my supervisor Prof. Dr. Feride SEVERCAN for her guidance, patience, encouragement and supervision throughout this thesis study.

I would also like to thank to Prof. Dr. Rüştü ONUR and Assos. Prof. Dr. Yıldırım SARA for his suggestions and guidance with the animal studies.

I would like to express my thanks to all my thesis committee for their suggestions and criticism.

I also compassionately express my special thanks to Sevgi Görgülü owing to their precious help and lovely attitude in the course of experimental period and writing this thesis.

I would like to thank to my labmates, for their sincere friendship and supports.

I would like to send my ultimate appreciation to my father Yalçın Özek, my mother Emine Şimşek, Fatma Özek and my sister Fatma Şimşek for their endless patience, encouragement, support and love.

TABLE OF CONTENTS

LIST OF FIGURES

LIST OF TABLES

ABBREVATIONS

FTIR Fourier Transform Infrared Spectroscopy

ATR-FTIR Attenuated Total Reflectance- Fourier Transform Infrared Spectroscopy

EDL Extensor Digitorium Longgus

DIA Diaphragm

SOL Soleus

CHAPTER 1

INTRODUCTION

In this study the effects of Simvastatin on three types of skeletal muscles, namely Extensor Digitorum Longus (EDL), Diaphragm (DIA) and Soleus (SOL) were reported at molecular level via Fourier transform infrared (FTIR) and Attenuated Total Reflectance Fourier transform infrared (ATR-FTIR) spectroscopic techniques. In this chapter a detailed preliminary survey including statins, structural properties of skeletal muscle, types of skeletal muscles and their structural properties, the effects of statins on skeletal muscle tissue, and basis of infrared spectroscopy have been conducted.

1.1 Skeletal Muscle

Skeletal muscle is the largest tissue mass in the human body, representing about 40% to 45% of total body weight. The main function of skeletal muscle is to perform mechanical work at the expense of potential chemical energy, usually for movement. In addition, it is involved in many other physiological processes. For example, it is a key player in thermogenesis and as a metabolic organ, it is important in fuel and energy homeostasis. In order to achieve these functions, muscle has a very complex structure that is composed of several contractile components (Storey, 2004).

1.1.1 Structural Organization of Skeletal Muscle

Skeletal muscles are a discrete organ, made up of hundreds to thousands of muscle fibres or myofibers which are the most basic structural element of the

skeletal muscle. The structural organization of muscle and muscle fibers is shown in Figure 1.1. The entire muscle is surrounded by a fibrous connective tissue called epimisyum. Groups of muscle fibers are arranged in bundles called fascicles, and are surrounded by a connective tissue sheath known as the perimysium. The perimysium contains blood vessels and nerves that maintain blood flow and innervate the fasicles. Within a fascicle, a fine layer of connective tissue, which further covers each muscle fiber and separates it from neighboring fibers, is called the endomysium. This connective tissue layer contains:

1-Capillary networks that supply oxygen and nutrients to individual muscle fibers.

2-Satellite cells, embryonic stem cells that function in the repair of the damaged muscle tissue

3- Nerve fibers that control the muscle.

Beneath the endomysium, each fiber is surrounded by the plasma membrane (sarcolemma) which has the properties of excitable cells and propagates action potentials. The sarcolemma contains proteins and strands of collagen. It makes thin tubular invaginations called transverse tubules (T-tubules) repeatedly found along the muscle cell and that deeply plunge into the center of the fiber. These T-tubules propagate action potentials throughout the muscle fiber, thereby causing muscle contraction. The cytoplasm of the muscle fiber, called sarcoplasm, contains organelles (required for its own functioning) and cytoskeleton. The sarcoplasm contains enzymes, fat and glycogen particles, nuclei, mitochondria and other organelles. Each myofiber contains a multitude of nuclei derived from myoblasts located at the periphery of the myofibers. In addition, separate cells called satellite cells are located between the basal lamina and plasma membrane and play a key role in the muscle regeneration process (Storey, 2004).

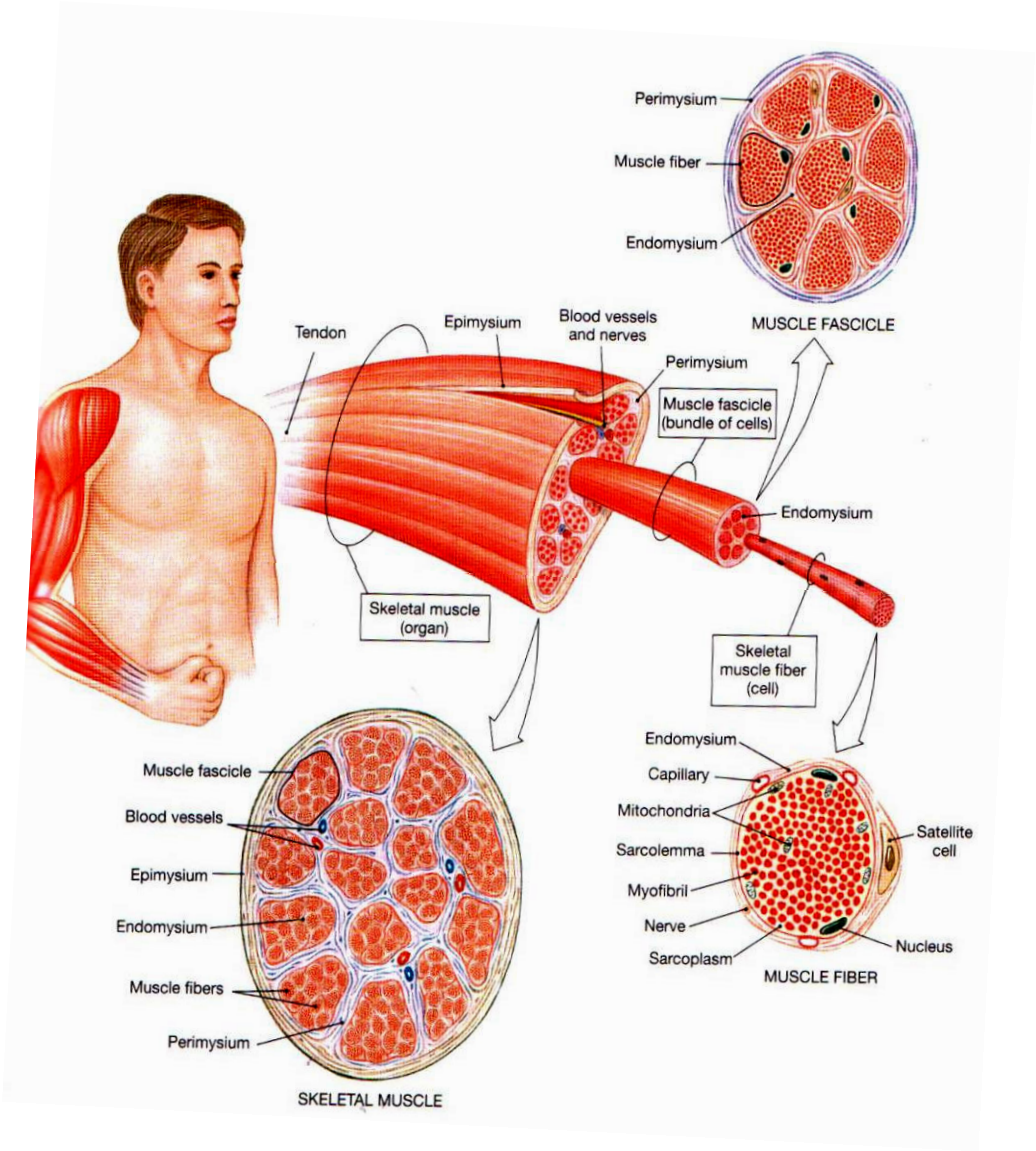

Figure 1.1. The structural organization of skeletal muscle (Martini, 2004).

Water constitutes approximately 75% of skeletal muscle, and about 20% of skeletal mass is composed of proteins. Most abundant skeletal muscle proteins are myosin, actin, tropomyosin and troponin. Actin and myosin are contractile protein while the others are regulatory proteins in muscle contraction. In addition to the proteins directly involved in the contraction process, there are a number of other sarcomeric proteins which are thought to play distinct

physiological roles such as membrane stabilization, force transmission, and ion channel anchorage (Vigoreaux, 1994; Berthier and Blaineau, 1997). These are

namely titin, nebulin, spectin, vinculin, talin, desmin, the muscle isoform of creatine kinase (CK), M protein, myomesin and skelemins. In addition, the oxygen binding protein, myoglobin, is also found in skeletal muscle tissue. The remaining 5 % is composed of enzymes, salts, minerals, and other substances, including high-energy phosphates, urea, lactate, calcium, magnesium, phosphorous, sodium, potassium, chloride ions, amino acids, fats and carbohydrates (Greisheimer and Wiedeman, 1972; Shier *et al*., 1996).

1.1.2 The Structure of Myofibrils

Each skeletal muscle fiber contains hundreds to thousands of myofibrils. Myofibrils consist of myofilaments which are organized into repeating functional units called sarcomeres. A sarcomere contains
(1) thick filaments, (2) thin filaments, (3) proteins that stabilize the positions of the thick and thin filaments, and (4) proteins that regulate the interactions between thick and thin filaments (Storey, 2004).

Differences in the size, density and distribution of thick and thin filaments account for the banded appearance of each myofibril (Figure 1.2 and 1.3). There are dark bands (A bands-anisotropic) and light bands (I bands-isotropic). The darker A bands are composed of thick myosin filaments and the lighter I bands are composed of the thin actin filaments. The thin dark line that bisects I bands and adheres to the sarcolemma is called as Z line, which gives stability to entire structure. The center of A bands contain the clear H zone or band, a region of lower optical density due to the absence of actin filaments. The M band bisects the central portion of the H band, which shows the center of the Z lines, consisting of protein structures that support the arrangement of the

myosin filaments (McArdle, Katch, Katch, 2001; Greisheimer and Wiedeman, 1972; Garrett *et al.*, 1983).

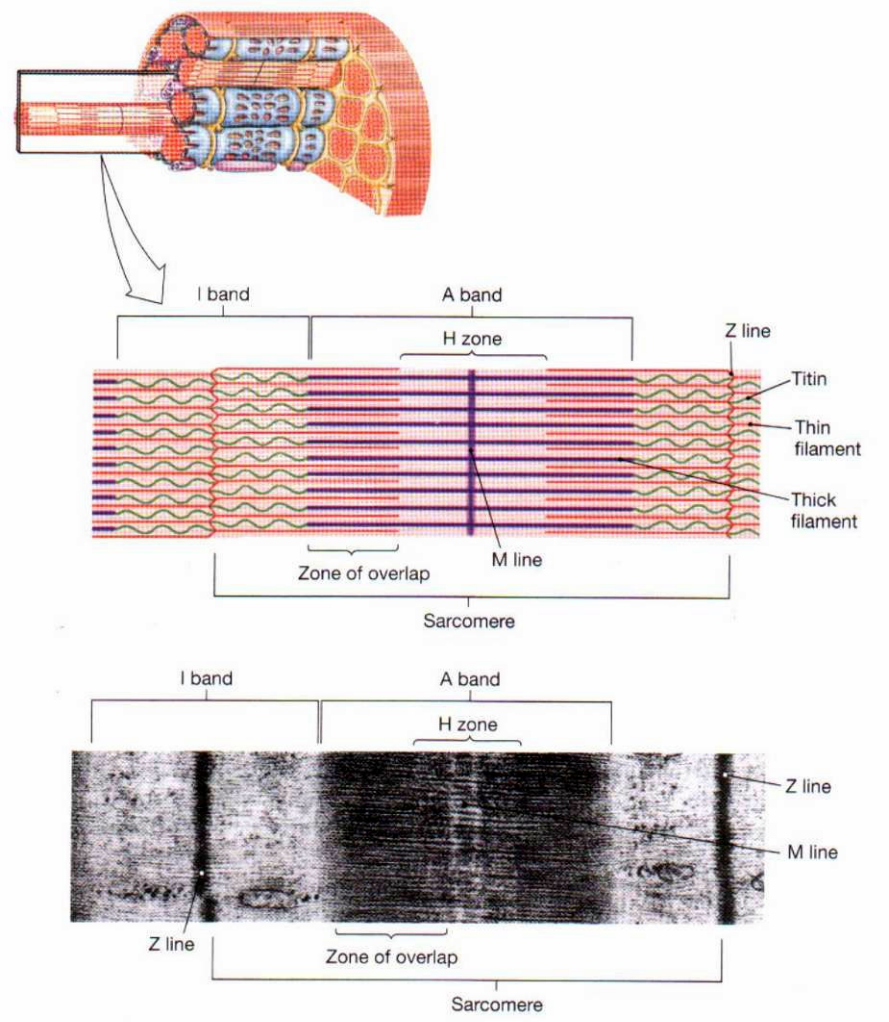

Figure 1.2. The arrangements of actin and myosin (Martini, 2004).

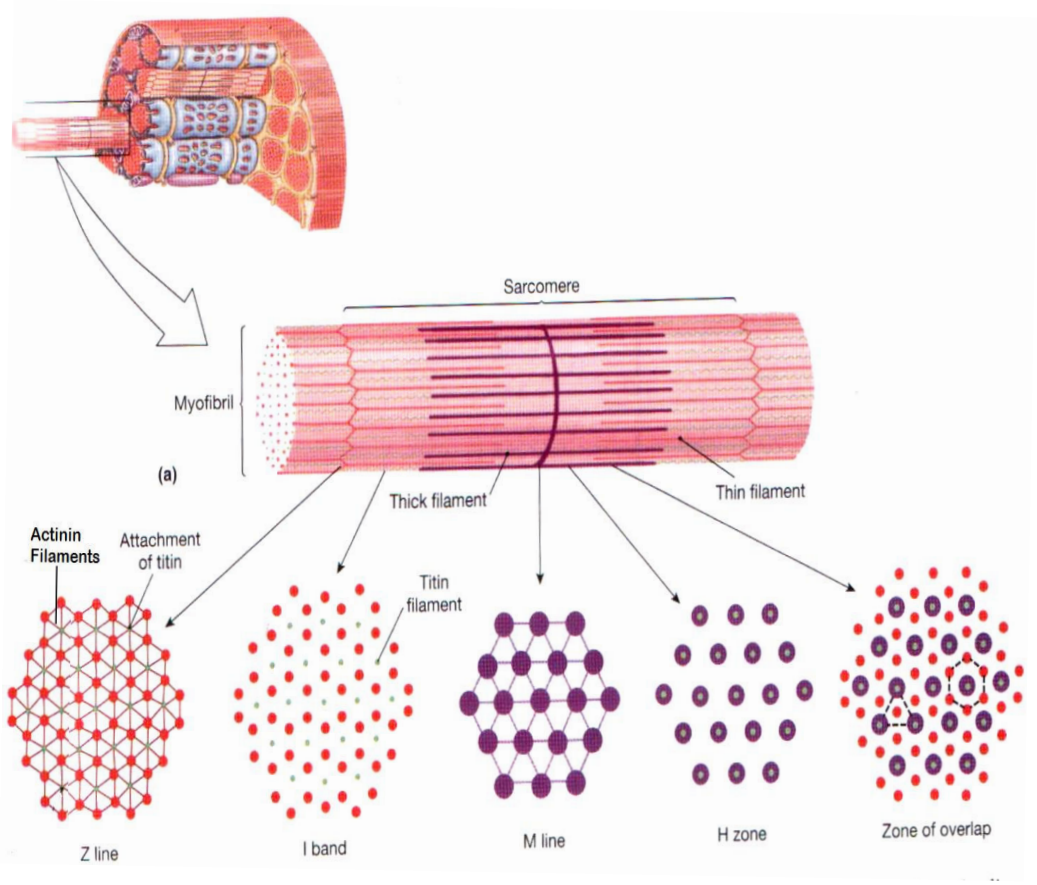

Figure 1.3. Structure of sarcomere (Martini, 2004).

The sliding filament model was proposed by Huxley and co-workers in 1950s. They hypothesized that muscle contraction resulted from filament movement due to elevated Ca^{2+} levels. In their theory, they describe how the thick and thin filaments slide past each other, causing the sarcomere to shorten. The overlap between myofilaments increases but their individual length remains constant. When muscles are relaxed, the sarcoplasmic Ca^{2+} levels are low and the tropomyosin in the thin filaments is disposed in such a way that the myosin binding site of actin is obstructed. Upon muscle stimulation, the myoplasmic Ca^{2+} levels increase, the released Ca^{2+} binds to troponin inducing a

conformational change that removes tropomyosin from the thin filament. Myosin can access its binding site on actin and the cross-bridges can form.

Myosin hydrolyzes ATP to ADP and inorganic phosphate. As a consequence, myosin in high-energy state changes its conformation and myosin heads bind to and rotate against actin filaments resulting in shortening of the fibers. Therefore contraction occurs. As Ca^{2+} levels lower during muscle relaxation, Ca^{2+} detach from the troponin complex, which in turn blocks tropomyosin and the myofilaments slide back to the resting configuration and then contraction stops (Martini, 2004).

1.2. Skeletal Muscle Metabolism

The skeletal muscles are able to use fatty acids, carbohydrates, ketone bodies and some amino acids as substrates to fulfill their energy requirements during rest and exercise (Newholme & Leech 1990). Under normal conditions, fatty acids and glucose are quantitatively the most important oxidizable substrates for muscle cells.

Glucose from glycogen in the liver has to be transported by the blood and taken up by the muscle before it can undergo glycolysis and be released as lactate, alanine or pyruvate, or be oxidized in the Krebs cycle. Glycogen stored in the skeletal muscle can undergo glycogenolysis, and hence directly glycolysis, and used for fuel in contractile processes.

Lipids are the predominant fuel at rest in the post absorptive and fasted state when the muscle glucose utilization is low. The capacity of the muscle fibers to synthesize fatty acid (FA) de novo is limited. However, over 50 % of the energy requirement of resting muscle is derived from their oxidation and thus, FAs have to be supplied first from extracellular sources. Fat is made available to the skeletal muscle cells via the blood as plasma nonesterified FAs or as

triacylglycerols (TGs) that form the lipid core of circulating TG-rich lipoproteins, very-low-density lipoprotein (VLDL) and chylomicrons (CM). Nonesterified FAs are liberated from the adipose tissue TG storage after lipolysis. From TG-rich lipoproteins, FAs are made available to the skeletal

muscle after hydrolysis by enzyme lipoprotein lipase (LPL). This enzyme is attached to the luminal surface of the endothelial cells in the capillary bed of the skeletal muscle (Braun and Severson 1992).

A resting muscle breaks down exogenous fatty acids entering the cell. At moderate levels of activity, muscle breaks down the fatty acids and glucose through aerobic metabolism. Glucose is obtained from glycogen in the muscle. If glycogen reserves are low, the muscle fiber can also break down other substrates, such as lipid or amino acids. However, at the peak levels, most of ATP are obtained from glycolysis. Fatty acid oxidation now provides only about one-third of the ATP consumed (Figure 1.4) (Martini, 2004).

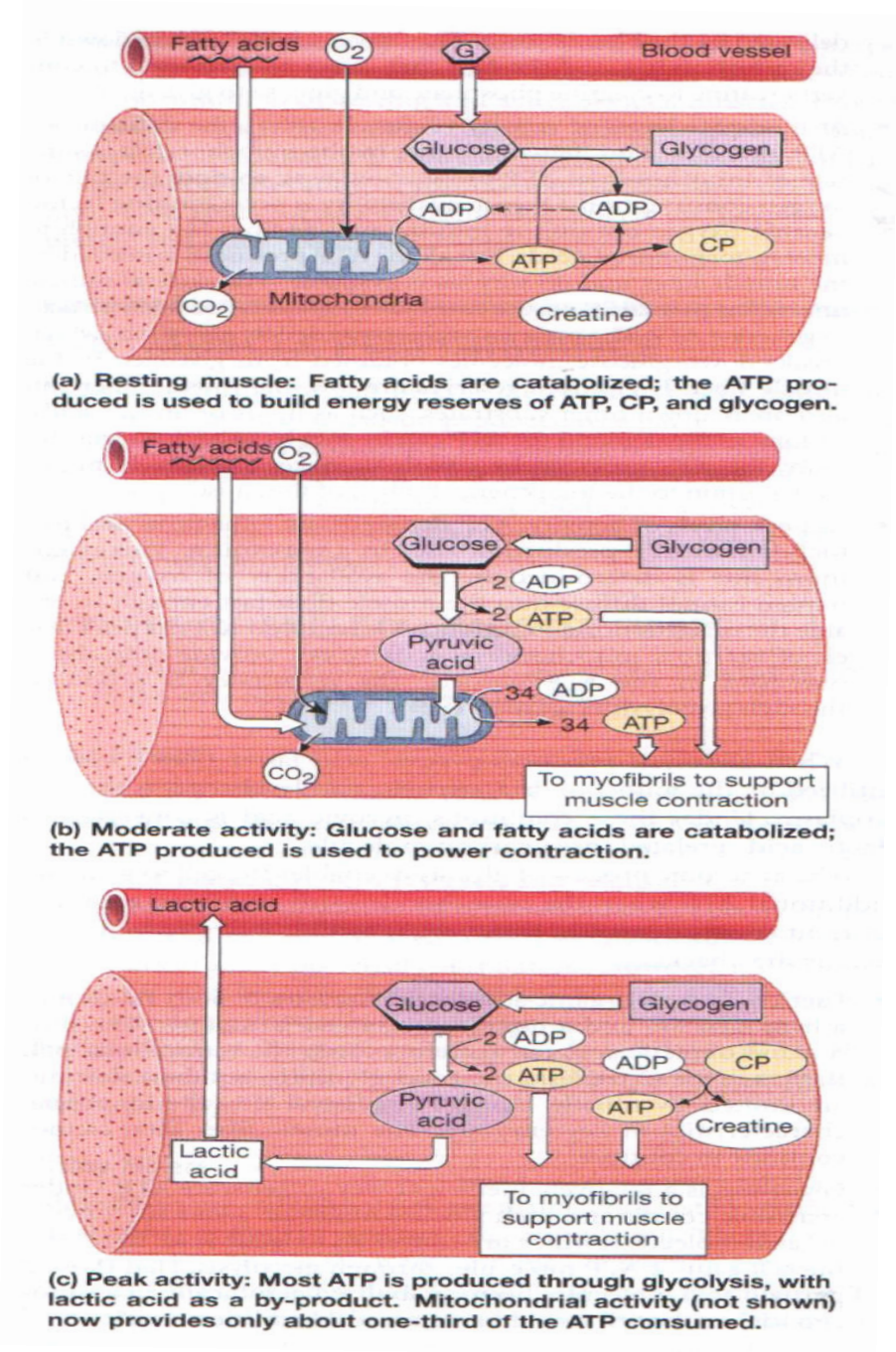

Figure 1.4. Skeletal Muscle Metabolism at resting (a), moderate (b) and peak (c) activity (Martini, 2004).

1.3 The Molecular Characteristics of Skeletal Muscle Fiber Types

Due to the various natures of movement, different muscle types are required to carry out different functional tasks. Muscle can be grouped into two main categories according to the functional and metabolic characteristics (Table 1.1) (Okumura *et al.,* 2005)

1- Slow twitch (Type I) Fibers
2- Fast twitch (Type II) Fibers

These fibers can be distinguished easily by special stains for specific enzymes, enzymes that take role in oxidative or glycolytic metabolism of fuels inside skeletal muscle structure. An example of the determination of skeletal muscle fiber types by staining ATPase was shown in Figure 1.5.

Slow twitch or type I fibers are red fibers due to the high myoglobin content and they are identified by a slow contraction time and a high resistance to fatigue. They have a small fiber diameter, a high mitochondrial and capillary density. They also contain many of the enzymes involved in the oxidative pathways (Krebs cycle, electron transport chain). Functionally, these fibers are used for aerobic activities requiring low force production, such as walking and maintaining posture (Storey, 2004).

Fast twitch or type II fibers have white fibers low myoglobin content and therefore it is known as white fibers. They are identified by a fast contraction time and a low resistance to fatigue. The fast twitch fibers can be divided into two groups: fast oxidative and fast glycolytic fibers. Fast oxidative/type IIa, fibers have a faster contraction speed than type I, but they still tend to be high in oxidative enzymes and ATPase activity and fatigue less quickly than other type II fibers. Fast glycolytic/type IIb fibers contract at a very quick rate and produce extremely large forces, but cannot maintain these tensions for more

than a few contractions without rest. These properties correlate with high ATPase and glycolytic activities and low oxidative capacity (Lieber, 2002).

Table 1.1 Ultrastructural and cytochemical properties of skeletal muscle fibers (Storey, 2004).

	Fiber Type			
	Characteristic	**Type I**	**Type II A**	**Type IIB/X**
Physiology	Contraction Velocity	Slow	Fast	Fast
	Myosin ATPase	Slow	Fast	Fast
	Contraction time (duration)	Long	Short	Short
	Ca^{+2} reuptake	Slow	Fast	Fast
	Fatigue resistant	+++	++	+
	Recruitment order	Early	Mid	Late
Enzyme Activities	Myosin ATPase	+	++	+++
	Hexokinase	+++	++	+
	Glycogen Phosphorylase	+	++	+++
	Glycolytic enzymes (α-Glycerophosphate Dehydrogenase)	+	++	+++
	Oxidative Enzymes (Succinate Dehydrogenase)	+++	++	+
	Myoglobin	+++	++	+
Morphology	Color	Red	Red	White
	Fiber diameter	+	+++	++++
	Capillary density	+++	++	+
	Mitochondrial density	+++	+++	+
	Z line thickness	+++	++	+
	Sarcoplasmic reticulum volume	+	+++	+++
	T tubules volume	-	+++	+++
	Motor-end-plate area	+	+++	+++
Metabolites	Glycogen	++	++	+++
	Triglycerides	+++	++	+
	Antibodies to fast myosin heavy chain	-	+++	+++
	Antibodies to slow myosin heavy chain	+++	-	-

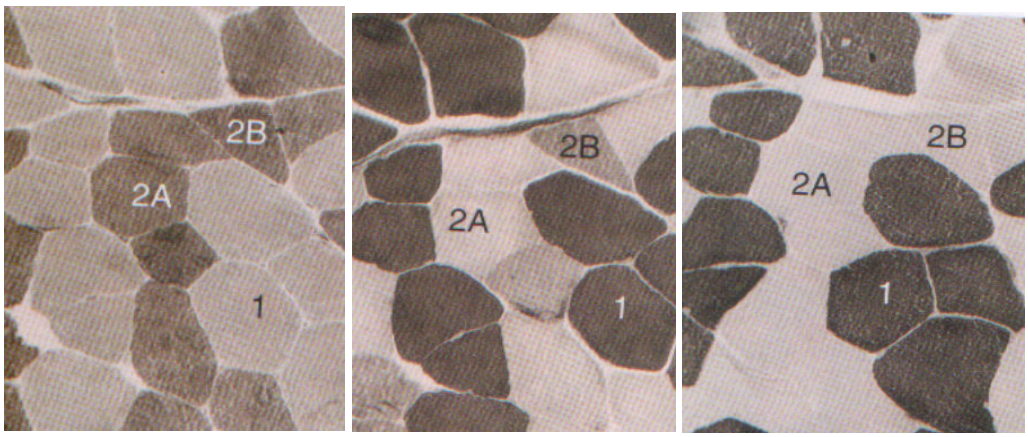

a **b** **c**

Figure 1.5. Serial sections stained with (a) ATPase pH 9.4 and following preincubation at (b) pH 4.6 and (c) pH 4.3 showing a checkerboard pattern of type 1 fibers and the subdivision of type 2 fibers into 2A and 2B (Dubowitz., 2006)

1.4 Statins and Simvastatin

1.4.1 The Functions of Cholesterol

Cholesterol is a vital building block molecule of life in many ways as given below.

1- It regulates the fluidity of cell membranes, preventing them from becoming both too rigid and too fluid and helps maintain the integrity of these membranes. It is also a primary component of lipid rafts, where it helps secure proteins involved in cell signaling (Alberts *et al.,* 2002).

2- It supports of the nervous system. It is a vital component of the myelin sheath, which allows neurons to conduct impulses necessary to communicate with each other, and has been found to be the rate-limiting factor in the formation of synapses, the formation of which is necessary for learning and the formation of memories. Cholesterol not only helps guide

the connecting parts of neurons to the right places, but also is necessary for their ability to grow in the first place (Bittman, 1997).

3- Cholesterol, more precisely 7-dehydrocholesterol, is the precursor to vitamin D. Vitamin D has long been recognized for its role in maintaining calcium balance and promoting bone health, but is more recently becoming known for a wide range of other functions, including the maintenance of mental health, a strong immune system, blood sugar regulation, and the prevention of cancer.

4- Cholesterol is also the precursor to all steroid hormones, including mineralocorticoids, glucocorticoids, and sex hormones. This makes all of the following important functions of cholesterol; athletic performance, regulating blood sugar, controlling blood pressure, regulating mineral balance, maintaining libido, building muscle mass (Harvey *et al.,* 2005).

5- It has a role in digestion. It is to be used by the liver to synthesize bile acids. Bile acids are secreted into the intestines where they are used to mix fats with the water-soluble enzymes that digest them (Harvey *et al*., 2005).

On the other hand, high levels of this lipophilic substance lead to atherosclerosis, a predisposing factor to the development of coronary artery disease. Atherosclerosis involves an accumulation of cholesterol esters and other blood lipids and lipoproteins in macrophage cells found in the intima of arteries. This type of diseases involves one or more specific cardiovascular pathologies, including myocardial infarction, ischemia, and angina (Roche, 2005).

1.4.2 The Synthesis Cholesterol and Statins

Cholesterol is synthesized in all types of cells but primarily in liver cells from the two-carbon acetate group of acetyl-CoA. Acetyl-CoAs are converted to 3-hydroxy-3-methyl glutaryl-CoA (HMG-CoA) and this is converted to mevalonate. The conversion of HMG CoA to mevalonate is catalyzed by

HMG-CoA reductase (HMGR) enzyme. Statins inhibits this enzyme and therefore it is named as HMG-CoA reductase inhibitors (Figure 1.6). HMGR enzyme consists of a single polypeptide chain of 888 amino acids (Istvan *et al.,* 2000a; 2000b). The amino terminal 339 residues are membrane bound and reside in the endoplasmic reticulum membrane while the catalytic activity of protein resides in its cytoplasmic, soluble C-terminal region portion (residues 460-888). A linker region (residues 340-459) connects the two portions of the protein. The three dimensional structure of catalytic portion of the HMGR shows a close association of two monomers in a dimer and of two dimmers in a tetramer. Statins consist of HMG-like moieties and different largely hydrophobic attachments. HMG-like moiety may be present in an active lactone form and it may occupy the HMG-binding pocket, thereby blocking HMG-CoA´s access to human HMG-CoA reductase. HMG-CoA reductase catalyzes the 4-electron reduction of HMG-CoA into CoA and mevalonate, a cholesterol precursor, with oxidation of two molecules NADPH (Figure 1.7). Statins target hepatocytes and inhibit the conversion of HMG-CoA to mevalonate, thus inhibiting an early step of the cholesterol biosynthetic pathway. The induction of a conformation change of HMG-CoA reductase in the active site makes the statins very specific and effective. The inhibition of the HMG-CoA reductase results in the activation of a protease which slices the sterol regulatory element binding proteins (SREBPs) from the endoplasmic reticulum. SREBPs are translocated at the level of the nucleus, where they increase the gene expression for LDL receptor. This has an influence on the reduction of circulating low density lipoproteins and its precursors

(intermediate density and very low density lipoproteins). As a consequence, low density lipoproteins and its precursors are cleared from the circulation (Goldstein and Brown, 1990). Furthermore, statins treatment lower triglyceride levels (5% to 10%) and raise the plasma concentration of anti-atherogenic high-density lipoproteins (HDL). On the other hand, statins have differences in the ability to decrease or increase in these parameters explained above. These differences were given in Table 1.2 (Ginsberg *et al.,* 1987; Vega *et al*., 1998; Bakker-Arkema *et al.,* 1996; Grundy 1998; Brown *et al*., 1998; Brown and Goldstein, 2004).

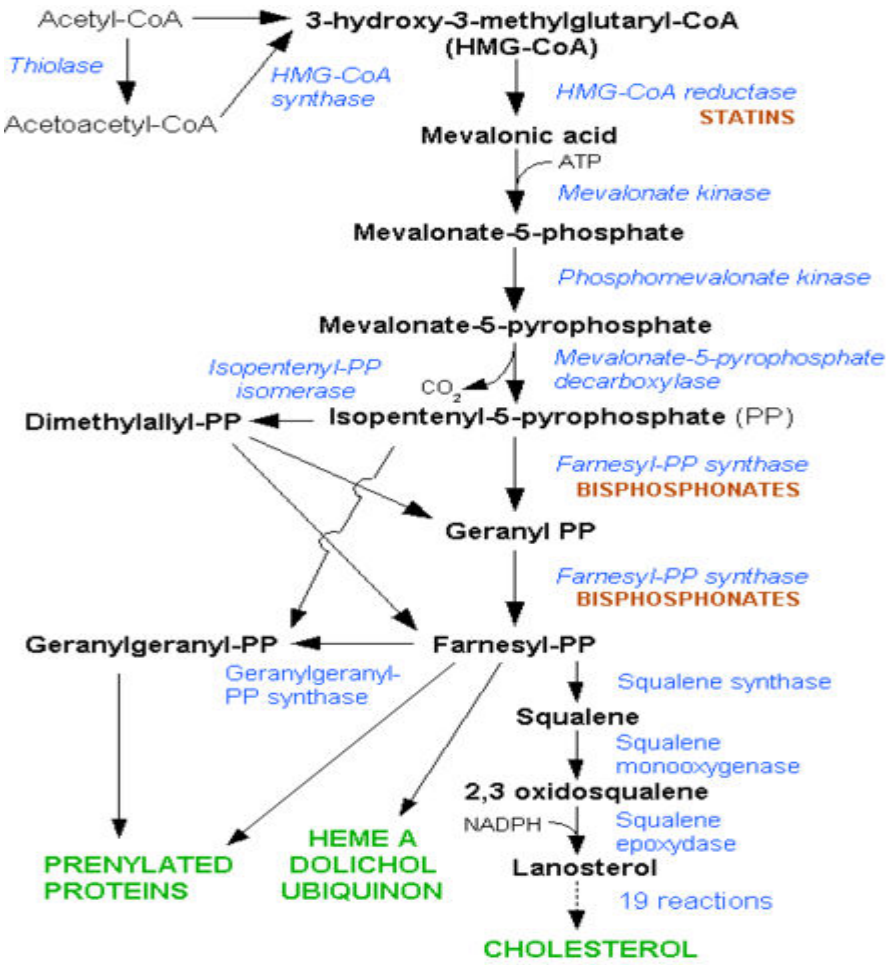

Figure 1.6. The cholesterol biosynthesis pathway

(http://goldbamboo.com/topic-t1183-a1-6Cholesterol.html)

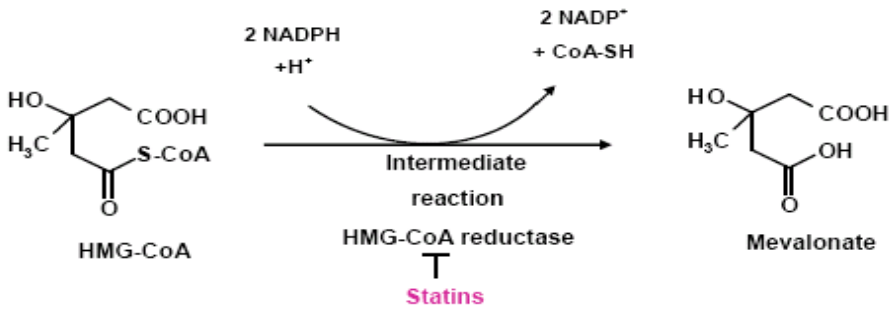

Figure 1.7. Inhibition of HMG CoA reductase by statins (Tchapda, 2005).

Table 1.2 Comperative efficacies of the different statins on various lipid fractions.
(% Serum LDL-C reduction, Serum HDL-C increase, Serum triglyceride reduction) .LDL-C, low-density lipoprotein cholesterol; HDL-C, high-density lipoprotein cholesterol, ATV-Atorvastain, CER-Cerivastatin, FLU-Fluvastatin,LOV-Lovastatin, PRA-Pravastatin, SIM-Simvastatin (Schachter, 2005)

	ATV 40 mg/day	**CER** 0.3 mg/day	**FLU** 40 mg/day	**LOV** 40 mg/day	**PRA** 40 mg/day	**SIM** 40 mg/day
Serum LDL-C reduction (%)	50	28	24	34	34	41
Serum HDL-C increase (%)	6	10	8	9	12	12
Serum triglyceride reduction (%)	29	13	10	16	24	18

Statins can be divided into two groups:

1- Non synthetic statins: They are obtained by fermentation. Pravastatin, Lovastatin and Simvastatin

For example, simvastatin is obtained from a chemical alteration of fungal products.

2- Synthetic statins: Atorvastatin, fluvastatin, cerivastatin and rosuvastatin.

Lovastatin and Simvastatin occur in an inactive closed lactones ring form. They are enzymatically hydrolyzed to their active hydroxyl acid forms in the liver. The others statins are administered as an active compound (acid form). The statins have rigid, hydrophobic groups that are covalently linked to the HMG-like moiety. Lovastatin, pravastain and simvastatin posses a hydroxy-hexahydro naphthalene ring system, to which different side chains are linked at C8 and C6. However synthetic statins have larger groups linked to the HMG-like moiety. These groups range in the character from very hydrophobic to partly hydrophobic (Shitara and Sugiyama, 2006). The chemical structure of statins is shown in Figure 1.8.

Although chemically related, statins differ in their physicochemical and pharmacokinetic properties (Table 1.3). Among available HMG-CoA reductase inhibitors, there are pharmacokinetic differences in distribution, half-lives, systemic exposure, maximum concentrations, bioavailability, protein binding, metabolic pathways, the presence of active metabolites and excretion routes, strictly related to their physicochemical and biochemical properties, which in turn may translate into differences in long-term safety (Garcia *et al.,* 2003, Schachter, 2005).

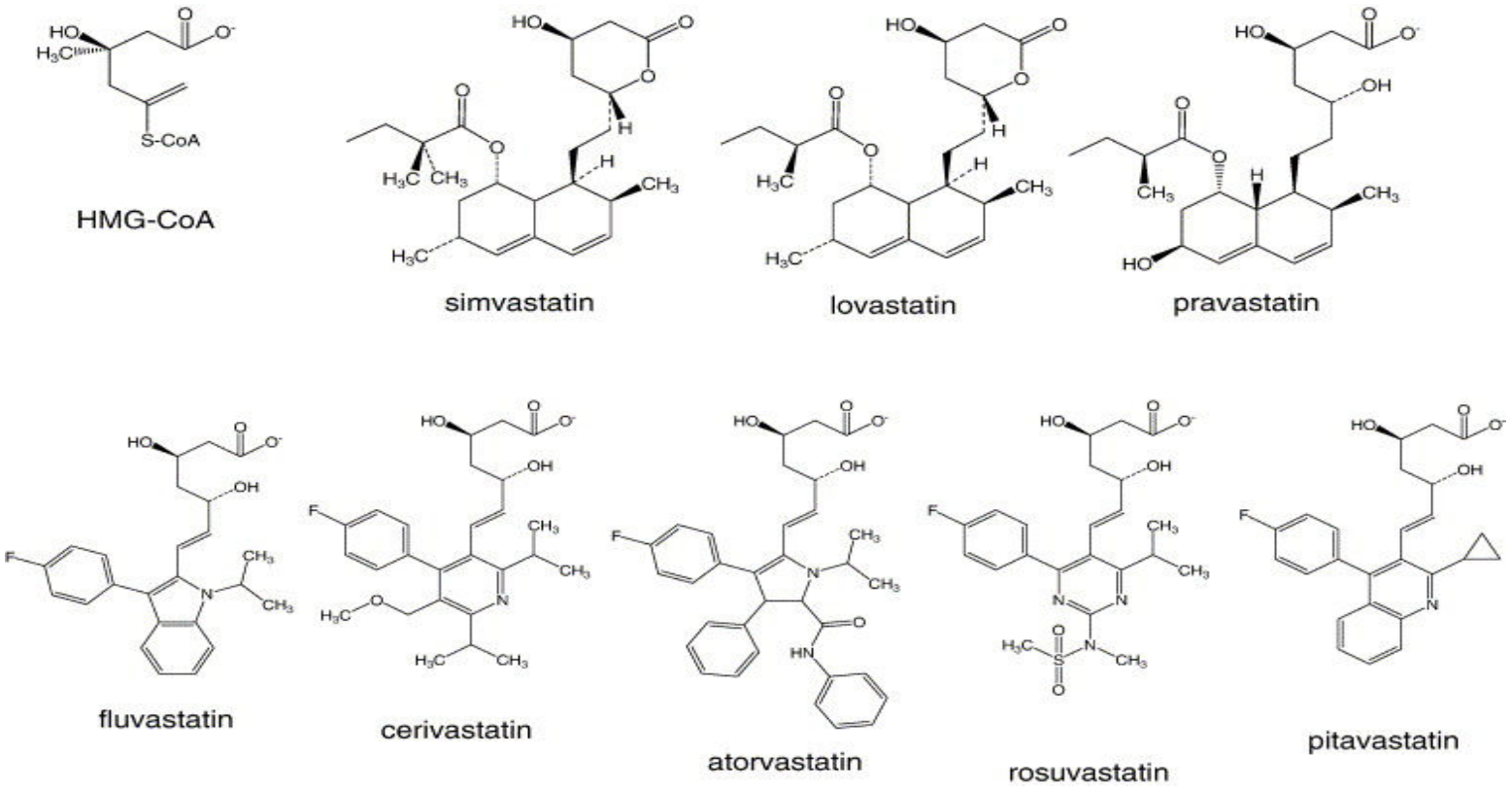

Figure 1.8 The chemical structures of the hydroxymethylglutaryl coenzyme A (HMG-CoA) reductase inhibitors (Shitara and Sugiyama, 2006).

Table 1.3 Lipophilicity and pharmacokinetic parameters of statins on the market. NA* : non available, ATV-Atorvastain, CER-Cerivastatin, FLU-Fluvastatin,LOV-Lovastatin, PRA-Pravastatin, SIM-Simvastatin

Parameter	**ATV**	**CER**	**FLU**	**LOV**	**PRA**	**SIM**
Absorption						
Fraction absorbed (%)	30	98	98	30	34	60-80
T_{max}(hr)	2-	2.5	0.5-1	2-4	0.9-1.6	1.3-2.4
C_{max} (ng/mL)	27-66	2	448	10-20	45-55	10-34
Bioavailability	12	60	19-29	5	18	5
% Effect of food	↓13%	0	↓15% to ↑ 25%	↑ 50%	↓30%	0
Distribution Fraction absorbed (%)	80-90	>99	>99	>95	43-55	94-98
Lipophilicity, (log P)	4.06	1.47	3.24	4.27	-0.22	4.68
Metabolism						
Hepatic metabolism	CYP3A4	CYP3A4/2 C8	CYP2C9	CYP3A4	Sulfation	CYP3A4
Clearance (L/hr/kg)	0.25	0.20	0.97	0.26-1.1	0.81	0.45
Mainly cleared as	Metabolites	Metabolites	Metabolites	Metabolites	Metabolites	Metabolites
Hepatic extraction (%)	>70	NA*	>68	>70	46-66	78-87
Systemic metabolites	Active	Active	Inactive	Active	Inactive	Active
Excretion						
$t_{1/2}$ (hr)	15-30	2.1-3.1	0.5-2.3	2.9	1.3-2.8	2-3
Urinary excretion (%)	Negligible	30	6	10	20	13
Fecal excretion (%)	Major route	70	90	83	71	58
Other parameters						
Prodrug	No	No	No	Yes	No	Yes
Max. dose (mg/day)	80	0.8	40	80	40	80

1.4.3 Pleiotropic Effects of Statins

Pleiotropic effects of a drug are actions other than those for which the agent was specifically developed. These effects may be related or unrelated to the primary mechanism of action of the drug, and they are usually unanticipated. Pleiotropic effects may be undesirable (such as side effects or toxicity), neutral, or, as is especially the case with HMG-CoA reductase inhibitors (statins), beneficial. The general pleiotropic effects of statin were shown in Figure 1.9 (Paul and Gahtan, 2003).

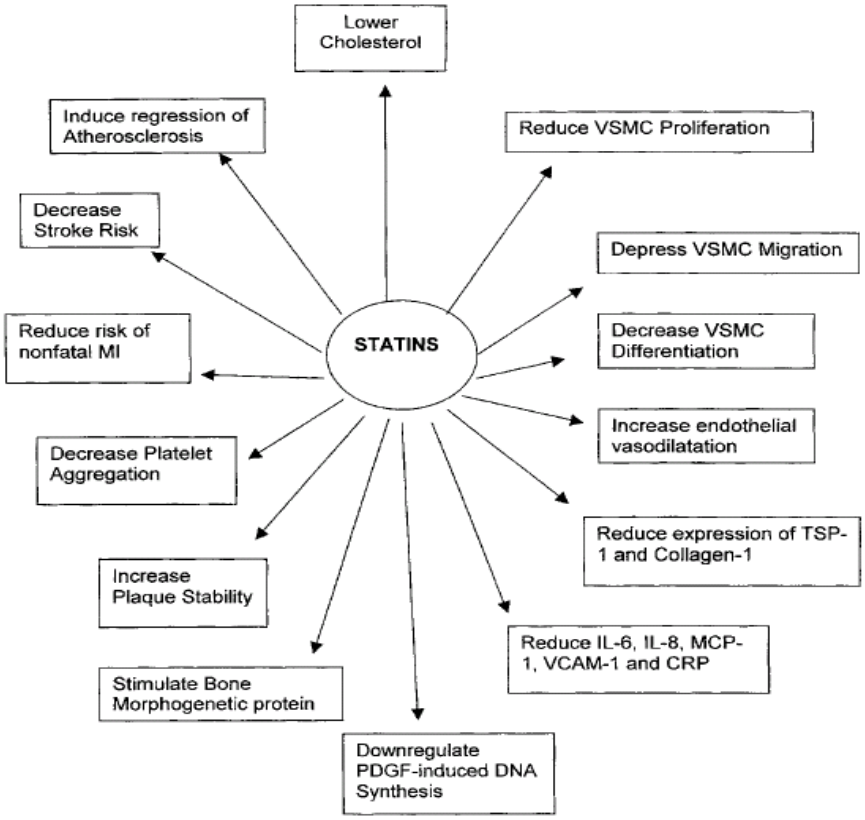

Figure 1.9. The pleiotropic effects of statins. The important clinical, cellular, and molecular systems influenced by this class of drugs are represented.VSMC = vascular smooth muscle cell; MCP-1 =monocyte chemoattractant protein-1; MI = myocardial infarction; VCAM-1 = vascular cell adhesion molecule-1; TSP-1 = thrombospondin-1; CRP= C-reactive protein; IL-6 =interleukin-6; PDGF =platelet-derived growth factor; IL-8 = interleukin-8; DNA =deoxyribonucleic acid (Paul and Gahtan, 2003).

1.4.3.1. Impact on Cardiovascular System

Statins directly prevent atherosclerosis and cardiovascular diseases by inhibition of cholesterol biosynthesis associated with the inhibition of HMG-CoA reductase. However, statins also prevent cardiovascular diseases by other mechanisms which are related to the pleiotropic effects of statins (Corsini *et al*., 1999). The general mechanisms for direct vascular actions of statins are given in Table 1.4.

Table 1.4. Mechanisms for direct vascular actions (Shitara and Sugiyama, 2006)

Lipid effects
Inhibition of cholesterol biosynthesis; Increased uptake and degradation of LDL Inhibition of LDL oxidation
Inhibition of lipoprotein secretion
Inhibition of modified LDL endocytosis
Antiatherosclerotic effects
Inhibition of migration and proliferation of arterial myocytes
Inhibition of macrophage growth
Inhibition of cholesterol accumulation in macrophages
Inhibition of cell adhesion
Inhibition of tissue factor expression and activity
Inhibition of superoxide generation
Inhibition of endothelin-1 synthesis and expression; Increased expression and activity of eNOS; Increased fibrinolytic activity
Induction of myocytes apoptosis in proliferative lesions

1.4.3.2. Impact on Kidney

The potential to ameliorate the impact of diabetes and to slow the progression of end stage renal disease are among the most promising roles for statins in the field of nephrology. Renal injury initiates inflammatory cascades that involve similar cellular events as seen in vascular tissue. Statins inhibit key events in this process that alter the progression of renal injury. Usui *et al*. (2003)

demonstrated a decrease in glomerular hypertrophy and albuminuria with cerivastatin treatment. One potential mechanism for this benefit was that cerivastatin inhibited leukocyte adhesion molecule expression on the glomerular endothelial cells, hence decreasing macrophage migration into the glomeruli (Almuti *et al*., 2006). Statins have also been reported to attenuate renal injury after an ischemic event.

1.4.3.3. Impact on Central Nervous System (CNS).

Statins have shown promise in the prevention of ischemic stroke in patients with coronary artery disease. Furthermore, some of the beneficial CNS effects of statins may be due to their augmentation of NO production as NO may improve CNS collateral blood flow, enhance cerebral vasodilator responses and prevent apoptosis (Del Zoppo, 1998).

In Alzheimer's disease (AD), elevated CNS cholesterol levels are thought to accelerate the cleavage of amyloid precursor protein (APP) to beta-amyloid (Aβ), a compound considered cytotoxic to oligodendrocytes and neurons. It has been found that the administration of simvastatin for a 6-month period to normo-cholesterolemic patients with mild AD decreased CNS Aβ levels (Fassbender *et al*., 2002; Locatelli *et al*., 2002).

1.4.3.4. Impact on Autoimmune System

Statins may have beneficial effects on autoimmune diseases such as rheumatoid arthritis, diabetes mellitus, psoriasis and inflammatory bowel disease. Modulation of T lymphocyte proliferation, differentiation and activation appears to be the primary mechanism (Almuti *et al*., 2006).

For instance, statins was found to decrease inhibit the expression of major histocompatibility antigen complex-II (MHC-II) on human macrophages and endothelial cells. Macrophages are thought to express MHC-II when they are activated. This allows them to activate T cells that, in turn, contribute to the

inflammatory process. This inhibition leads to a reduction of T cell proliferation and differentiation and subsequently to a reduction in the release of pro-inflammatory cytokines (Kwak *et al*., 2000).

1.4.3.5 .Impact on Bone

Statins have positive and negative effects on bone. Their negative effect is the inhibition of bone resorption. It has been found that murine osteoclast formation in cultures was inhibited by both lovastatin and alendronate (a nitrogen-containing bisphosphonate). On the other hand, they stimulate bone formation. Statins was found to increase the number of osteoblasts and the amount of new bone formation in mouse skull bones (Mcfarlane *et al*., 2002).

1.4.3.6. Impact on Gastrointestinal System

Statins may decrease the incidence of colon cancer. Lovastatin, in combination with the chemotherapeutic agents 5-FU (5-fluorouracil) and cisplatin, was found to increase apoptosis and to decrease the proliferation of cells in colon cancer cell lines, thereby inhibiting the progression of the disease. Furthermore, the addition of statins to the therapeutic regimen allowed for the use of lower doses of chemotherapeutic drugs resulting in milder side effects (Sacks *et al*., 1996; Pedersen *et al*., 1996)

1.4.4. Adverse Effects of Statins

It has been reported that statins have many adverse effects of organs and tissues (Kiortsis *et al*., 2006). These adverse effects are given below:

.

- Gastrointestinal side effects: Nausea, dyspepsia, abdominal pain, flatulence and diarrhoea or constipation
- Skin side effects: Alopecia, rash, cheilitis , lichenoid eruption , dermographism, chronic urticaria and toxic epidermic necrolysis
- Sensory organs: Cataract formation, ocular hemorrhage, nasal polyposis

- ❖ Central nervous system: Increase of suicides and violent deaths, depression, sleep disturbances, nightmares, headache, cognitive and memory problems.
- ❖ Peripheral Nervous system: Idiopathic polyneuropathy
- ❖ Renal effects: Proteinuria
- ❖ Autoimmune disorders: lupus erythematosus, arthralgia dermatomyositis, polymyositis, autoimmune hepatitis
- ❖ Erectile dsydunction, gynecomastia
- ❖ Hepato-toxicity

1.4.5. Effects of Statins on Skeletal Muscles

Even though statins are used very successfully clinically and well tolerated, some adverse effects may also arise in skeletal muscle. These effects may range from myalgia, myopathy to potentially life-threatening rhabdomyolysis. There are two reasons why skeletal muscle is primarily and profoundly affected tissue in the body from statin treatment. The first reason is that skeletal muscle is one of the lowest cholesterol biosynthetic tissues in body (Yokoyama *et al*., 2007)**.** The second one is that skeletal muscle accounts for the around 45 % of total weight and has a high metabolic rate and blood flow. As a consequence, it is highly exposed to drugs within the circulation (Evans and Rees, 2002A, 2002 B).

Myalgia and myopathy are characterized by diffuse muscle pain, tenderness, weakness associated with abnormal elevations in creatine kinase levels (< 10 times the upper limit of normal). Rhabdomyolysis is characterized by severe muscle destruction resulting in myoglobinuria and clinical features of muscle weakness, pain, swelling and cramps. This syndrome is the most harmful myotoxic effect of statin since it may cause death as a result of acute renal

failure. The incidence of these myotoxicities depends on several factors given below (Rosenson, 2004):

- The dosage of statin which is used
- The usage of statin with other drugs i.e. monotheraphy or polytheraphy
- The hydrophilic or lipophilic properties of statin drugs.

While the dose of drugs increases, the incidence of myotoxic effects raises. It has been shown a dose-dependent myotoxicity with simvastatin in both rats and humans. For example, the incidence of myopathy with patients receiving 20 mg simvastatin/d was found 0.04 % while this rate was observed 0.4 % in patients receiving 40 or 80 mg simvastatin/d (de Lemos *et al*.. 2004).

The usage of statin with other drugs such as cyclosporin, fibrate and gemfibrozil at the same time increases the rate of occurrence of myotoxic effects since these drugs inhibits CYP enzyme system and leads to increased bioavailability of statins, thereby increasing the potential for myotoxicity (Evans and Rees, 2002)**.**

The lipophilic or hydrophilic properties of statins also affect the incidence of the adverse effects in skeletal muscle since the lipophilic statins enter the cell by simple diffusion especially in unhepatic tissues. It has been shown that pravastatin is less myotoxic than simvastatin or lovastatin due to the its hydrophilicity, thus lower uptake of by myocytes (Masters *et al*., 1995). The incidence of rhabdomyolysis in different statin drugs was given in Table 1.5. (Cziraky *et al*., 2006).

Table 1.5 Incidence rate of Rhabdomyolysis in statins (Managed care claims database-USA) (Cziraky et al., 2006).

Drug	Patient-Years	Incidence Rates (per 10,000 person-years)
Atorvastatin	261,567	2.4 (1.9-3.1)
Fluvastatin	12,635	1.6 (0.2-5.7)
Lovastatin	26,122	2.3 (0.8-4.5)
Pravastatin	64,254	3.4 (2.1-5.2)
Rosuvastatin	8,213	2.4 (0.3-8.8)
Simvastatin	54,394	3.5 (2.1-5.6)
Cerivastatin	4,719	10.6 (3.4-24.7)

The sensitivities of skeletal muscle fibers to statin are different. These differences result from the metabolic and structural differences in the slow and fast twitch muscle. Histological experiments show that fast twitch fibers are ultimately affected from statin treatment. It has been indicated that the fibers show a necrotic response to statin administration and this response increases along with glycolytic metabolic nature of muscle fibers as decreases with oxidative metabolic properties of fibers. Least sensitive $\rightarrow$ I < IIA < IID < IIB $\rightarrow$ Most sensitive (Westwood *et al* 2005).

There are many histological, biochemical, physiological and some genetic studies to explain statin-induced myotoxicity in animals and humans.

Histological studies about statin induced myotoxicity revealed that they induce

- myofiber necrosis with interstitial edema (Smith *et al*.,1991)
- inflammatory cell infiltration (Smith *et al*.,1991)
- mitochondrial myopathy (England *et al*.1995)
- distruption of sarcomere (Schaefer *et al*., 2004)
- T-tubular injury (Draeger *et al*., 2006)

Physiological studies showed that statins induce:

- Decrease in membrane chloride conductance (Pierno *et al*., 1995)
- Decrease in action potential amplitude (Pierno *et al*., 1999)
- Decrease Na^+ channel function (Gray *et al*., 2000)
- Reduced flux through ATP-sensitive K^+ channel (Pierno *et al*., 1992)
- Decrease Na^+-K^+ ATPase density (Gray *et al*., 2000)
- Increase in sarcolemmal excitability (Pierno *et al*., 2006)
- Decrease in threshold value (Pierno *et al*., 2006)
- Increase in latency of the first action potential (Pierno *et al*., 2006, Pierno *et al*., 1995)
- Increase in Ca^{2+} release to sarcoplasma (Inonue *et al*.,2003; Sirvent *et al*., 2005; Liantonio *et al*., 2007)

Biochemical studies clarified that these drugs leads to:

- Increase (Phillips *et al*., 2002; Paiva *et al*., 2005) or no change (Yokoyama *et al*., 2007) in the level of tissue lipids
- Decrease in the level of tissue proteins (Master *et al*., 1995)
- Decrease in the level of tissue and mitochondrial DNA (Schick *et al*., 2007)

Genetic studies revealed that statins cause:

- Upregulation of genes which are responsible for protein degradation (Urso *et al*., 2005)
- Genetic abnormalities (Vladutiu *et al*., 2006)

Based on these studies, three theories about the mechanisms of statin induced myotoxicity has been proposed.

THEORY 1: Blocking cholesterol synthesis by statins reduces cholesterol content of skeletal muscle membranes and this makes them unstable.

As a result of cholesterol reduction, the membrane fluidity, its electrical properties and the functions of ion channel in membrane change. These changes affect the muscle cell functions.

THEORY 2: Statins lead to a reduced synthesis of ubiquinone (coenzyme Q10), an essential element of mitochondria, thereby disturbing normal cell respiration and energy production.

Ubiquinone (coenzyme Q10) is an essential cofactor of electron transport chain where ATP is generated. In addition, it serves as an important antioxidant in both mitochondria and lipid membranes and decreases oxidative DNA damage in human lymphocytes. The inhibition of cholesterol synthesis decreases the synthesis of precursors of ubiquinone. This leads to the impairment energy metabolism and increase in the amount of reactive oxygen species (Baker and Tarnopolsky, 2001)

THEORY 3: Reduction of small GTP-binding proteins leads to muscle apoptosis.

Cholesterol biosynthesis pathway is also known as mevalonate pathway. The intermediate products of this pathway are important for regulations of many cellular functions. Mevalonic acid, the synthesis of which is inhibited by statins, is a precursor of not only cholesterol but other metabolites including isopentyl
adenosine contained in transfer RNA, dolichols for the synthesis of glycoproteins and CoQ_{10}. In addition, metabolites of mevalonic acid including farnesyl pyrophosphate and geranylgeranylpyrophosphate mediate the prenylation of some specific proteins. Prenylated proteins are involved in a

number of processes, including cell signal transduction, differentiation, proliferation, and myelination and cytoskeletal dynamics. The inhibition of cholesterol synthesis reduces the synthesis of the intermediary products, thereby inhibiting protein prenylation and stopping the cellular growth and functions i.e. apoptosis. The general apoptotic mechanisms of statin is given in figure 1.10 (Dirks and Jones, 2006; Laufs and Liao, 2003; Matzno *et al*., 2005)

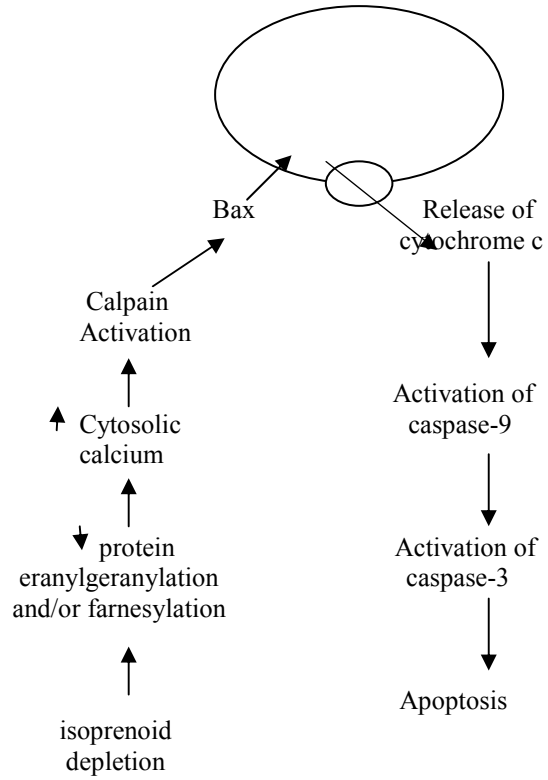

Figure 1.10. Hypothetical Scheme of statin induced apoptosis (Dirks and Jones, 2006).

1.5 Spectroscopy

Spectroscopy is defined as the study of the interaction of electromagnetic wave with matter excluding chemical effects.

The energy (*E*) of the electromagnetic wave is given by the Bohr equation as:

$$\Delta E = h\nu$$

ν is the frequency of the applied radiation and h is Planck's constant (h = 6.6×10^{-34} joule second).

$$c = \lambda \nu$$

where c is the speed of light in vacuum (3.0×10^{8} ms^{-1}) and λ is the wavelength of light. These two equations can be used to identify a common spectroscopic unit called wavenumber, which is denoted by ν. Wavenumber is the number of waves in a length of one centimeter and expressed in terms of cm^{-1}. It is given by the following relationship (Stuart, 1997):

$\bar{\nu}$ = wavenumber = $1/\lambda = \nu/c$

Thus, $E = h\nu = hc\bar{\nu}$,

From these equations, it is clear that both wavenumber and frequency are directly proportional to energy. However, in practical applications of spectroscopy wavenumber is used because in the frequency, the numbers involved are often large.

As a result of electromagnetic radiation with matter, redirection of the radiation can be scattered (i.e. its direction of propagation changes), absorbed (i.e. its energy is transferred to the molecule) or emitted (energy is released by the molecule). The relative probability of the occurrence of each process is a property of the particular molecule encountered. When the energy of the light is absorbed, the molecule is said to be *excited or* in an excited state. An excited molecule can possess any one

of a set of discrete amounts (quanta) of energy described by the laws of quantum mechanics. These amounts are called the *energy levels* of the molecule. A typical energy-level diagram describing these energy levels is presented in Figure 1.11. The major energy levels are determined by the possible spatial distributions of the electrons and are called electronic energy levels; on these are superimposed vibrational levels, which indicate the various

modes of vibration of the molecule (e.g., the stretching and bending of various covalent bonds). There are even smaller subdivisions called rotational levels, but they are of little importance in absorption spectroscopy. The lowest electronic level is called the ground state and all others are excited states (Freifelder, 1982).

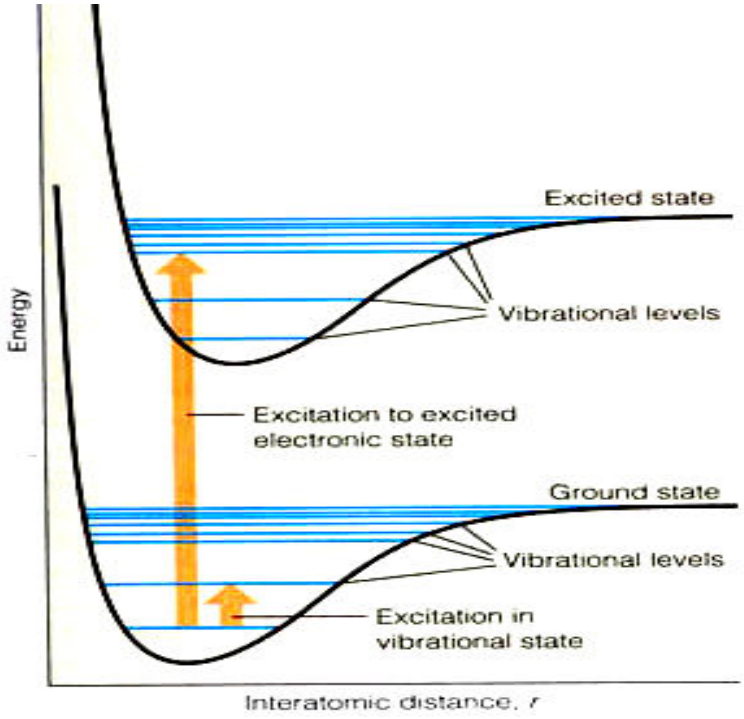

Figure 1.11. Typical energy-level diagrams showing the ground state and the first excited state. Vibrational levels are shown as thin horizontal lines. A possible electronic transition between the ground state and the fourth vibrational level of the first excited state is indicated by the long arrow. A vibrational transition within the ground state is indicated by the short arrow (Freifelder, 1982).

For most purposes, it is convenient to treat a molecule as if it possesses several distinct reservoirs of energy. The total energy is given by:

$$E_{\text{total}} = E_{\text{transition}} + E_{\text{rotation}} + E_{\text{vibration}} + E_{\text{electronic}} + E_{\text{electron spin orientation}} + E_{\text{nuclear spin orientation}}$$

Each *E* in the equation represents the appropriate energy as indicated by its subscript.

1.5.1 Infrared Spectroscopy

Infrared spectroscopy is the study of the interaction of infrared light with the electric dipole moment of the matter. The multiplicity of vibrations occurring simultaneously produces a highly complex absorption spectrum, which is the plot of absorption as a function of wavenumber (ν) expressed in terms of cm^{-1}. The value of infrared spectral analysis comes from the fact that the modes of vibration of each group are very sensitive to the changes in chemical structure, conformation and environment. In addition, as each different material has a unique combination of atoms, no two compounds produce the exact same infrared spectrum. Therefore, an infrared spectrum can result in a positive identification of every different kind of material.

The term "infrared" covers the range of the electromagnetic spectrum between 0.78 and 1000 μm (Figure 1.15). The infrared spectrum can be divided into three regions: the *far infrared* (400-20 cm^{-1}), the *mid infrared* (4000-400 cm^{-1}) and the *near infrared* (14285-4000 cm^{-1}). Most infrared applications employ the mid-infrared region, but the near and far infrared regions can also provide information about certain materials.

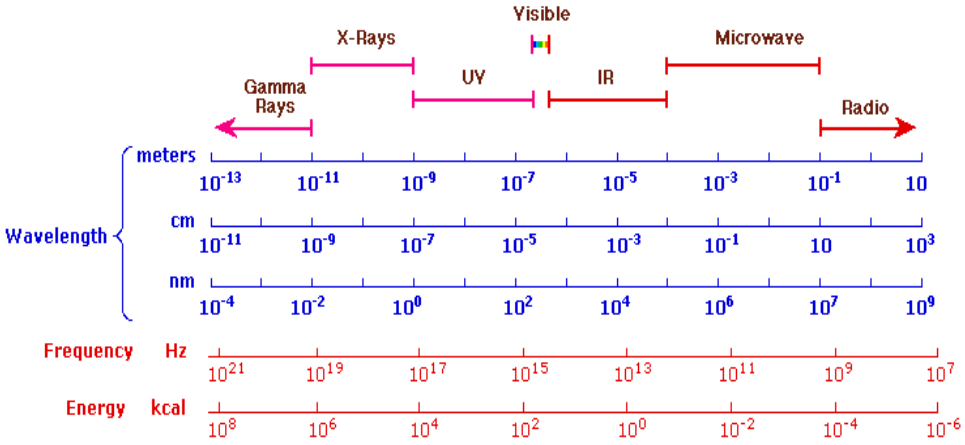

Figure 1.12. The Electromagnetic spectrum

Infrared spectroscopy has been used in a number of branches of science as a quantitative and qualitative tool (Diem, 1993, Garip *et al*, 2007, Gorgulu *et al*., 2007, Dogan *et al*., 2007, Bozkurt *et al*., 2007, Akkas *et al*., 2007). It is a nondestructive tool, which gives information about the structure of material.

An IR Spectrum of sample is obtained by scanning the intensity of IR radiation before and after passage of the IR beam. The IR Spectra of most materials consist of a large number of absorption bands. These bands originate from the interaction between discrete vibrational and rotational modes of the molecules which are excited by the absorption of IR radiation. Since the components of typical biological sample are present in a condensed phase (solids, liquids or solutions), only vibrational modes are observed. Consequently, IR spectra of biological specimens are only vibrational spectra (Colthup *et al*., 1990).

Different descriptive names are often given to vibrational modes. Vibrations can be subdivided into two classes, depending on whether the bond length or angle is changing:

1- Stretching (Symmetric and asymmetric): It produces a change of bond length. A stretch is a rhythmic movement along the line between the atoms so that the interatomic distance is either increasing or decreasing. A stretch can be symmetric or asymmetric
2- Bending (scissoring, rocking, wagging and twisting): results in a change in bond angle. Bending can occur in the plane of the molecule or out of plane; it can be scissoring, like blades of a pair of scissors, or rocking, where two atoms move in the same directions

Consequently, infrared spectra are generated by the characteristic motions of various functional groups (e.g. methyl, carbonyl, amide etc.). The sensitivity of these modes of vibration to any alteration in chemical structure, conformation, and environment presents the value of infrared spectroscopy. Figures 1.13, 1.14 and 1.15 demonstrate the main types of variations schematically.

For a vibration to give rise to absorption of infrared radiation, there are two criteria:

* A molecule should have a frequency of vibration similar to electromagnetic wave.
* Change of dipole moment should take place.

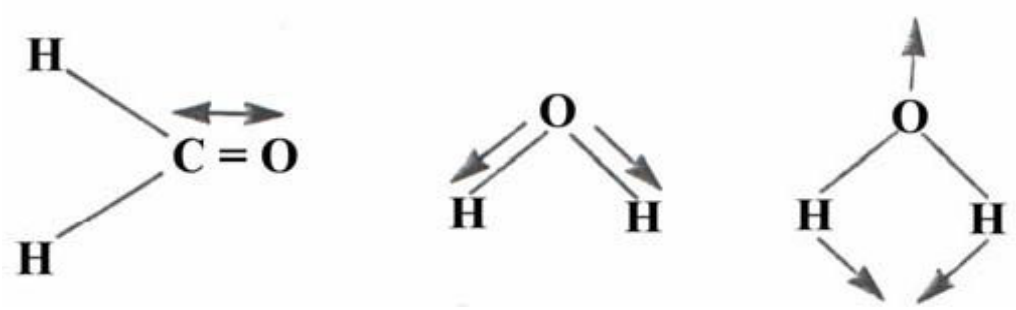

Stretching Stretching Bending

Figure 1.13. Stretching and bending vibrations (Stuart, 1997).

Symmetric stretching

Asymmetric stretching

Figure 1.14. Symmetric and asymmetric stretching vibrations (Stuart, 1997).

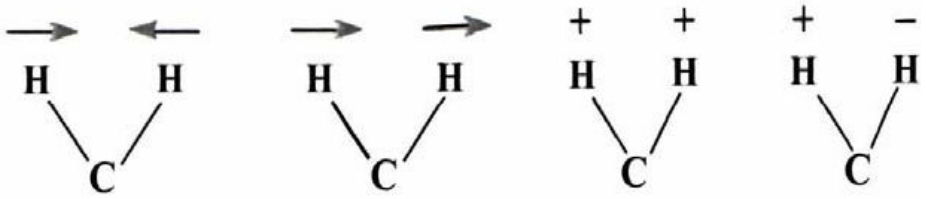

Deformation Rocking Wagging Twisting

Figure 1.15. Types of bending vibrations (Stuart, 1997).

Upon interaction with infrared radiation, portions of the incident radiation are absorbed at particular wavelengths.

1.5.2 Fourier Transform Infrared Spectroscopy (FTIR)

Fourier transform infrared (FTIR) spectroscopy has found increasing favor in laboratories since early eighties. This method is based on the idea of the interference of radiation between two beams to yield an *interferogram,* which is a signal produced as a function of the change of pathlength between the two beams.

The most important feature of an interferogram is that every individual data point of this signal contains information over the entire infrared region. This process is carried out by an interferometer. It encodes the initial frequencies into a special form, which the detector can observe. For rapid-scanning interferometers, liquid nitrogen cooled *mercury cadmium telluride (MCT)* detectors are used. For slower scanning types of interferometer, pyroelectric detectors (e.g. a *deuterated triglycine sulfate (DTGS)* detector element) can be used. In essence, the detector is always observing all frequencies at the same time (Griffiths and De Haseth*,* 1986). The two domains of distance and frequency are interconvertible by the mathematical method of Fourier transformation. Therefore, Fourier transformation is simply a mathematical means of sorting out the individual frequencies for the final representation of an infrared spectrum.

The basic components of an FTIR spectrometer are shown schematically in Figure 1.16. The radiation emerging from the source is passed through an interferometer to the sample before reaching a detector. Upon amplification of the signal, in which, high frequency contributions have been eliminated by a filter, the data are converted to a digital form by an analog-to-digital converter and then transferred to the computer for Fourier transformation to be carried out.

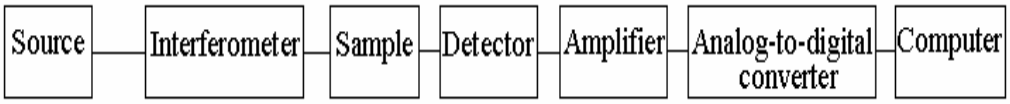

Figure 1.16. Basic components of an FTIR spectrometer**.** (Stuart 2004)

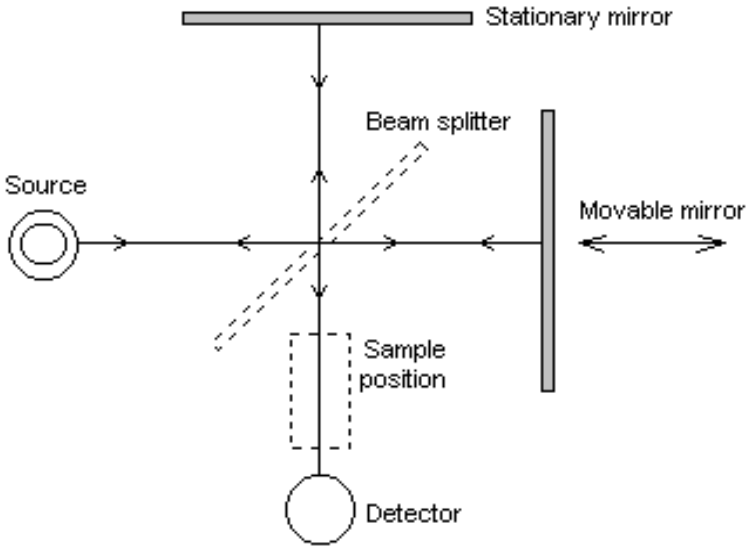

Figure 1.17. Schematic of a Michelson interferometer (Stuart 2004)

The most common interferometer used in FTIR spectrometry is a Michelson interferometer (Figure 1.17), which consists of two perpendicularly plane mirrors, one of which can travel in a direction perpendicular to the plane. A semi-reflecting film, a beamsplitter, bisects the planes of these two mirrors. The beamsplitter material has to be chosen according to the region to be examined. FTIR spectrometers use a Globar or Nernst source for the mid-infrared region. If the far-infrared region is to be examined, then a high-pressure mercury lamp can be used.

For the near-infrared, tungsten-halogen lamps are used as sources. The moving mirror is a crucial component of the interferometer. It has to be accurately aligned and must be capable of scanning two distances so that the path difference corresponds to a known value. A number of factors associated with the moving mirror need to be considered when evaluating an infrared spectrum. The interferogram is an analogue signal at the detector that has to be digitized in order that the Fourier-transformation into a conventional spectrum can be carried out (Stuart, 2004).

1.5.3 Attenuated Total Reflectance FTIR Spectroscopy

FTIR spectra can be obtained from the transmission or reflection of IR radiation from the sample. In transmission measurements, the IR beam passes through the sample and it is applicable to solids, liquids, gases and polymers that allow transmission of source light whilst reflectance measurements are based on the reflection of IR radiation on the sample. They are classified as diffuse reflectance and Attenuated Total Reflectance (ATR) (Stuart, 2004).

ATR is especially useful for opaque solid samples regardless of thickness with a minimum time of preparation. Thin films, pastes, powders, suspensions, paper, coatings, and fibers can easily be analyzed with ATR technique. This technique utilizes the phenomenon of total internal reflection. A beam of radiation entering a crystal will undergo total internal reflection when the angle of incidence at the interface between the sample and crystal is greater than the critical angle, where the latter is a function of the refractive indices of the two surfaces.The beam penetrates a fraction of a wavelength beyond the reflecting surface and when a material that selectively absorbs radiation is in close contact with the reflecting surface, the beam loses energy at the where the material absorbs (Figure 1.18). The resultant attenuated radiation is measured and plotted as a function of wavelength

by the spectrometer and gives rise to the absorption spectral characteristics of the sample (Stuart, 2004; Günzler and Gremlich, 2002).

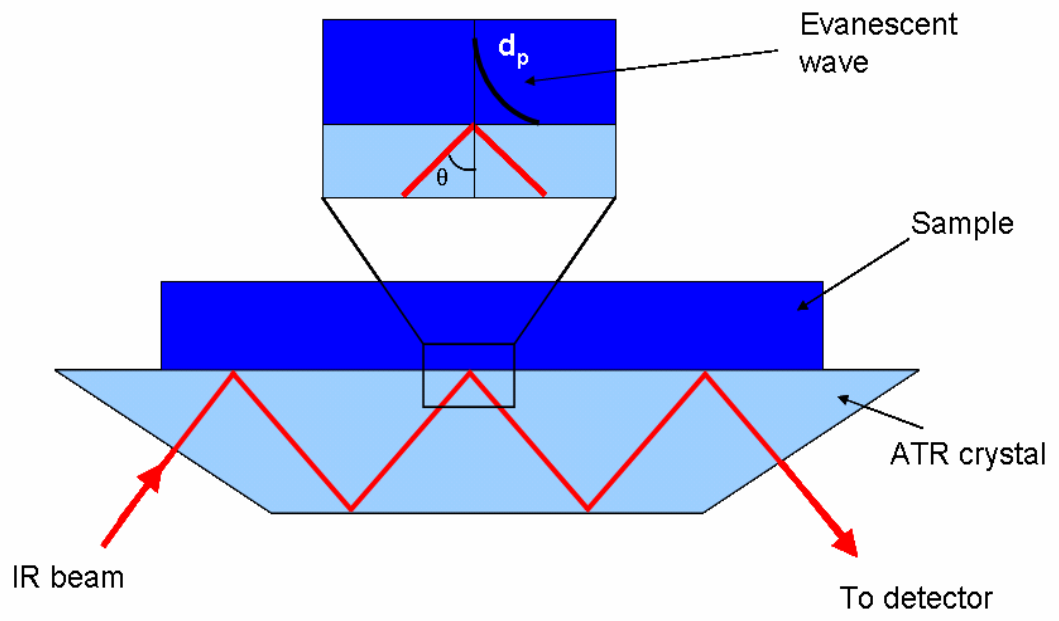

Figure 1.18. Schematic of a typical attenuated total reflectance cell

The depth of penetration in ATR spectroscopy is a function of the wavelength (λ), the refractive index of the crystal (n_2) and the angle of incident radiation,(θ). The depth of penetration (d_p) for a non-absorbing medium is given by the following:

$$d_p = (\lambda/n_2)/\{ 2\pi[\sin\theta - (n_1/n_2)^2]^{1/2}\}$$

where n_1 is the refractive index of the sample.

The crystals used in ATR cells are made from materials that have low solubility in water and are of a very high refractive index. Such materials include zinc selenide (ZnSe), germanium (Ge) and thallium-iodide (KRS-5).

The properties of these commonly used materials for ATR crystals are summarized in table 1.6.

Table 1.6. Materials used as ATR crystals and their properties (Stuart 2004).

Window material	Useful range (cm^{-1})	Refractive index	Depth of penetration (μm)
KRS-5	20 000-400	2.37	1.73
ZnSe	20 000-650	2.4	1.66
Si	8300-1500	2.37	1.73
Diamond	45000-2500	2.4	1.66
Ge	5000-550	4.0	0.65

Different designs of ATR cells allow both liquid and solid samples to be examined. It is also possible to set up a flow-through ATR cell by including an inlet and outlet in the apparatus. This allows for continuous flow of solutions through the cell and permits spectral changes to be monitored with time (Stuart, 2004).

1.5.4. The Advantages of FTIR and ATR-FTIR Spectroscopy

The reason why infrared spectroscopy is commonly used is that

- The spectra of almost any biological material can be obtained in a wide variety of environments.

- ❖ It provides a precise measurement method, which requires no external calibration.
- ❖ It is possible to examine all wavelengths arriving at the detector simultaneously, compared to being able to sample only one spectral element at a time by the detector (Diem, 1993).
- ❖ This method is a rapid and sensitive technique, which is easy to perform to improve the signal-to-noise ratio (noise adds up as the square root of the number of scans, whereas signal adds linearly). The data processing is simple with the computer softwares. Moreover, system permits permanent data storage, manipulation of data and quantitative calculations (Rigas *et al.,* 1990; Manoharan *et al.*, 1993; Yono *et al.*, 1996; Ci *et al.*, 1999).
- ❖ The instrumentation is inexpensive compared to the cost of X-Ray diffraction, NMR, ESR, and CD spectroscopic equipment.
- ❖ Small sample quantities as low as few micrograms are sufficient to analyse and in vivo studies are possible (Mendelsohn and Mantsch, 1986).
- ❖ It is a non-destructive technique (Melin *et al.*, 2000, Severcan and Haris, 1999, Cakmak *et al.*, 2003) and there is no light scattering or fluorescent effects.
- ❖ The system can be applied to the analysis of any kind of material and that is not limited to the physical state of the sample. Samples may be solutions, viscous liquids, suspensions, inhomogeneous solids or powders (Colthup *et al.*, 1990). Indeed, kinetic and time-resolved studies are possible (Mantsch *et al*., 1984; Mendelson and Mantsch, 1986; Haris and Severcan, 1999).
- ❖ Frequency and bandwidth values can be determined routinely with uncertainties of better than ±0.05 cm^{-1}.

Moreover, due to its somewhat different technology, it is used to examine functional groups that are not accessible with ultraviolet and visible light absorption spectrometers (Freifelder, 1982).

In addition to all advantages mentioned above, the other advantages of ATR-FTIR spectroscopy are the following: (Zhongsheng *et al*., 2007),

- A pure spectrum of any kind of sample is obtained easily in a short time as compared to transmission spectroscopy.
- ATR sampling is fast and easy because little or no sample preparation is required
- Other techniques, such as infrared transmission, often require the sample to be heated, pressed or ground in order to collect the spectrum. These processing steps for transmission analysis take time and can cause structural changes to the sample. In addition, samples that must be diluted for transmission analysis are usually mixed with salts which may have spectral features of their own.
- Most samples can be run in their natural state (Grdadolnik, 2002).
- The ATR-FTIR spectra have better signal-to-noise ratio and increased sensitivity.
- The ATR-FTIR spectra are similar to absorption spectra, but without significant spectral distortion.
- Compared to transmission experiments, it avoids the handling problems which are caused by the required short pathlength.

1.6 Aim of the Study

Statins are the most prescribed drugs in the world due to the higher efficacy. The mechanism of 3-hydroxyl-3-methylglutaryl-coenzyme-A reductase inhibitor-induced muscle side effects is not yet understood. A variety of statins have been shown to cause myopathy and rhabdomyolysis in animals and humans. A number of in vitro studies have investigated statin-induced myotoxicity; however there is currently no data about statin induced structural and functional changes of macromolecules in skeletal muscle and comparison of these changes in different type of muscles. To obtain a better understanding of the nature of the side effects of statins in muscle the present study examined

simvastatin-tissue interactions with regard to their ability to induced myotoxicity within the different rat skeletal muscle tissues, namely EDL, DIA and SOL. For this purpose FTIR and ATR-FTIR spectroscopy were used.

As mentioned before FTIR and ATR-FTIR spectroscopy are valuable techniques due to their high sensitivities in detecting changes, simultaneously in the functional groups belonging to tissue components. Both techniques are especially useful for the analysis of secondary structural characterization of proteins. These techniques are non-destructive, and highly selective because their ability to be a spectral fingerprint for molecular components.

The other aim of this study is to apply FTIR and ATR-FTIR spectroscopy as rapid and suitable methods to evaluate the effect of simvastatin on skeletal muscle tissues at molecular level and to compare these findings with biochemical and physiological data obtained in other studies.

CHARTER 2

MATERIALS AND METHODS

2.1 Reagents

Simvastatin (Zocor) were purchased from Merck, Sharp and Dohme (West Point, PA, USA) as tablets containing 40 mg in each. Potassium bromide (KBr), acetonitrile and isopropanol were obtained from Merck (Merck Company, Darmstadt, Germany), Butylated hydroxy toluene and cholesterol was purchased from Sigma (Sigma Chemical Company, Saint Louis, Missouri, USA). All chemicals were obtained from commercial sources at the highest grade of purity available.

2.2. Preparation of Experimental Animals

Twenty adult male Wistar rats (12-14 weeks) weighing 250-300 g which are obtained from Experimental Animal Center, Hacettepe University, Ankara, were selected randomly. The rats were fed with a standard diet with water ad libitum, and kept in conventional room with controlled light (12:12, dark:light), temperature (22±1 °C), relative humidity (40-50%) and ventilation (15 air changes per hour). They were allowed to adapt to their environment for one week prior to the experiments. All procedures were approved by the Ethics Committee of Hacettepe University.

The rats were separated into two groups as control (n=10) and simvastatin treated (n=10). The control group received only serum physiologic solution. Simvastatin in serum physiologic (50 mg/kg) were given to the treatment group daily through

gavage during 30 days (Figure 2.1). During the experiment, rats were weighed weekly. A definite amount of water and foods were given to the rats and remained food weighed and water measured by a graduated cylinder daily.

At the end of this period the rats were decapitated. The blood samples were taken for HPLC studies. EDL, SOL and DIA muscles were dissected separately and stored at −80 °C until FTIR spectroscopy study. In Figure 2.2 the surface of the tibia and the muscles of the left limb of rat, SOL muscle and tendon of EDL muscle can be seen. Figure 2.3 shows the caudal and dorsal surface of the rat diaphragm muscle. In this figure, the numbers between 4-10 represents the different parts of the rat diaphragm.

Figure 2.1. Oral gavage method

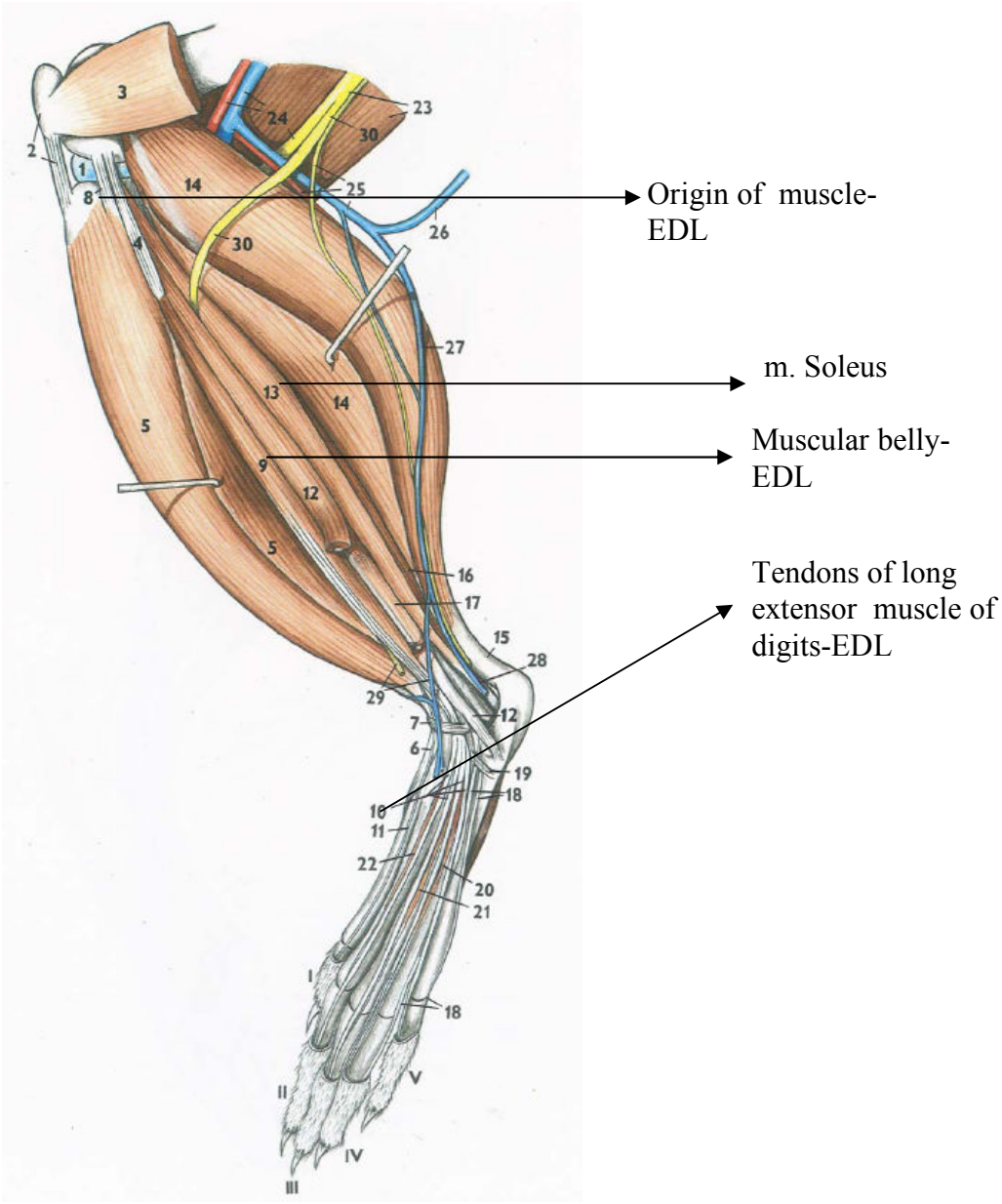

Figure 2.2. Rat lateral surface of the tibia and the muscles of the left limb; view of the dorsolateral surface, 8-10 m. extensor digitorium longus-long extensor muscle of digits, 13-m. soleus-soleus muscle (Popesko *et al*., 2002).

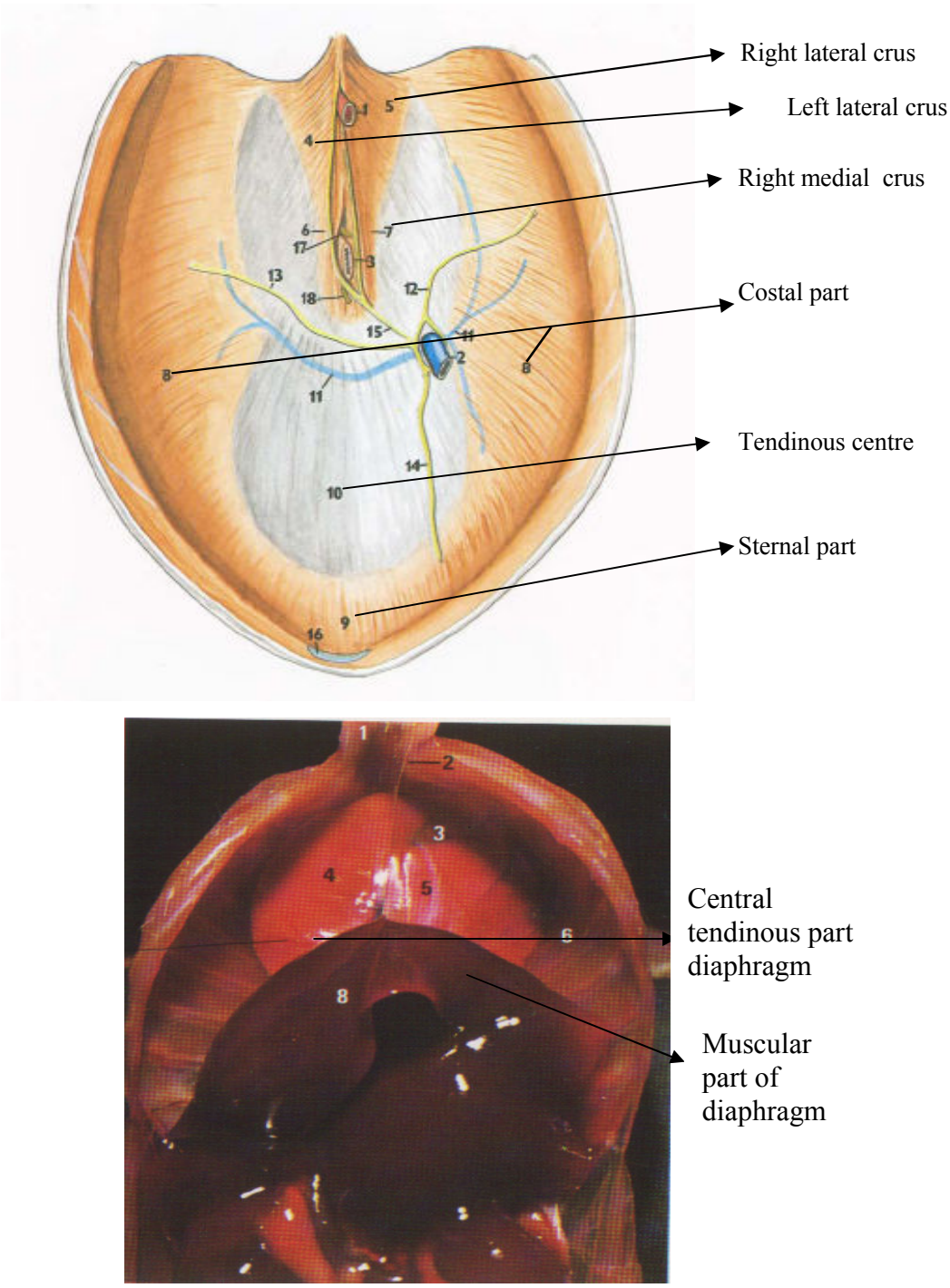

Figure 2.3. The dorsal and caudal surface of rat diaphragm. 4-10 diaphragm (Popesko *et al.* , 2002; Olds, 1988).

2.3. High Pressure Liquid Chromatography (HPLC) Studies

Total cholesterol analysis in serum: Blood samples were collected in tubes for biochemical analysis, and centrifuged at 5000 x *g* at 4°C for 10 min to separate cells and serum. The serum samples were used for total cholesterol determination. 200 µL serum samples were extracted in 3 ml acetonitrile/isopropyl alcohol (70:30, v/v)-containing tubes and the mixture were vortexed for 30 s and centrifuged at 6000×*g* for 10 min at 4 ºC. Supernatants were transferred to autosampler vials of the HPLC instrument. In order to prevent the oxidation of cholesterol, BHT is added to both standard and serum cholesterol solutions. Acetonitrile-isopropyl alcohol (70:30 v/v) was used as mobile phase at a flow rate of 1 ml/ min. Supelcosil LC 18 DB column (250 x 4.6 mm, 5 µ m) was used as the HPLC column. Detection was performed by UV at 202 nm and 40 º C column oven. Quantification was carried out by external standardization using *Class VP software*. The results were expressed µg/ml for serum samples (Yilmaz *et al*., 2007).

2.4. Fourier Transform Infrared (FTIR) and Attenuated Total Reflectance Fourier Transform Infrared (ATR-FTIR) Spectroscopic Measurements

2.4.1 Sample Preparation for FT-IR and ATR-FTIR Studies

The EDL and SOL samples were dried in a LABCONCO freeze drier (Labconco FreeZone®, 6 liter Benchtop Freeze Dry System Model 77520) for overnight in order to remove water content. The dried samples were then ground in a liquid nitrogen-cooled colloid mill (Retsch MM200) to obtain tissue powder. The tissue powder was mixed with dried potassium bromide at the ratio of 0.5 mg sample to 150 mg KBr in a mortar. KBr is most commonly used alkali halide disk serving as a beam condensing system. It is completely transparent in the mid-infrared region (Stuart, 1997). The mixture was dried again in the freeze drier for 18 hours to remove all traces of remaining water.

The mixture then was compressed under a pressure of ~100kg/cm^2 (1300psi) for 6 min to obtain a thin KBr disk. This sinters the mixture and produces a clear transparent disk (Stuart, 1997).

Diaphragm muscle has a very thin structure (Figure 2.3) and the distribution of muscle fiber types changes from costal to sternal part of the tissue. Due to the requirements of small samples and difficulties in the grinding of the diaphragm muscle tissues for FTIR studies, these tissues were studied with ATR-FTIR spectroscopy. For ATR-FTIR studies, the samples in size of 0.5 cm x 0.5 cm x 0.1 cm were cut from costal part of rat diaphragm muscles.

2.4.2 FTIR and ATR-FTIR spectroscopy

Infrared spectra of EDL and SOL samples were obtained using Perkin-Elmer Spectrum 100 FTIR spectrometer (Perkin-Elmer Inc., Norwalk, CT, USA) equipped with a MIR TGS detector. Water and carbondioxide molecules in the air affect the IR spectrum. Moreover, although KBr is always infrared spectroscopic grade, it may give some small absorption bands interfering with sample spectra. To overcome these problems the spectrum of air and KBr transparent disk was recorded together as background and substracted automatically by using appropriate software (Spectrum1000 software).

The spectra of EDL and SOL samples were recorded in the 4000–400 cm^{-1} region at room temperature. A total of 50 scans were taken for each interferogram at 4 cm^{-1} resolution

The infrared spectra of diaphragm muscle samples were collected in the one-bounce ATR mode in a Spectrum 100 FTIR spectrometer (Perkin-Elmer Inc., Norwalk, CT, USA) equipped with a Universal ATR accessory. The small diaphragm muscle samples were placed on a Diamond/ZnSe crystal plate (Figure 2.4) (PerkinElmer) and compressed (150 Gauge) with a sponge to

obtain good surface contact. The tissues were scanned from 4000 to 650 cm^{-1} for 50 scans with a resolution of 4 cm^{-1} at room temperature. Water was used as a reference. Since the diaphragm tissue contains water, this water was subtracted automatically from the tissue spectra by using Spectrum 100 software.

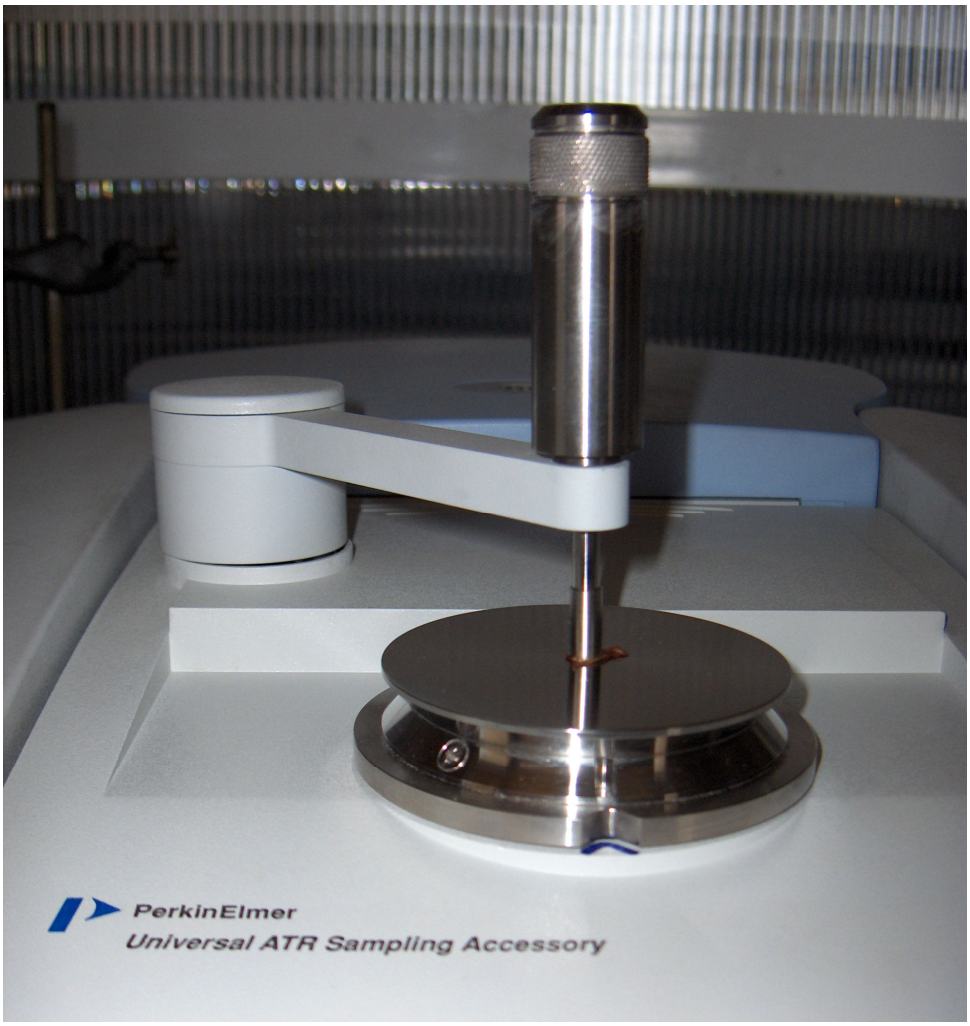

Figure 2.4. The sample position on ATR-FTIR Spectroscopy

Each sample was scanned under the same conditions with three different pellets, all of which gave identical spectra. The average spectra of these three replicates were used in detailed data analysis and statistical analysis.

Collections of spectra and data manipulations were carried out using Spectrum 100 software (Perkin-Elmer). The band positions were measured using the frequency corresponding to the center of weight. Using the same software, the spectra were first smoothed with nineteen-point Savitsky-Golay smooth function to remove the noise. After the averages of three replicates of the same samples were taken, the spectra were baseline corrected. The spectra were normalized with respect to specific bands for visual demonstration. The purpose of the normalization is to remove differences in peak heights between the spectra acquired under different conditions. It allows a point-to-point comparison to be made (Smith, 1999). The ratios of the intensities and shifting of the frequencies were examined before the normalization process. Band areas were calculated from smoothed and baseline corrected spectra using Spectrum 100 software. The bandwidth values of specific bands were calculated as the width at 0.75x height of the signal in terms of cm^{-1}.

2.4.3. Cluster Analysis

In order to the spectral differentiation of control and simvastatin-treatment groups in each type of skeletal muscle and control groups of EDL, SOL and DIA muscles, cluster analysis was applied by using OPUS 5.5 software (Bruker Optics, GmbH). For cluster analysis, second derivative of each spectrum was taken in 3800-850 cm^{-1} region and subsequently vector normalization was applied over the investigated frequency range. As input data for this analysis, spectral distances were calculated between pairs of spectra as Pearson's correlation coefficients. Cluster analysis for the separation of control and treatment groups were based on the Euclidean distances. Ward's algorithm was used to construct dendrograms.

2.5 Statistical Test

The results were expressed as ‘mean ± standard deviation (SD)’. Control and simvastatin treated data were analyzed statistically using non-parametric Mann–Whitney U test. A ‘p’ value less than or equal to 0.05 was considered as statistically significant. The degree of significance was denoted as less than or equal to $p<0.05$*, $p<0.01$**, $p<0.001$***.

CHAPTER 3

RESULTS

This current study was specifically conducted to reveal the effects of high dose of simvastatin treatment on the macromolecular compositions, structure and function of different rat skeletal muscle tissue types: EDL, SOL and DIA by using ATR-FTIR and FTIR spectroscopy.

3.1 Body Weights, Food, Drug Intake and Serum Cholesterol Levels of Rats

Animals were weighed both before treatment and decapitation. A definite food and water was given to animals everyday and remaining food and water amount were measured. The body weights, food and water consumption values of control and treated groups were given in Table 3.1. Simvastatin treatments caused significant decrease in the body weight ($p<0.05$), food ($p<0.01$) and water intake ($p<0.001$).

After decapitation, serum cholesterol levels were measured by HPLC. The results were given in Figure 3.1. As seen from the Figure, the total cholesterol values in rat serum samples decreased significantly from 172.06±11.83 µg/ml to 146.63±11.22 µg/ml ($p<0.01$) as a result of the simvastatin treatment as expected.

Table 3.1. Food intake, water intake and body weight in rats treated with simvastatin. The values are the mean ± S.D. for each group. Comparisons were done by Mann–Whitney U-test. The degree of significance was denoted as: $p < 0.05$*, $p < 0.01$**, $p < 0.001$***. Downward arrow indicates a decrease and upward arrow indicates an increase with respect to the control.

Animal Group	Control	Simvastatin Treated Group
Initial body weight (g)	262±12	277±11
Final body weight(g)	267±15 ↑	260±13↓*
Food intake (g/rat)	19.11±2.65	15.50±3.05↓**
Water intake (ml/one rat)	29.75±4.20	21.18±3.27↓***

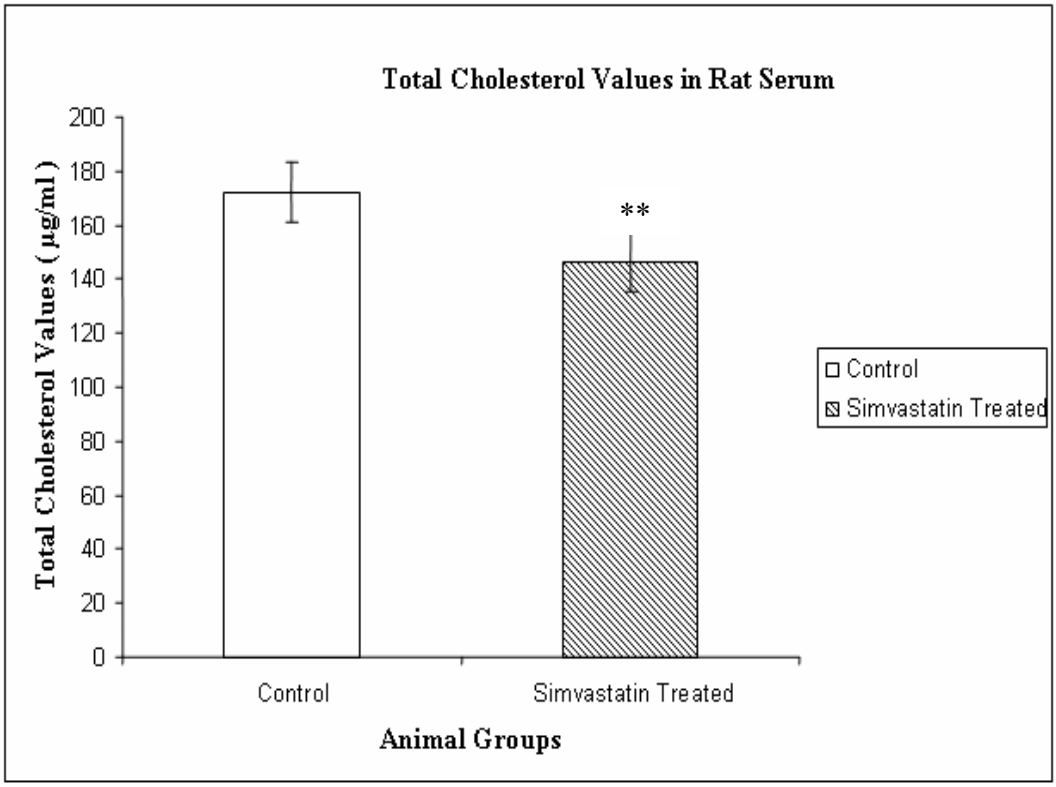

Figure 3.1. Serum total cholesterol values in control and simvastatin treated animals

3.2. Infrared Spectroscopy Studies

3.2.1. General FTIR and ATR-FTIR Spectrum and Band Assignment of Skeletal Muscle Tissue

The present FT-IR study primarily based on the investigation of the structural and compositional variations in macromolecules and lipid fluidity in between simvastatin treated and untreated different rat skeletal muscles, namely, EDL, SOL and DIA. EDL is largely composed of type II fibers whereas SOL muscle largely composed of type I fibers. On the other hand, rat DIA consists of a substantial proportion of type I fibers (Kilarski and Sjostrom, 1990; Ariano *et al.*, 1973; Delp *et al.*, 1996).

Since the positions and intensities of many of the infrared absorption bands can be correlated with the presence of specific groups of atoms in the system studied (Steele, 1971), it is possible to assign specific wavelength molecular absorption bands to specific vibrational modes of particular functional groups. In the present study, the same approach was applied.

Figure 3.2 A and 3.2 B demonstrate the representative infrared spectra of control EDL, SOL and DIA muscles in the region of 3850-850 cm^{-1}. The main bands are labeled in the figures and detailed band assignments are based upon this work and other studies cited in literature are given in Table 3.2 (Rigas *et al.*, 1990; Wong *et al.*, 1991; Takahashi *et al.*, 1991; Wang *et al.*, 1997; Jamin *et al.*, 1998; Melin *et al.*, 2000; Jackson *et al.*, 1998; Lyman *et al.*, 1999; Chiriboga *et al.*, 2000; Çakmak *et al.*, 2003, Banyay *et al.*, 2003; Toyran *et al.,* 2006, Cakmak *et al.*, 2006).

As seen from the figures, there are marked differences in the intensity/area and frequency values of the control groups of EDL, SOL and DIA muscles.

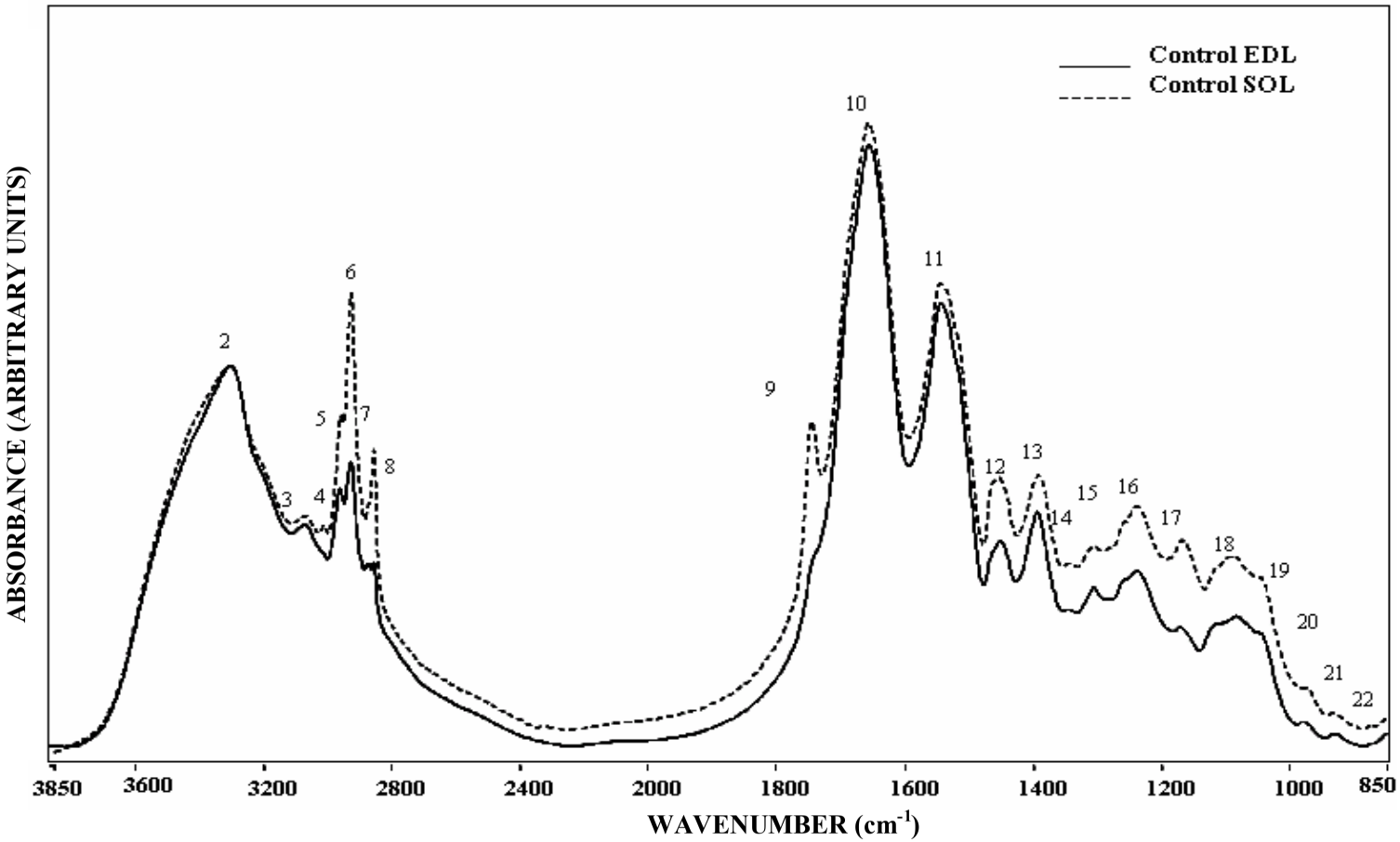

Figure 3.2. A The representative infrared spectra of control groups of EDL and SOL muscles in the 3850-850 cm^{-1} region. (The spectra were normalized with respect to the Amide A band. around 3350 cm^{-1})

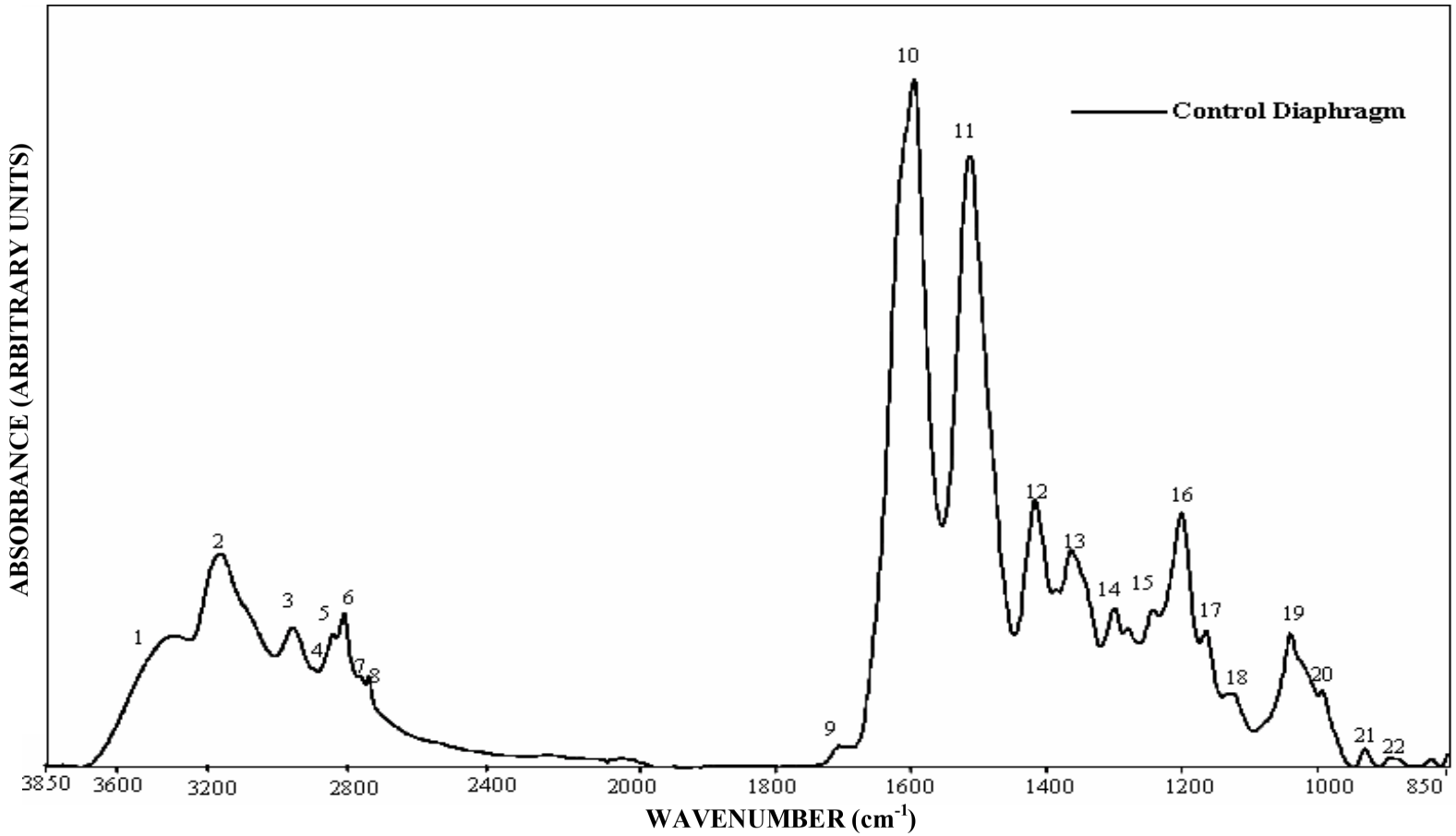

Figure 3.2. B The representative infrared spectrum of control groups of Diaphragm muscle in the 3850-850 cm^{-1} region. (The spectra were normalized with respect to the Amide A band. around 3350 cm^{-1})

Table 3.2. General band assignment of rat skeletal muscle

Peak no.	Wavenumber (cm^{-1})	Definition of the spectral assignment
1	3400	O-H stretching (Amide A), hydrogen-bonded intermolecular OH groups of proteins and glycogen
2	3330-3290	Mainly N-H stretching (Amide A) of proteins with the little contribution from O-H stretching of polysaccharides and intermolecular H bonding
3	3062	C-N and N-H stretching (Amide B) of protein
4	3014	Olefinic=CH stretching vibration: unsaturated lipids, cholesterol esters
5	2962	CH_3 asymmetric stretching: mainly lipids, with the little contribution from proteins, carbohydrates, nucleic acids
6	2929	CH_2 asymmetric stretching: mainly lipids, with the little contribution from proteins, carbohydrates, nucleic acids
7	2874	CH_3 symmetric stretching: mainly proteins, with the little contribution from lipids, carbohydrates, nucleic acids
8	2855	CH_2 symmetric stretching: mainly lipids, with the little contribution from proteins, carbohydrates, nucleic acids
9	1739–1744	Ester C=O stretch: triglycerides, cholesterol esters
10	1656	Amide I (protein C=O stretching)
11	1540	Amide II (protein N-H bend, C-N stretch)
12	1452	CH_2 bending: mainly lipids, with the little contribution from proteins
13	1392	COO^- symmetric stretching: fatty acids
14	1343	Amide III vibrations of collagen
15	1261	PO^-_2 asymmetric stretching, non-hydrogen-bonded: mainly nucleic acids with the little contribution from phospholipids
16	1236	PO^-_2 asymmetric stretching, fully hydrogen-bonded: mainly nucleic acids with the little contribution from phospholipids
17	1170	CO–O–C asymmetric stretching: ester bonds in cholesterol esters and phospholipids
18	1080	PO^-_2 symmetric stretching: nucleic acids and phospholipids C-O stretch: glycogen, polysaccharides, glycolipids
19	1040	C-O stretching: polysaccharides (glycogen)
20	976	$C\text{-}N^+\text{-}C$ stretch: nucleic acids, ribose-phosphate main chain vibrations of RNA
21	929	Z type of DNA
22	876	Vibrations in N-type sugars in nucleic acid backbone

3.2.2 Comparison of Spectra of Skeletal Muscle Fiber Types

3.2.2.1 Comparison of Control and Simvastatin EDL Skeletal Muscle Fiber

Although the FTIR spectral data were collected over the frequency range of 4000-400 cm^{1}, in order to display the details of spectral changes, the analysis was performed in three distinct frequency ranges: 3750-3025 cm^{-1}, 3025-2800 $cm^{-1}$and 1850-850 cm^{-1}. It is seen that the control spectra are almost overlapped with each other. The simvastatin treated spectra are also almost overlapped with each other. For this reason, only one control and simvastatin treated spectra are chosen as a representative spectrum for each group in the the following discussion.

Figure 3.3 and Figure 3.4 show the representative infrared spectra of control and simvastatin treated EDL muscle in 3750-3025 $cm^{-1}$and 3025-2800 cm^{-1} regions, respectively.As it could be seen from these figures control and simvastatin treated spectra noticeably differ in peak positions, peak heights and bandwidths in these regions.

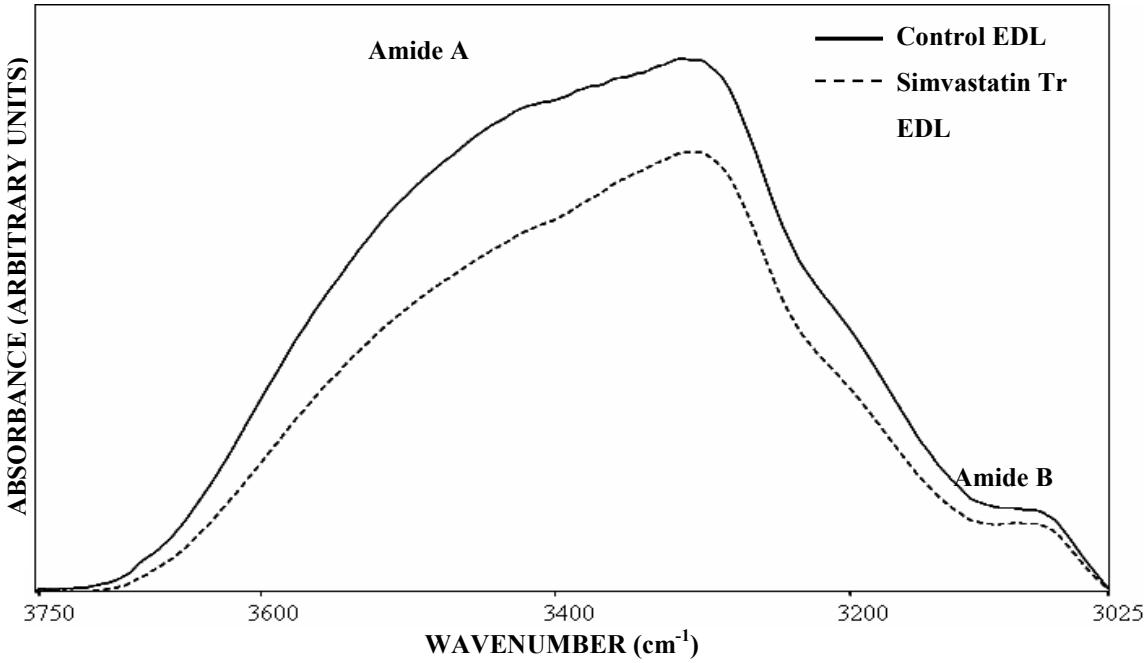

Figure 3.3. The representative infrared spectra of control and simvastatin treated EDL muscles in the 3750-3025 cm^{-1} region (The spectra were normalized with respect to the CH_2 asymmetric stretching mode at 2925 cm^{-1})

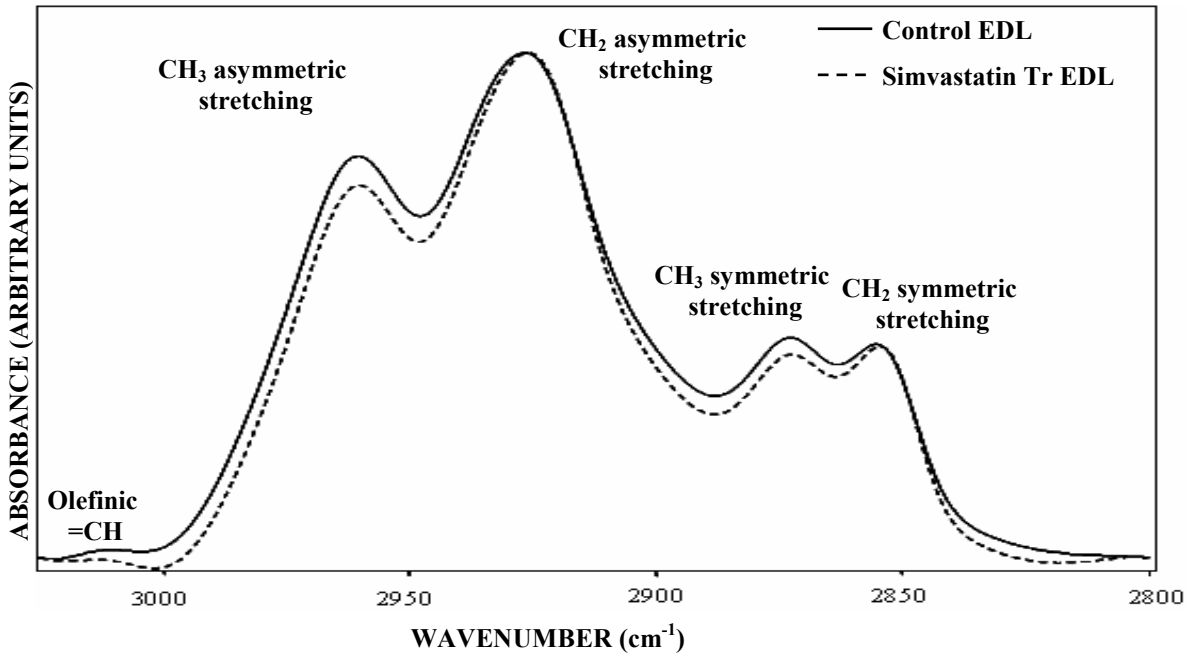

Figure 3.4. The representative infrared spectra of control and simvastatin treated EDL muscles in the 3025-2800 cm^{-1} region (The spectra were normalized with respect to the CH_2 asymmetric stretching mode at 2925 cm^{-1})

Figure 3.5 demonstrates the representative infrared spectra of control and simvastatin treated EDL muscle in 1850-850 cm^{-1} region. As it could be seen from the figure, the control and simvastatin treated spectra represent remarkable differences in bandwidth, intensity and frequency values in this region. These differences between the control and simvastatin treated spectra will be discussed in detail.

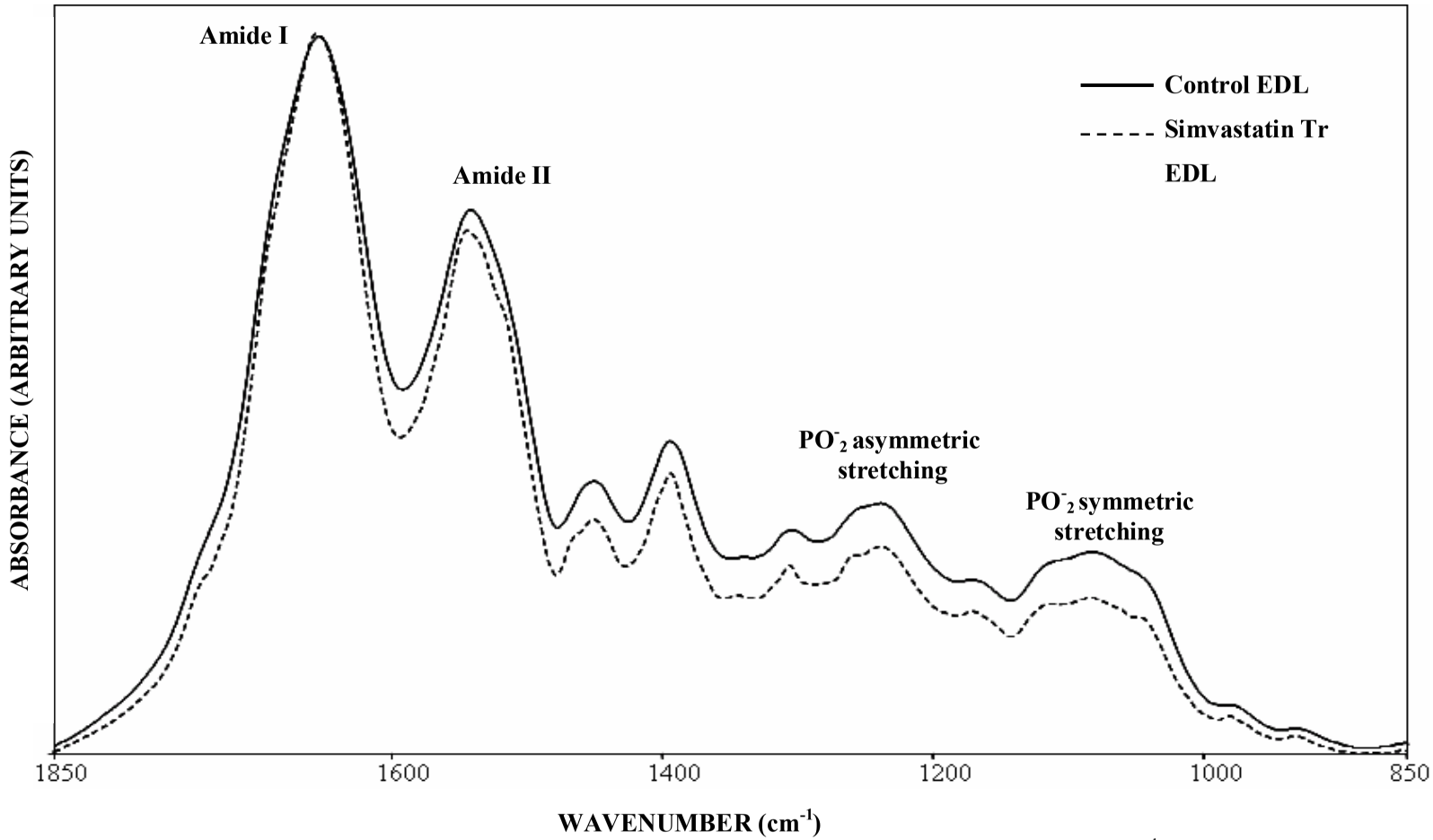

Figure 3.5. The representative infrared spectra of control and simvastatin treated EDL muscles in the 1850-850 cm^{-1} region (The spectra were normalized with respect to the Amide I at 1645 cm^{-1})

Concerning these spectral differences, the control and simvastatin treated EDL muscles were differentiated using cluster analysis with a high accuracy (success rate 7/10 for treated, 8/10 control for tissues). The result is demonstrated in Figure 3.6.

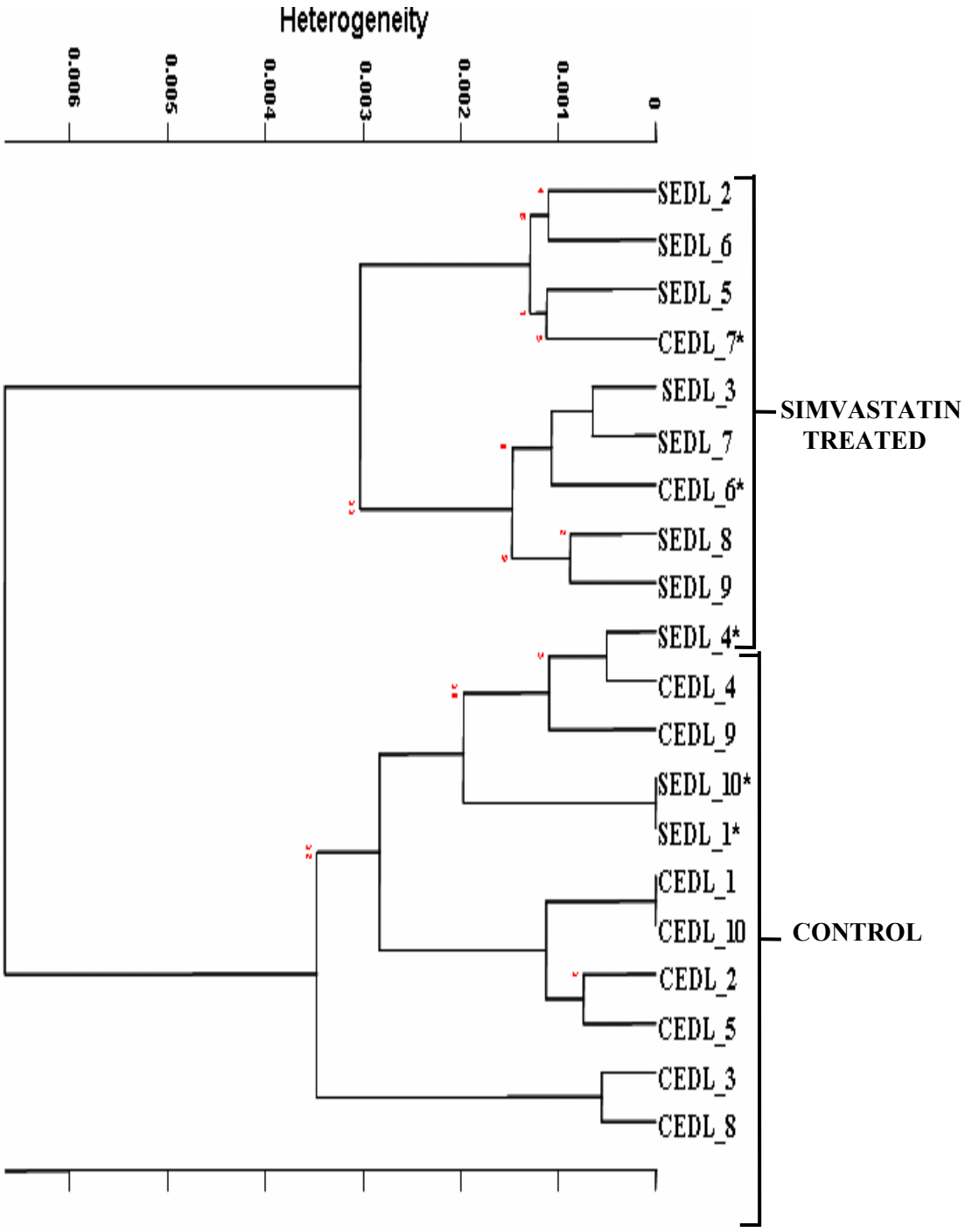

Figure 3.6. Hierarchical clustering of control and simvastatin treated EDL muscles using second derivative spectra (spectral range: 3850-850 cm^{-1}). The sample labeled with * was not clearly differentiated, and not used in statistical analysis.

3.2.2.2 Comparison of Control and Simvastatin Treated DIA Skeletal Muscle

Figure 3.7, Figure 3.8 and Figure 3.9 show the infrared spectra of control and simvastatin treated DIA muscle in 3750-3025 cm^{-1}, 3025-2800 cm^{-1} and 1800-850 cm^{-1} regions, respectively. As it could be seen from these figures, the control and simvastatin treated spectra considerably differ in peak positions, peak heights and widths in all regions. These differences between the control and simvastatin treated samples will be discussed later more specifically. The differences in variables are seemed to be similar to main spectral bands observed in part 3.2.2.1, the spectra of EDL muscle.

Cluster analysis was performed based on second derivative FTIR spectrs to differentiate between the control and simvastatin treated DIA muscles. As seen from the Figure 3.10, the control and simvastatin treated samples are discriminated with a high accuracy (success rate 8/10 for treated, 9/10 for control tissues).

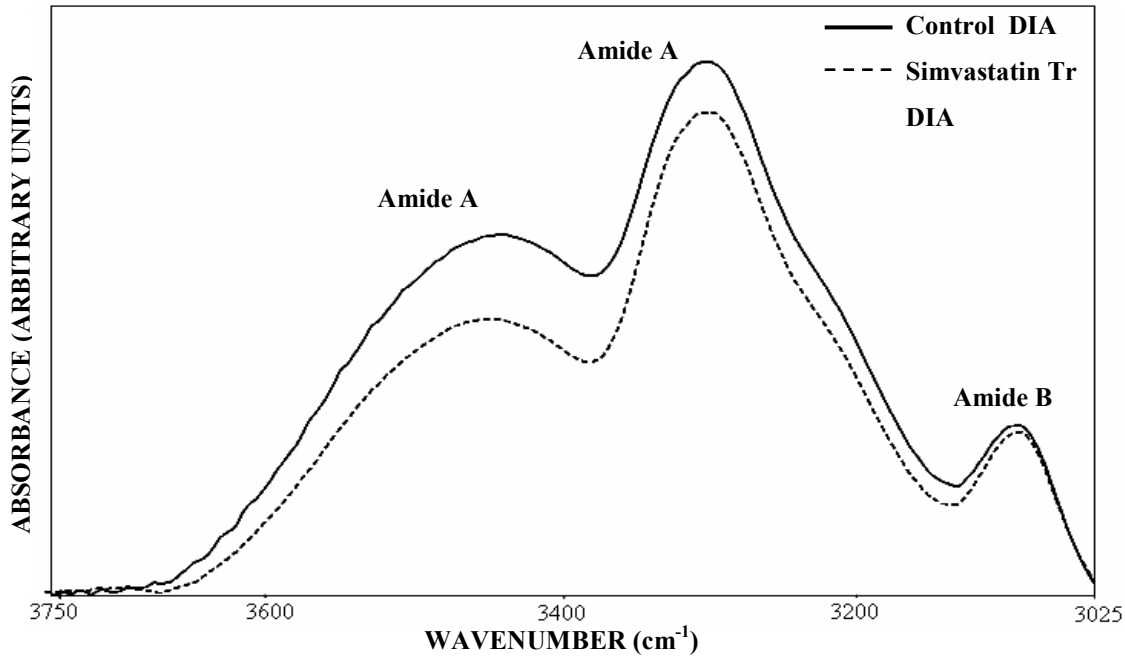

Figure 3.7. The representative infrared spectra of control and simvastatin treated EDL muscles in the 3750-3025 cm $^{-1}$ region (The spectra were normalized with respect to the CH_2 asymmetric stretching mode at 2925 cm^{-1})

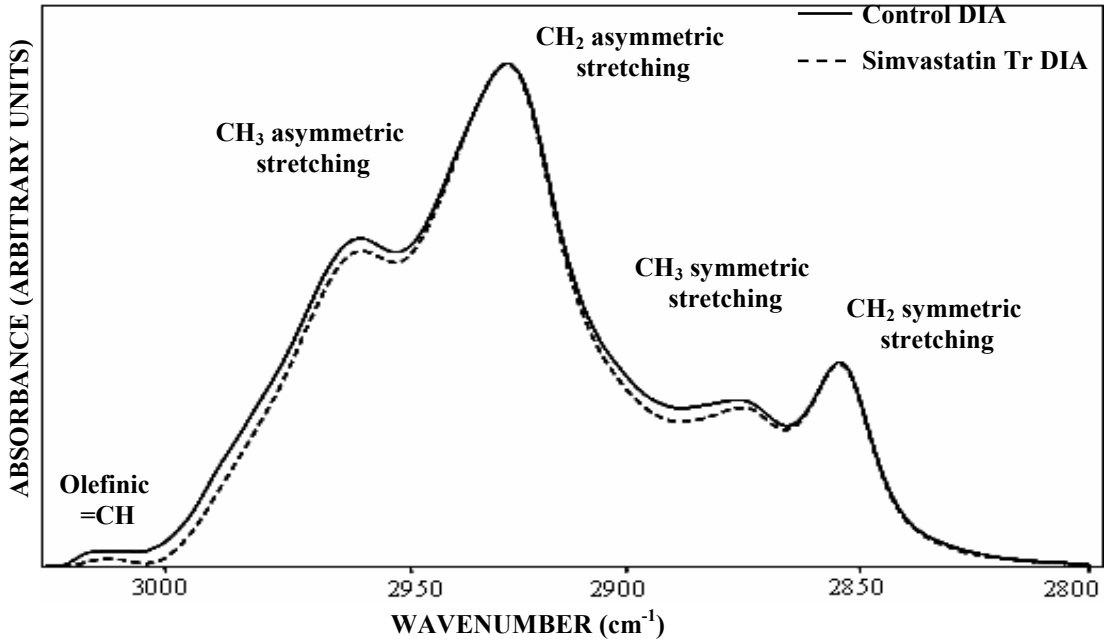

Figure 3.8. The representative infrared spectra of control and simvastatin treated EDL muscles in the 3025-2800 cm $^{-1}$ region (The spectra were normalized with respect to the CH_2 asymmetric stretching mode at 2925 cm^{-1}

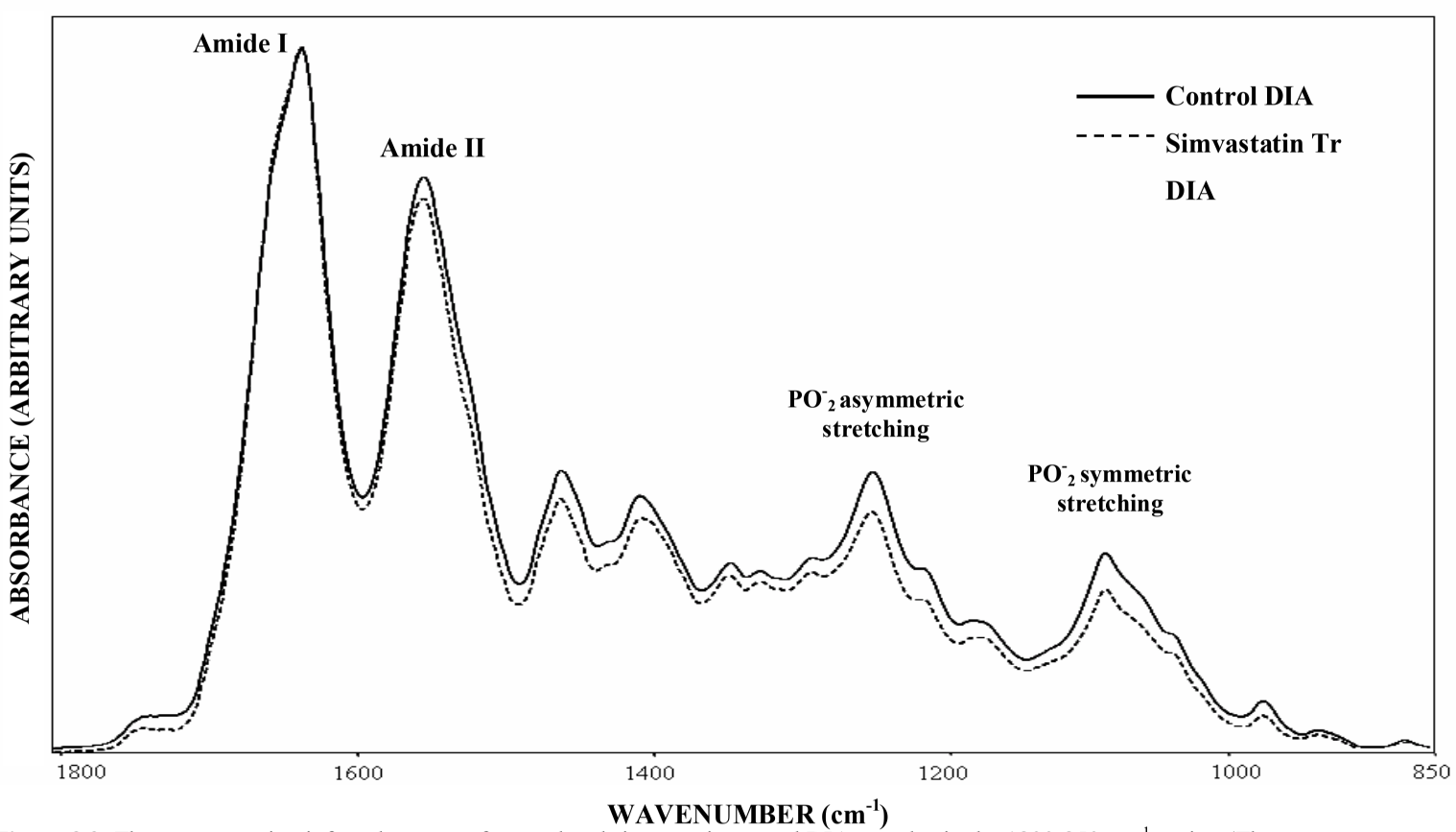

Figure 3.9. The representative infrared spectra of control and simvastatin treated DIA muscles in the 1800-850 cm^{-1} region (The spectra were normalized with respect to the Amide I at 1645 cm^{-1})

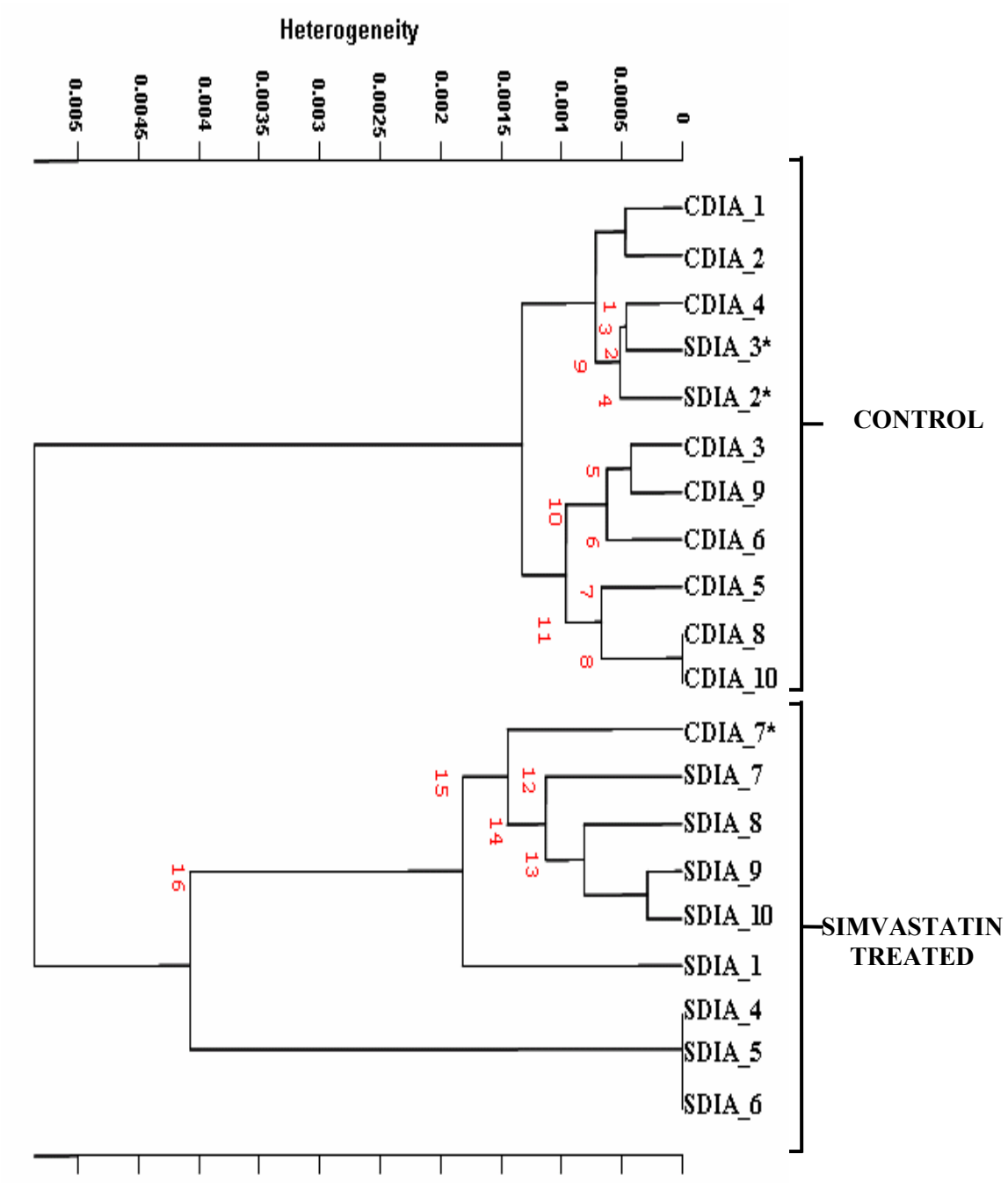

Figure 3.10. Hierarchical clustering of control and simvastatin treated DIA muscles using second derivative spectra (spectral range: 3850-850 cm^{-1}). The sample labeled with * was not clearly differentiated, and not used in statistical analysis.

3.2.2.3 Comparison of Control and Simvastatin Treated SOL Skeletal Muscle

The infrared spectra of control and simvastatin treated SOLmuscle in 3750-3025 cm^{-1}, 3025-2800 cm^{-1} and 1850-850 cm^{-1} regions are shown in Figures 3.11, 3.12 and 3.13 respectively. There are variations in peak positions, peak heights and bandwidths in the three regions which are seen in these figures. These differences between the control and simvastatin treated spectra will be discussed later more specifically. The differences in variables are seemed to be similar to the other skeletal muscles observed in part 3.2.2.1 and part 3.2.2.2, the spectra of EDL and DIA muscles, respectively.

To obviously view these spectral differences, cluster analysis was performed based on the second derivative FTIR spectra to differentiate between the control and simvastatin treated SOL muscles. As seen from the Figure 3.14, the control and treated groups can be differentiated with a high accuracy (success rate 9/10 for treated, 9/10 for control tissues).

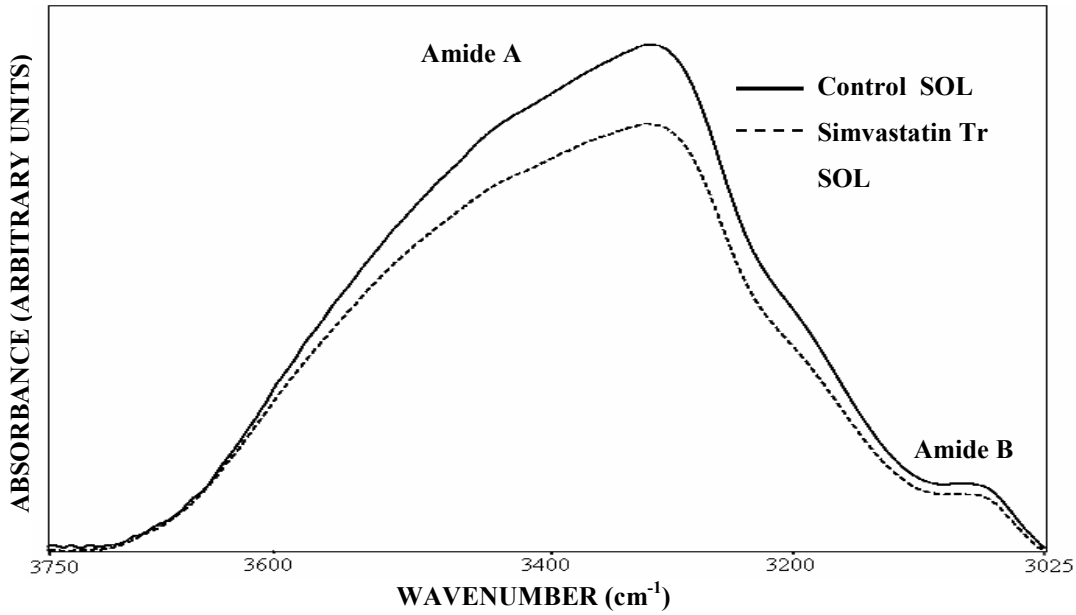

Figure 3.11. The representative infrared spectra of control and simvastatin treated SOL muscles in the 3750-3025 cm^{-1} region (The spectra were normalized with respect to the CH_2 asymmetric stretching mode at 2925 cm^{-1})

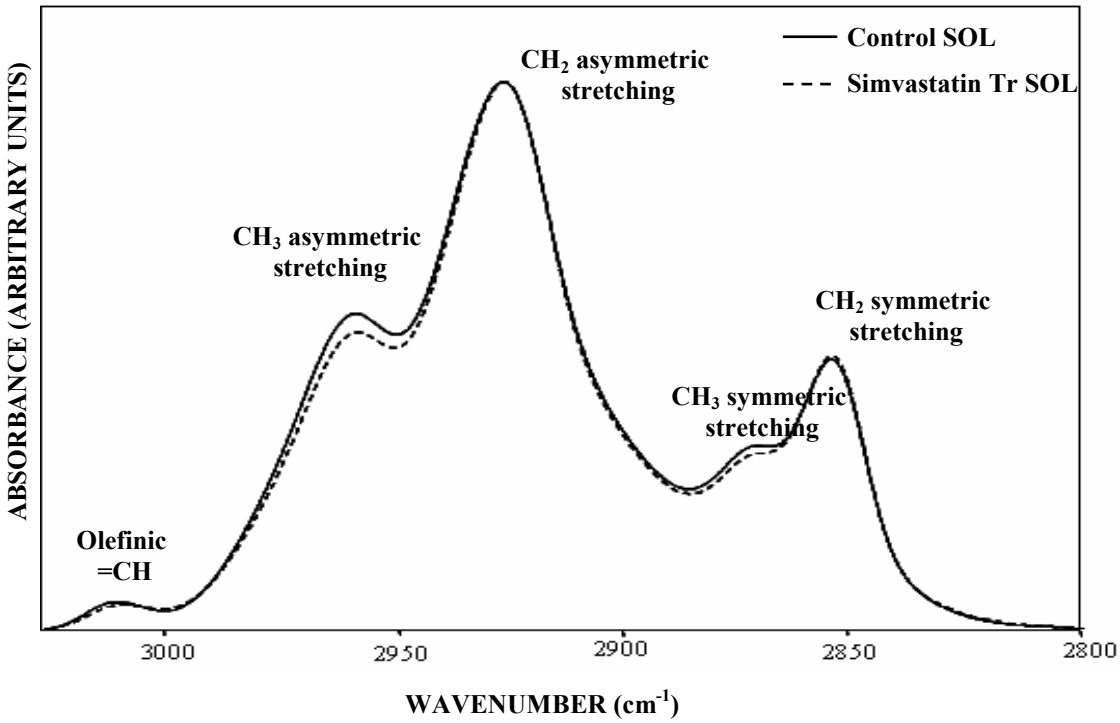

Figure 3.12. The representative infrared spectra of control and simvastatin treated SOL muscles in the 3025-2800 cm^{-1} region (The spectra were normalized with respect to the CH_2 asymmetric stretching mode at 2925 cm^{-1}

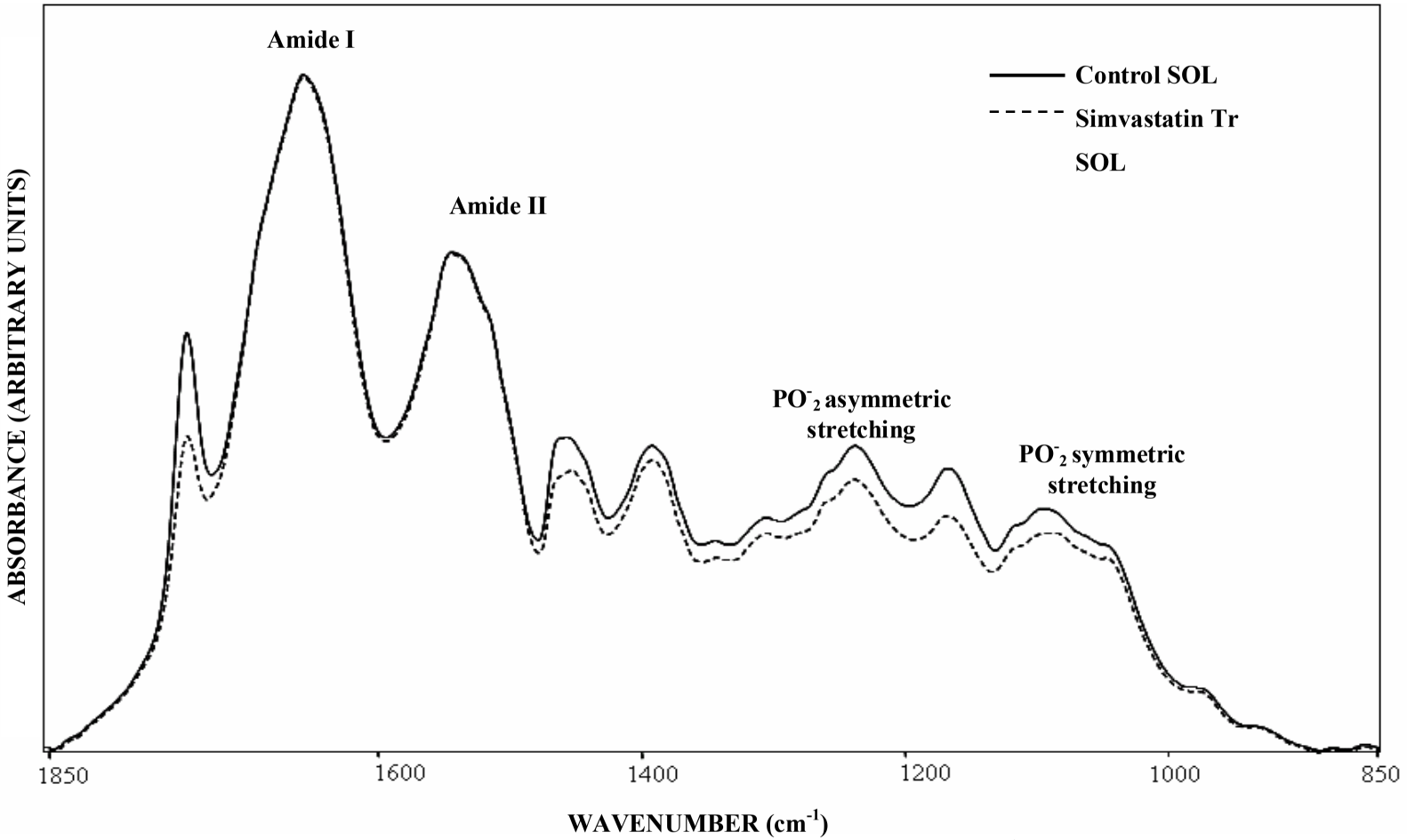

Figure 3.13. The representative infrared spectra of control and simvastatin treated SOL muscles in the 1850-850 cm^{-1} region (The spectra were normalized with respect to the Amide I at 1645 cm^{-1})

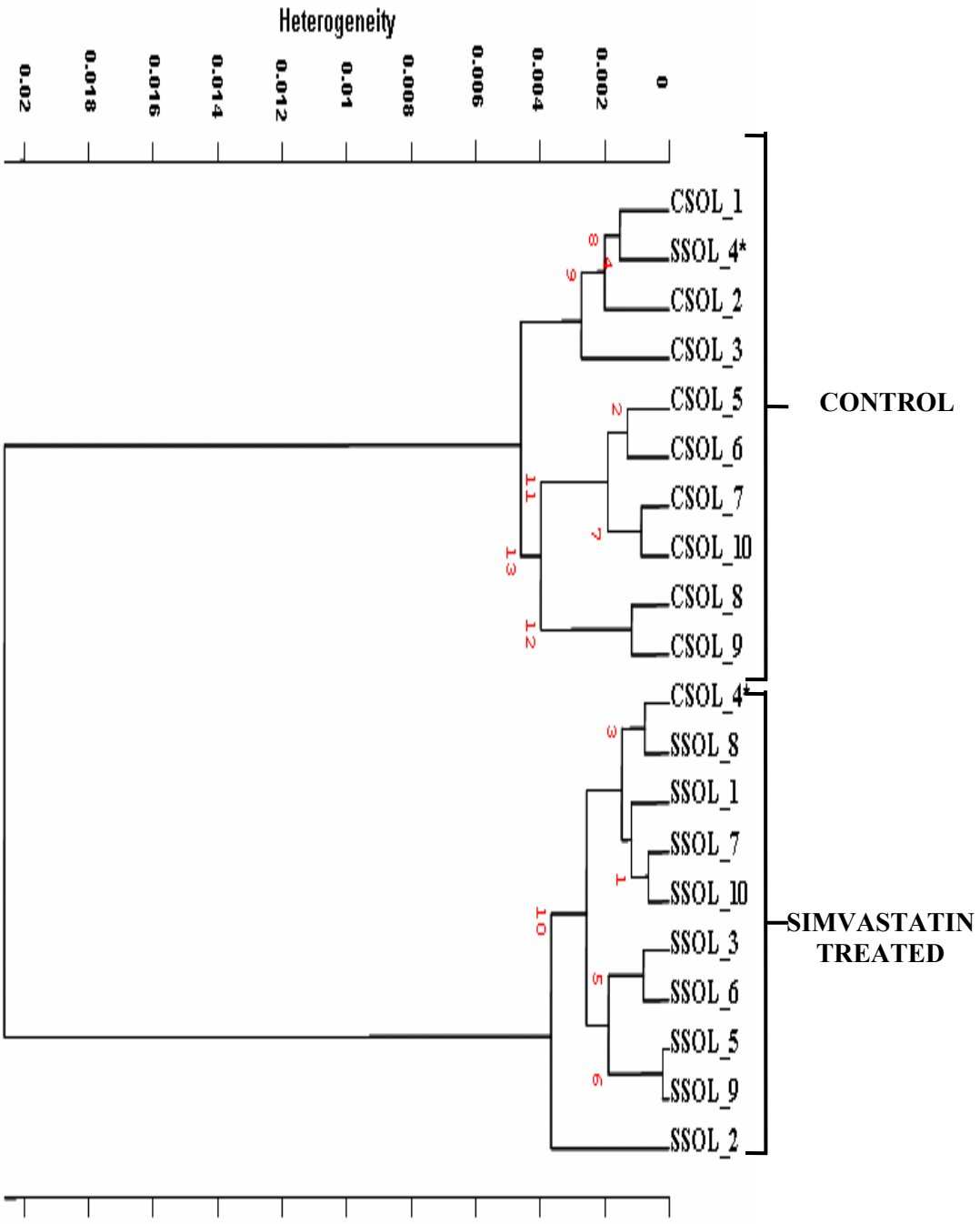

Figure 3.14. Hierarchical clustering of control and simvastatin treated SOL muscles using second derivative spectra (spectral range: 3850-850 cm^{-1}). The sample labeled with * was not clearly differentiated, and not used in statistical analysis.

3.2.3 Numerical Comparisons of the Bands of Control and Simvastatin Treated Spectra of EDL, DIA and SOL Muscles

In order to clarify the possible spectral differences that could be observed between the individuals of even the same group, the means and the standard deviations of the band areas and direction of the shifts with respect to the control were taken into consideration for the control and simvastatin treated groups of EDL, DIA and SOL muscles. Mann-Whitney U-test was applied and the significance values were calculated.

3.2.3.1 Comparisons of Control and Simvastatin Treated Spectra of EDL, DIA and SOL Muscles in the 3750-3025 cm^{-1} Region

Figure 3.3, 3.7 and 3.11 demonstrate the normalized infrared spectra of the control and simvastatin treated EDL, DIA and SOL muscles in the 3750-3025 cm^{-1} region, respectively.The band located between 3370-3330 cm^{-1} (Amide A) contains strong absorptions arising from the N-H and the O-H stretching modes of proteins and polysaccharides intermolecular H bonding. This band was located at 3330 cm^{-1} and 3357 cm^{-1} in the spectrum of EDL and SOL, respectively. On the other hand, amide A appeared as two separated bands (3420 cm^{-1}, 3290 cm^{-1}) in the spectrum of diaphragm. As it can be seen from the figures and Table 3.3, simvastatin–treatment lowered the area value of this band in the three muscle types, but most dramatically for EDL muscle ($p<0.05$*). A more clear representation of the changes in the areas of all types of the muscles is shown in Figure 3.15. The relative weak band located at 3072 cm^{-1} (Amide B) arises from C-N and N-H stretching of protein. A great decrease was also observed in the area of this band for EDL muscle ($p<0.05$*). As it can be seen from Table 3.4, the frequency of Amide A band shifted to a higher values in all muscles but this shifting was and more profound and significant for EDL muscle. The frequency of Amide B also shifted to higher values in simvastatin treated DIA and SOL muscles from 3075.76± 0.78 to

3077.88± 1.15 ($p<0.01$**) and from 3065.72± 0.98 to 3067.31± 1,26 cm^{-1} ($p<0.05$*) respectively. However, in simvastatin treated EDL muscle the frequency of this band shifted to more profoundly the higher values from 3062.60±1.34 to 3071.82± 2.08 cm^{-1} ($p<0.01$**).

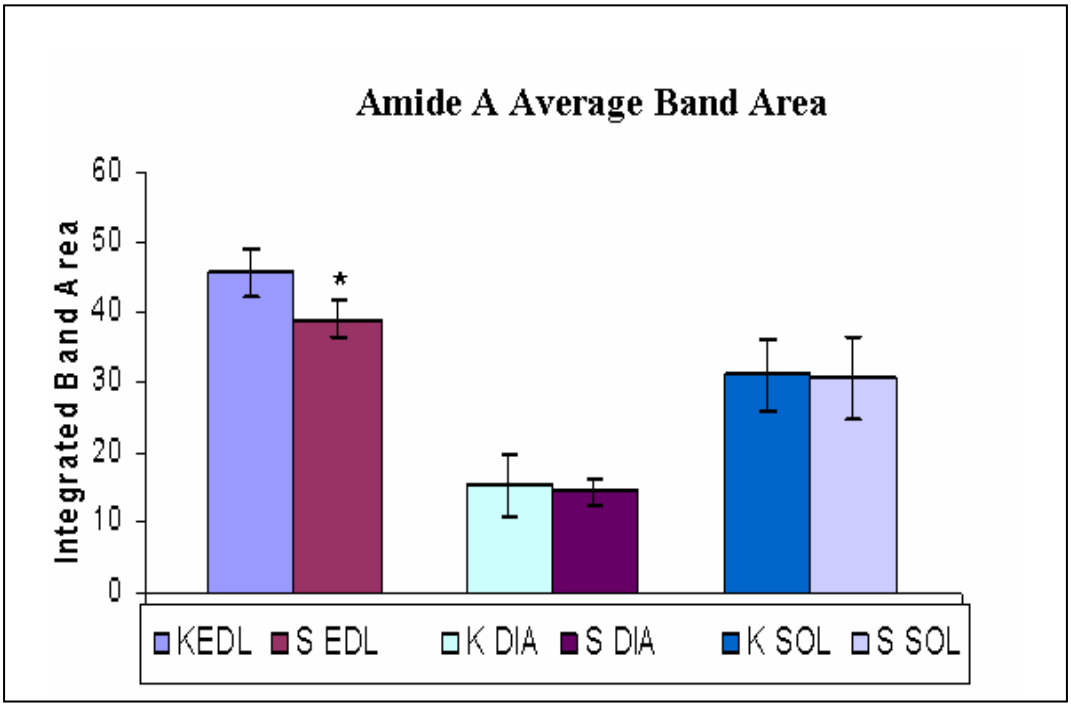

Figure 3.15. Comparison of Amide A area for control and simvastatin treated groups of EDL, DIA and SOL muscles. * shows significance of $p<0.05$.

Table 3.3. The changes in the band area values of the control and simvastatin treated EDL, DIA and SOL spectra in 3750-3025 cm $^{-1}$ region. The values are the mean ± Standart Deviation for each sample. The degree of significance was denoted as $p<0.05$*.

	BAND AREA					
Band No	**Control EDL (n=8)**	**Sim.Tr. EDL (n=7)**	**Control DIA (n=9)**	**Sim.Tr. DIA (n=8)**	**Control SOL (n=9)**	**Sim.Tr. SOL (n=9)**
1			9.50±0.97	8.77± 1.15↓		
2	45.71±3.38↓	39.10± 2.63*↓	15.48± 4.36	14.48± 1.85↓	31.11± 5.05	30.61±5.74↓
3	4.87± 0.81	3.97± 0.47 *↓	4.96± 0.53	4.61± 0.45↓	2.64± 0.51	2.47± 0.79↓

Table 3.4. The changes in the band frequency values of the control and simvastatin treated EDL, DIA and SOL spectra in 3750-3025 cm $^{-1}$ region. The values are the mean ± Standart Deviation for each sample. The degree of significance was denoted as $p<0.05$*, $p<0.01$**.

	BAND FREQUENCY					
Band No	**Control EDL (n=8)**	**Sim.Tr.EDL (n=7)**	**Control DIA (n=9)**	**Sim.Tr. DIA (n=8)**	**Control SOL (n=9)**	**Sim.Tr. SOL (n=9)**
1			3429.55± 3.14	3431.58± 5.56↑		
2	3336.33 ± 8.43	3346.26± 6.77*↑	3290.65± 1.56	3290. 81± 0.89↑	3356.76±14.38	3357.76± 10.73↑
3	3062.60±1.34	3071.82± 2.08 **↑	3075.76± 0.78	3077.88± 1.15**↑	3065.72± 0.98	3067.31± 1,26*↑

3.2.3.2 Comparisons of Control and Simvastatin Treated Spectra of EDL, DIA and SOL Muscles in the 3025-2800 cm^{-1} Region

Figure 3.4, 3.8 and 3.12 show the normalized infrared spectra of control and simvastatin treated EDL, DIA and SOL muscles in 3025-2800 cm^{-1} region, respectively. The band located at 3010 cm^{-1}, which is due to the CH stretching mode of the HC=CH groups, can be used as a measure of unsaturation in the phospholipid acyl chains (Takahaski *et al*., 1991; Melin *et al*., 2000; Liu *et al.*, 2002; Severcan *et al.*, 2005). There was a decrease in the area of this band in all muscle types, and this decrease was more dramatic in EDL muscle ($p<0.01$**)(Table 3.5). A more clear representation of the changes in the areas of all types of the muscles is shown in Figure 3.16. The frequency of this band shifted significantly to a higher value in simvastatin treated EDL muscle from 3010.49 ± 0.69 to 3011.56 ± 0.94 cm^{-1} ($p<0.05$*) (Table 3.6).

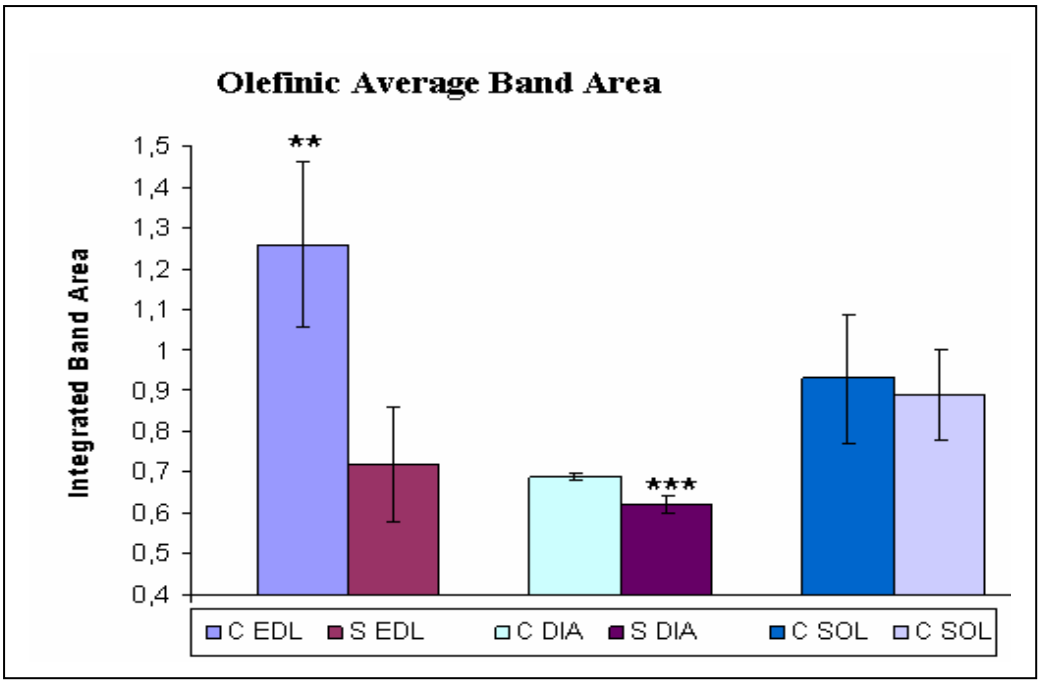

Figure 3.16. Comparison of =CH olefinic band area for control and simvastatin treated groups of EDL, DIA and SOL muscles. ** and *** show significances of $p<0.01$ and $p<0.001$ respectively.

The CH_3 asymmetric (2959 cm^{-1}), the CH_2 asymmetric (2927 cm^{-1}), and the CH_2 symmetric (2857 cm^{-1}) stretching bands originate mainly from lipids, whereas the the CH_3 (2876 cm^{-1}) symmetric stretching band originate mainly from proteins (Table 3.2) (Mantsch, 1984; Severcan *et al*. 1997; Severcan *et al.*, 2000; Severcan *et al.*, 2003, Cakmak *et al.*, 2006).

Table 3.5. The changes in the band area values of the control and simvastatin treated EDL, DIA and SOL spectra in 3025-2800 cm $^{-1}$ region. The values are the mean ± Standart Deviation for each sample. The degree of significance was denoted as $p<0.05$*, $p<0.01$**, $p<0.001$***.

	BAND AREA					
Band No	**Control EDL (n=8)**	**Sim.Tr.EDL (n=7)**	**Control DIA (n=9)**	**Sim.Tr. DIA (n=8)**	**Control SOL (n=9)**	**Sim.Tr. SOL (n=9)**
4	1.26± 0.20	0.72± 0.14**↓	0.69± 0.08	0.62± 0.02***↓	0.93± 0.16	0.89± 0.11↓
5	2.86± 0.47	2.39± 0.25*↓	2.19± 0.18	2.13± 0.07↓	2.21± 0.32	1.92± 0.31*↓
6	3.44 ± 0,22	3.08± 0.28*↓	2.90± 0.25	2.71± 0.10↓	4.15± 0.67	3.98± 0.54↓
7	0.79± 0.13	0.58± 0.11*↓	0.53± 0.05	0.49± 0.19*↓	0.49± 0.06	0.42± 0.03↓
8	0.88± 0.12	0.73± 0.09*↓	0.61± 0.06	0.53± 0.02*↓	1,07± 0.29	0.96± 0.18↓

Table 3.6. The changes in the band area values of the control and simvastatin treated EDL, DIA and SOL spectra in 3025-2800 cm $^{-1}$ region. The values are the mean ± Standart Deviation for each sample. The degree of significance was denoted as $p<0.05$*.

	BAND FREQUENCY					
Band No	**Control EDL (n=8)**	**Sim.Tr.EDL (n=7)**	**Control DIA (n=9)**	**Sim.Tr.DIA (n=8)**	**Control SOL (n=9)**	**Sim.Tr.SOL (n=9)**
4	3010.49 ± 0.69	3011.56± 0.54*↑	3011.32± 0.79	3011.98± 0.41↑	3010.56± 1.34	3010.59± 0.94↑
5	2961.09± 0.57	2960.56± 0.84↓	2958.31± 0.69	2958.26± 1.14 ↓	2958.12± 0.73	2957.89± 1.33↓
6	2927.60± 0.27	2926.82± 0.54*↓	2927.71± 1.27	2927.39± 0.6↓	2925.99± 0.28	2925.89± 0.20↓
7	2873..81± 0.48	2873.35± 0.63↓	2873.78± 0.73	2873.63± 0.60 ↓	2873.55± 0.37	2873.4± 1.76↓
8	2854.68± 0.53	2854.45± 0.28↓	2854.72± 0.62	2854.53± 0.20↓	2854.67± 0.33	2854.49± 0.83↓

In all simvastatin treated groups for different muscle types there was a reduction in the areas of the CH_3 asymmetric and symmetric stretching vibrations but more profoundly for simvastatin treated EDL muscle ($p<0.05$*) (Table 3.5). The frequency of these bands in simvastatin treated groups shifted to lower frequency values for all muscle types. However these changes were insignificant (Table 3.6).

The CH_2 stretching vibrations depend on the degree of conformational disorder; hence they can be used to monitor the average trans/gauche isomerization (order/disorder state of lipids) in the system (Mantsch *et al.*, 1984; Severcan, 1997; Bizeau *et al.*, 2000). An increase in the frequency of the CH_2 stretching means an increase in the number of gauche conformers in the fatty acyl chains (Rana *et al.*, 1990; Schultz *et al.*, 1991; Melin *et al.*, 2000; Cakmak *et al.*, 2003; Cakmak *et al.*, 2006). As seen from Figures 3.4, 3.8 and 3.12, the areas of the CH_2 asymmetric and symmetric stretching vibrations located at 2927 cm^{-1} and 2854 cm^{-1} respectively, decreased in all three types of muscles. This decrease was more profound for EDL muscle in both bands ($p<0.05$*). The frequency of the CH_2 asymmetric stretching band shifted to a lower frequency value in simvastatin treated EDL muscle from 2927.60 ± 0.27 to 2926.82 ± 0.54 cm^{-1}, with a significance value of $p<0.05$*. In simvastatin treated DIA and SOL muscle the frequency of this band shifted slightly to a lower frequency and the changes were insignificant. A more clear representation of the variations in the band frequencies of all types of the muscles is shown in Figure 3.17. The frequency of the CH_2 symmetric stretching band shifted to a lower frequency value in all muscle types insignificantly.

The bandwidth of the CH_2 symmetric modes gives information about the membrane fluidity. As it can be seen from Table 3.7, there was a significant increase in the bandwidth value of this band in all muscle types but more profoundly for EDL muscle ($p<0.01$**).

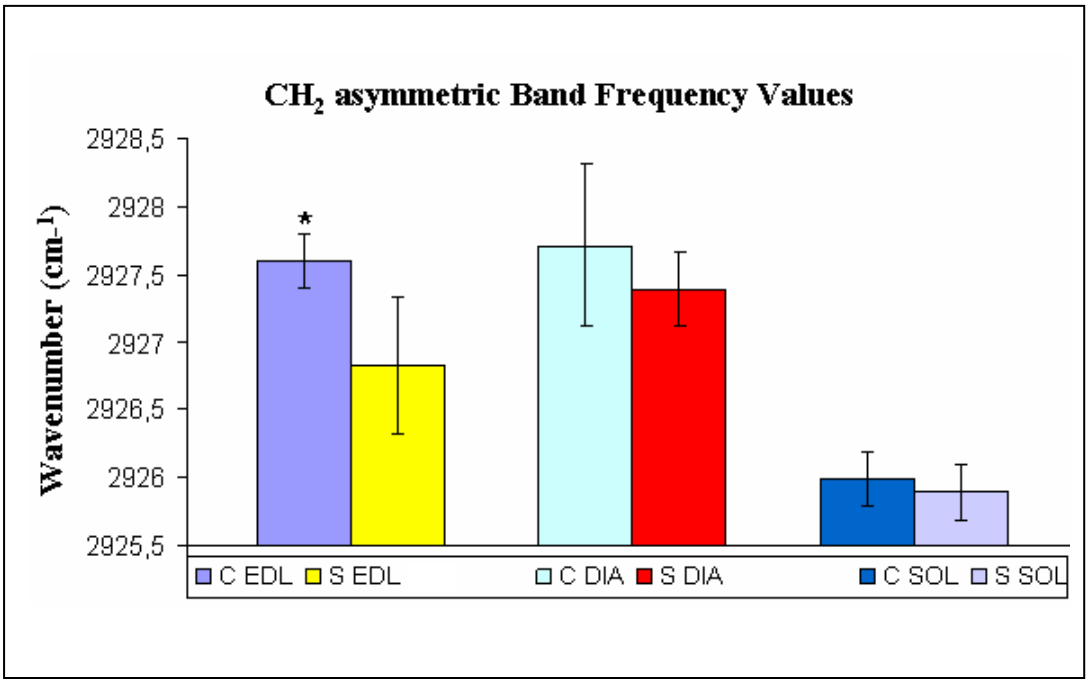

Figure 3.17. Comparison of CH_2 asymmetric band frequency value for control and simvastatin treated groups of EDL, DIA and SOL muscles. * shows significance of $p<0.05$.

The amount of proteins and lipids in the membranes is an important factor affecting the membrane structure and dynamics (Szalontai *et al.*, 2000). From the FTIR spectrum, a precise lipid-to-protein ratio can be derived by taking the ratio of the sum of the areas of the lipid bands namely CH_2 asymmetric and symmetric stretching bands to the area of the CH_3 symmetric stretching band (protein). As it is seen from Table 3.8, an increase in this ratio was observed in the treatment groups which is more profound for EDL muscle ($p< 0.05$*).

Table 3.7. The changes in the bandwidth of the control and simvastatin treated EDL, DIA and SOL spectra. The values are the mean ± Standart Deviation for each sample. The degree of significance was denoted as $p<0.05$*, $p<0.01$**.. The degree of significance was denoted as $p<0.05$*.

	BANDWIDTH					
Band Name	**Control EDL (n=8)**	**Sim.Tr.EDL (n=7)**	**Control DIA (n=9)**	**Sim.Tr DIA (n=8)**	**Control SOL (n=9)**	**Sim.Tr. SOL (n=9)**
CH_2 symmetric	11.34±0.17	11.59 ±0.29**↑	10.30 ±0.1	10.44±0.26*↑	11.78±0.06	11.89±0.10*↑

Table 3.8 The changes in the lipid-to-protein ratio of the bands for control and simvastatin treated EDL, DIA and SOL muscles. The values are the mean ± Standart Deviation for each sample. The degree of significance was denoted as $p<0.05$*.

Ratio of Peak Areas (lipid to protein)	**Control EDL (n=8)**	**Sim.Tr.EDL (n=7)**	**Control DIA (n=9)**	**Sim.Tr DIA (n=8)**	**Control SOL (n=9)**	**Sim.Tr. SOL (n=9)**
CH_2 Asym.strech. + CH_2 Sym. strech./ CH_3 Sym. Strech.	5.57 ± 0.07	6.80 ± 0.17*↑	6.55±0.20	6.69±0.29↑	10.61±0.89	11.65±1.80↑

3.2.3.3 Comparison of Control and Simvastatin Treated Spectra of EDL, DIA and SOL Muscles in the 1850-850 cm^{-1} Region

The 1850-800 cm^{-1} frequency range is called as fingerprint region, includes several bands that originate from the interfacial and head-group modes of the membrane lipids, protein and nucleic acid vibrational modes (Mendelsohn and Mantsch, 1986). Figure 3.5, 3.9 and 3.13 demonstrate the normalized infrared spectra of control and simvastatin treated EDL, DIA and SOL muscles in 1850-850 cm^{-1} region, respectively.

The band centered at 1742 cm^{-1} is mainly assigned to the >C=O ester stretching vibration in phospholipids (Melin *et al.*, 2000; Cakmak *et al.*, 2003; Severcan *et al.*, 2003). As illustrated in the Figure 3.5, 3.9 and 3.13 and Table 3.9, the area of this band decreased in the all simvastatin treated skeletal muscle types. However, this decrease was significant for EDL muscle ($p<0.05$*). A more clear representation of the changes in the areas of all types of muscles is shown in Figure 3.18. In addition, the wavenumber values of this vibration shifted to higher values in three muscle types but more dramatically for EDL muscle ($p < 0.01$**) (Table 3.10).

Table 3.9. The changes in the band area values of the control and simvastatin treated EDL, DIA and SOL spectra in 1850-850 cm $^{-1}$ region. The values are the mean ± Standart Deviation for each sample. The degree of significance was denoted as $p<0.05$*, p<0.01**, p<0.001***.

	BAND AREA					
Band No	**Control EDL (n=8)**	**Sim.Tr.EDL (n=7)**	**Control DIA (n=9)**	**Sim.Tr.DIA (n=8)**	**Control SOL (n=9)**	**Sim.Tr. SOL (n=9)**
9	3,08± 0,35	2.57± 0.27*↓	0.32± 0.07	0.31± 0.06↓	3.38± 0.41	2.73± 0.66↓
10	30,4± 4,88	18.90± 4.57**↓	20.63± 1.76	18.23± 1.27↓	16.32± 2.82	14.68± 4.47↓
11	11,79± 3,46	5.96± 1.46**↓	17.25±0.88	15.94± 0.95*↓	11.26± 1.88	10.56± 2.58↓
12	3,47± 0,42	2.92± 0.28*↓	5.72±0.28	5.07+0.40**↓	3.44± 0.40	3.08± 0.52↓
13	4,93± 0,27	4.36± 0.38*↓	5.38±0.33	4.98+ 0.17***↓	4.27± 0.40	3.81± 0.73↓
14	1,18± 0,14	0.99± 0.12**↓	2.58±0.19	2.37± 0.18↓	1.07± 0.12	1.01± 0.10↓
15	1,43± 0,12	1.11± 0.13**↓	2.22±0.12	1.96± 0.13**↓	1.21± 0.10	1.10± 0.11↓
16	3,88± 0,49	3.15± 0.44*↓	5.93±0.30	5.41± 0.30**↓	3.33± 0.28	3.15± 0.34↓
17	1,59± 0,12	1.53± 0.08↓	2. 10±0.14	2.07± 0.06↓	3.17± 0.35	2.95± 0.26↓
18	2,36± 0,21	1.85± 0.25**↓	4.94±0.29	4.59± 0.12*↓	2.28± 0.07	2.17± 0.08*↓
19	1,62± 0,14	1.31± 0.12*↓	1.54±0.10	1.38± 0.06**↓	1.94± 0.11	1.81± 0.09*↓
20	0,27± 0,05	0.24± 0.06↓	0.44±0.04	0.41±0.03↓	0.41± 0.04	0.39± 0.02↓
21	0,14± 0,02	0.10± 0.03*↓	0.20±0.01	0.17± 0.01*↓	0.11± 0.01	0.10± 0.01↓
22	0,09± 0,01	0.02± 0.05*↓	0.06±0.01	0.04± 0.01↓	0.01± 0.00	0.01± 0.00↓

Table 3.10. The changes in the band frequency values of the control and simvastatin treated EDL, DIA and SOL spectra in 1850-850 cm $^{-1}$ region. The values are the mean ± Standart Deviation for each sample. The degree of significance was denoted as $p<0.05$*, $p<0.01$**.

	BAND FREQUENCY					
Band No	**Control EDL (n=8)**	**Sim.Tr.EDL (n=7)**	**Control DIA (n=9)**	**Sim.Tr.DIA (n=8)**	**Control SOL (n=9)**	**Sim.Tr. SOL (n=9)**
9	1742.94± 0.46	1746.41± 0.92 **↑	1742.60± 1.77	1743.26± 1.43 ↑	1744.28±1.30	1745.34± 1.11↑
10	1655.13± 0.52	1656.40± 0.58 **↑	1636.32± 1.25	1637.26± 1.01↑	1656.77± 1.11	1657.20± 0.63↑
11	1541.38± 0.31	1542.24± 0.47 **↑	1548.52± 0.63	1549.15± 0.69↑	1540.75± 0.93	1541.25± 0.60↑
12	1451.72± 0.68	1452.86± 0.55*↑	1453.66± 0.61	1453.49± 0.55↓	1455.79±1.05	1455.27± 1.42↓
13	1393.87± 1.03	1394.49± 0.45↑	1400.22± 2.07	1398.56± 2.05↓	1393.11± 1.79	1392.66±1.24↓
14	1344.21± 0.48	1344.32± 0.49↑	1337.78± 0.44	1338.11± 0.50↑	1343.85± 0.5	1344.03± 1.07↑
15	1260.39± 0.97	1263.44± 2.44 *↑	1282.57± 1.65	1281.84± 1.25↓	1261.82± 0.86	1260.77± 1.00↓
16	1238.61± 0.36	1239.03± 0.26*↑	1240.57± 1.62	1240.41± 0.81↓	1238.69± 0.21	1238.46± 1.58↓
17	1171.21± 0.62	1170.57± 0.29↓	1163.10± 1.04	1166.06± 2.80↑	1168.41± 1.90	1169.58± 1.75↑
18	1082.77± 0.44	1085.15± 2.10*↑	1080.55± 0.37	1079.31± 0.65**↓	1088.76± 4.43	1086.84± 2.61↓
19	1044.41±0.49	1045.23± 0,70*↑	1034.2± 0.43	1034.042± 0.59↓	1045.41± 0.70	1043.45±1.05↓
20	977.31±0.96	979.04± 2.17*↑	972.35± 1.04	972.21± 0.36↓	975.60± 1.70	972.17± 3.01↓
21	930.11±0.80	931.24± 0.74*↑	934.85± 0.95	933.60± 1.98↓	929.26± 1.48	927.60± 3.47↓
22	874.67±0.43	875.41± 0.23**↑	876.19± 0.90	875.25± 0.64↓	874.49± 0.59	874.26± 1.25↓

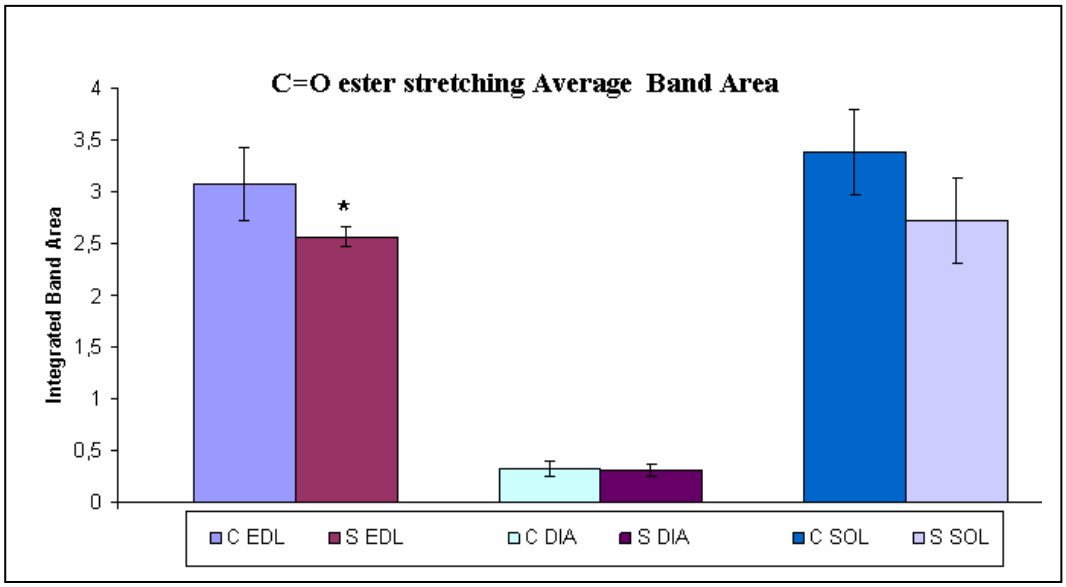

Figure 3.18. Comparison of C=O Ester stretching band area value for control and simvastatin treated groups of EDL, DIA and SOL muscles. * shows significance of $p<0.05$.

The bands at 1656 and 1540 cm^{-1} are attributed to the amide I and II vibrations of structural proteins, respectively. The band centered at 1656 cm^{-1} (amide I) corresponds to the C=O stretching and the C-N stretching (% 60) vibrational modes weakly coupled with the N-H bending (% 40) of the polypeptide and protein backbone. The Amide I band was located at 1656 cm^{-1} for EDL and SOL muscles while it was located at 1636 cm^{-1} for DIA muscle. The band located at 1540 cm^{-1} (amide II) is assigned to the N-H bending (% 60) and the C-N stretching (% 40) modes of proteins (Melin *et al.*, 2000; Takahashi *et al.*, 1991; Wong *et al.*, 1991; Haris and Severcan, 1999; Çakmak *et al.*, 2003). This band was located at 1540 cm^{-1} for EDL and SOL muscles whereas it was placed at 1548 cm^{-1} for DIA muscle. The band areas of amide I and amide II bands decreased in the all simvastatin treated muscle types but more dramatically for EDL muscle ($p<0.01$**). For example, for EDL muscles the Amide I and Amide II band decreased as 38 % and 49.5 %, respectively which can be clearly in Figures 3.19 and 3.20.

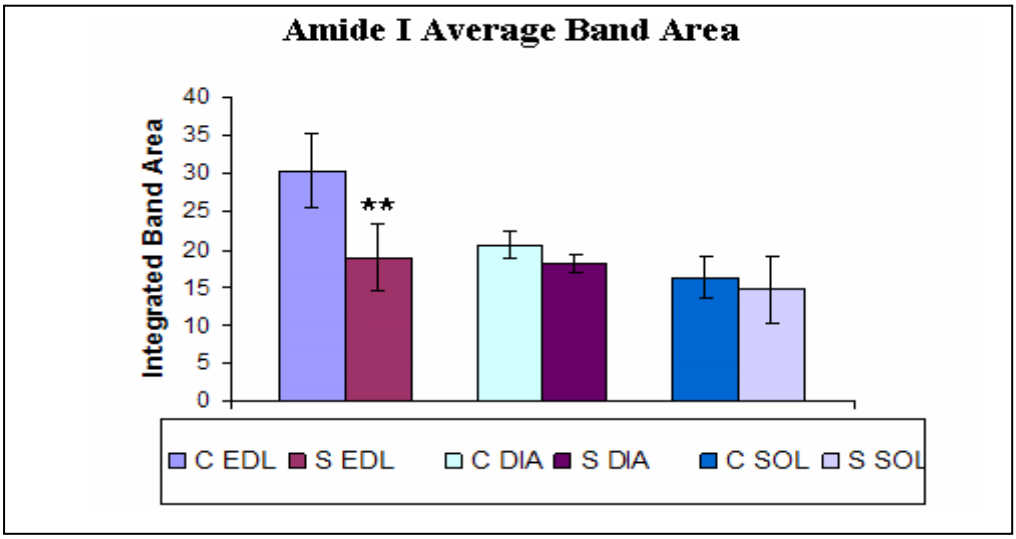

Figure 3.19. Comparison of Amide I band area value for control and simvastatin treated groups of EDL, DIA and SOL muscles. **shows significance of $p<0.01$.

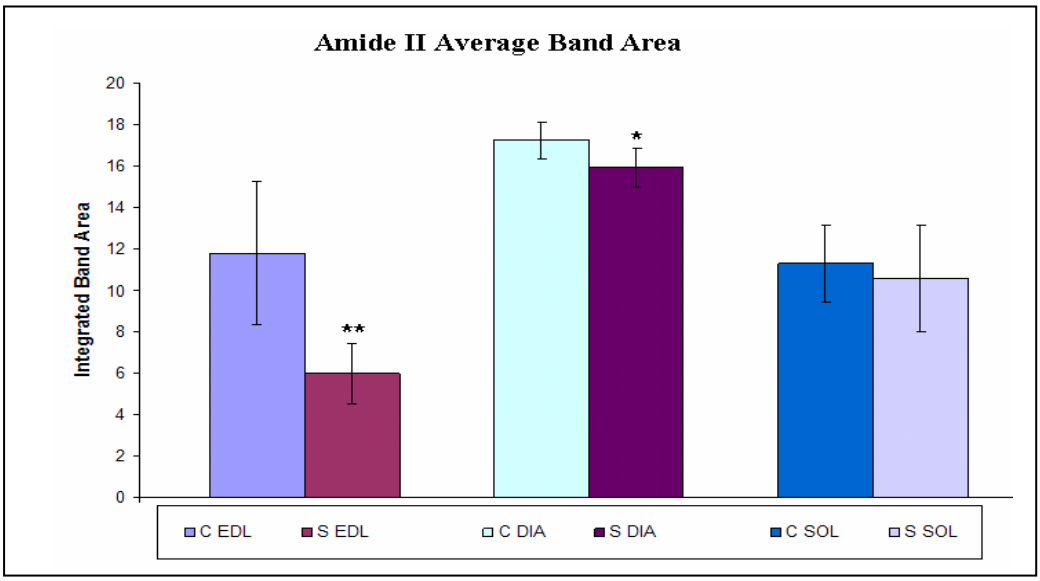

Figure 3.20. Comparison of Amide II band area value for control and simvastatin treated groups of EDL, DIA and SOL muscles. ** and * show significances of $p<0.01$ and $p<0.05$ respectively.

The shifts in the frequencies of amide I and amide II band to higher values were observed for all simvastatin treated muscle types but more significantly for EDL muscle ($p<0.01$**). For Amide I band, this shift was from 1655.13± 0.52 to 1656.40± 0.58 cm^{-1} in EDL ($p<0.01$**) while this shift was insignificant in DIA and in SOL. For Amide II band, the shift was from 1541.38± 0.31 to 1542.24± 0.47 cm^{-1} in EDL ($p<0.01$**) while this shift was found to be insignificant in DIA and in SOL.

As it can be seen from Figures 3.5, 3.9, 3.13 and Table 3.11, there was a decrease in the bandwidth of amide I band for all simvastatin treated muscles but this change is more profound for EDL muscle ($p<0.05$*).

Table 3.11. The changes in the bandwidth values of the control and simvastatin treated EDL, DIA and SOL spectra. The values are the mean ± Standart Deviation for each sample. The degree of significance was denoted as $p<0.05$*.

	BANDWIDTH					
Band Name	**Control EDL (n=8)**	**Sim.Tr.EDL (n=7)**	**Control DIA (n=9)**	**Sim.Tr. DIA (n=8)**	**Control SOL (n=9)**	**Sim.Tr. SOL (n=9)**
Amide I	26.46±0.91	25,43±3.03 *↓	21.64±1.79	21.45±1.15↓	29.9±2.8	28.49±2.40↓

The intense band at 1452 cm^{-1} is assigned to CH_2 bending mode of protein and lipids. A decrease in the area (Manoharan *et al.*, 1993; Cakmak *et al.*, 2003) of this band was observed for all simvastatin treated groups but more profoundly for EDL muscle ($p<0.05$*). As seen from Table 3.9, the frequency of this vibration significantly shifted to higher values in EDL muscle ($p<0.05$*), while it was shifted to lower values in the other muscle types.

A decrease in the area of the band at 1392 cm^{-1} which is due to the COO^- symmetric stretching vibration of amino acid side chains and fatty acids (Jackson *et al.*, 1998; Çakmak *et al.*, 2003; Cakmak *et al.*, 2006) was observed

for all the treatment muscles, which was more obvious for EDL muscle ($p<0.05$*).

The absorption bands of collagen are seen in a broad range in the spectrum. The main bands of collagen arise from peptide bond vibrations detected in amide A, I, II and III bands (Camacho *et al.*, 2001). The amide III vibrations of collagen are seen in the spectral range between 1355 and 1167 cm^{-1} (Gough *et al.*, 2003). The band located at 1343 cm^{-1} falls into this region of the Amide III vibrations, more specifically originates from the C-N and the C-C stretching and the N-H bending vibrations of collagen (Camacho *et al.*, 2001, Gough *et al.*, 2003; West *et al.*, 2004). As it can be seen from Table 3.9, the area of this band located at 1343 cm^{-1} decreased in all the three types of muscles but more profoundly for EDL muscle ($p<0.01$*).

In the 1280-900 cm^{-1} frequency range, several macromolecules (e.g. polysaccharides and phosphate composing of macromolecules such as phospholipids and nucleic acids) give absorption bands (Melin *et al.*, 2000; Cakmak *et al.*, 2003). The relatively strong bands at 1261, 1236 cm^{-1} are mainly due to the asymmetric and the band of 1080 cm^{-1} is due to symmetric stretching modes of phosphodiester groups, which monitors the P=O bond present in the phosphate moieties (PO_2^-) of nucleic acid backbone structures and phospholipids (Wong *et al.*, 1991; Wang *et al.*, 1997; Diem *et al*, 1999; Cakmak *et al.*, 2003). The band located at 1260 cm^{-1} is due to non-hydrogen-bonded PO_2^- groups and the band located at 1238 cm^{-1} is due to more hydrogen-bonded PO_2^- groups (Rigas *et al.*, 1990; Wong *et al.*, 1991). There was a decrease in the area of 1261 cm^{-1} band in all treated muscles but more profoundly for EDL. This decrease was significant for EDL ($p<0.01$**) and DIA ($p<0.01$**) while insignificant for SOL. In addition, a decrease in the area of 1238 cm^{-1} band in treated muscles was observed which was more profound for EDL muscle ($p<0.05$*). The frequencies of these two bands shifted significantly to higher values in EDL muscles ($p<0.05$*) as it shifted to lower

values in DIA and SOL muscles.

The PO_2 symmetric stretching band is generally assigned at 1080 cm^{-1} (Lyman *et al.*, 2001; Banyay *et al.*, 2003). As seen from Table 3.9, a significant reduction in the area of this band was observed in all muscle types but more significantly for EDL muscle ($p<0.05$*). Furthermore, although a significant shift to higher values in the frequency of this band was observed in EDL muscle ($p<0.05$*), this shifting occurred to lower values for DIA ($p<0.01$**) and SOL.

The DNA to protein ratio calculated by the ratio of the area of the PO_2 symmetric stretching band to the area of the amide II band was given in Table 3.12. As seen from the table, there was an increase in this ratio in all muscle types, more intensely for EDL muscle ($p<0.05$*).

Table 3.12. The variations in the DNA to protein ratio of the control and simvastatin treated EDL, SOL and DIA muscles. The values are the mean ± Standart Deviation for each sample. The degree of significance was denoted as $p<0.05$*.

Ratio of Peak Areas (DNA to protein)	**Control EDL (n=8)**	**Sim.Tr.EDL (n=.7)**	**Control DIA (n=9)**	**Sim.Tr. DIA (n=8)**	**Control SOL (n=9)**	**Sim.Tr. SOL (n=9)**
PO_2 sym./ Amide II	0.21±0.07	0.32±0.07*↑	0.287±0.01	0.289±0.01↑	0.20±0.03	0.21±0.05↑

The area of the band at 1170 cm^{-1} which is due to asymmetric stretching mode of the CO-O-C groups arising from ester bonds in cholesterol esters and phospholipids decreased for all muscle types but more profoundly for EDL muscle (Jackson *et al.,* 1998, Toyran *et al*.,2007) (Table 3.9). The frequency of this band shifted to lower values in EDL muscle whereas it shifted to higher values for other muscles (Table 3.10).

The band at 1044 cm^{-1} is mainly assigned to the C-O stretching vibrations of polysaccharides especially glycogen. As seen from Figure 3.5, 3.9, 3.13 and Table 3.9, a decrease in the areas of this band was observed which was more dramatic in EDL muscle ($p<0.05$*). A more clear representation of the change in areas of all types of muscles is shown in Figure 3.21 (Melin *et al.*, 2000; Toyran *et al.*, 2006; Lyman and Murray-Wavelet, 1999).

The band centered at 976 cm^{-1} is generally assigned to symmetric stretching mode of dianionic phosphate monoester of cellular nucleic acids (Ci *et al.*, 1999; Chiriboga *et al.*, 2000; Cakmak *et al.*, 2003) and ribose-phosphate main chain vibrations of the RNA backbone (Banyay *et al.*, 2003, Tsuboi *et al.*, 1969). There was a decrease in the area of this band in each treated muscle which was more dramatic for EDL. A shift to higher values in the frequency of this band was only observed in EDL muscle ($p<0.05$*) however, it was shifted to lower values for the other muscles.

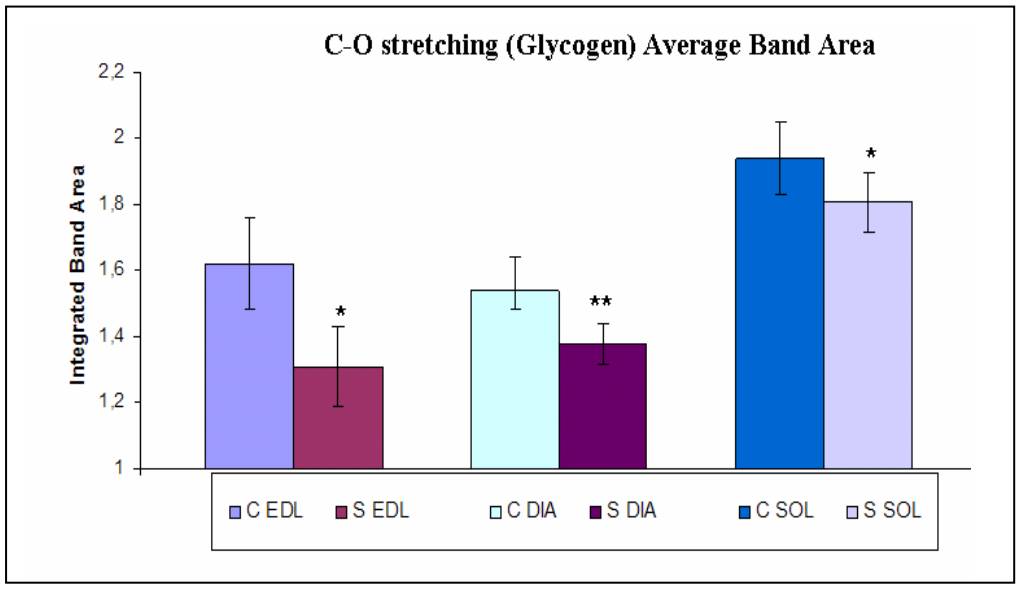

Figure 3.21. Comparison of C=O stretching band area value for control and simvastatin treated groups of EDL, DIA and SOL muscles. * and ** show significances of $p<0.05$ and $p<0.01$ respectively.

The band centered at 929 cm^{-1} arises from Z type of DNA (Banyay *et al*., 2003). A significant decrease in the area of this band was observed for both EDL and diaphragm muscle ($p<0.05$*). However this decrease was more profound for EDL. This decrease was found to be insignificant for SOL. In addition, the frequency of this band significantly shifted to higher values for EDL ($p<0.05$*).

The band centered at 873 cm^{-1} originates from the vibrations of N-type sugars in the sugar phosphate backbone of nucleic acids (Banyay *et al.*, 2003, Taillandier and Liquier, 1992). A decrease in the area of this band was observed for all muscles but more significantly for EDL muscle ($p<0.05$*). The frequency of this band shifted from 874.67±0.43 to 875.41± 0.23 ($p<0.01$**) in the frequency of this band was found in the EDL muscle.

CHAPTER 4

DISCUSSION

In the current study, we for the first time investigated and compared the effects of simvastatin on structure and functions of macromolecules in three types of skeletal muscle tissues, namely EDL, DIA and SOL. Statins are the largest class of drugs on the market and they widely used in the treatment of hypercholesterolemia due to the higher efficacy. Skeletal muscle accounts for around 45 % of the total body weight and has a high metabolic rate and blood flow. As a consequence, it is highly exposed to drugs within the circulation. Therefore, it may be primarily and greatly affected from statins. Skeletal muscle is composed of different fiber types. Rat SOL muscle is largely composed of type I fibers (84% type I, 16% type IIa, 0% type IIb) having a characteristic of slow-contracting oxidative muscle whereas Rat EDL is largely composed of type II fibers (3% type I, 57% type IIa, 40% type IIb) having a fast-contracting glycolytic characteristic. On the other hand, rat diaphragm consists of a substantial proportion of type I fibers (42-39 % Type I, 24-25 % type IIa, 33-34 % type IIb) (Kilarski and Sjöström, 1990; Ariano *et al.*, 1973, Delp *et al.*, 1996, Kanbara *et al*., 1997).

EDL muscle is composed of fast twitch glycolytic fibers and utilizes glucose as energy source. Decreased food consumption may induce a reduction in the amount of glycogen, which is a glucose source. This decrease in glycogen level stimulates muscle fibers to use fatty acids for energy production (Smith *et al*., 1991). Statin treatment leads to a decrease in the level of fatty acids. Due to the decrease in the levels of energy sources in skeletal muscle, the EDL muscle can not contract properly. Therefore EDL muscle is affected firstly and profoundly from statin treatment.

The amide A band located between 3370-3330 cm^{-1} arising from the N-H and the O-H stretching modes of H_2O, proteins and glycogen. Since water was largely removed during sample preparation for FT-IR spectroscopy, its contribution to this band can be neglected, and therefore; the contribution can be considered to be only due to proteins and glycogen. The intensity and more accurately band area gives information about the concentration of related functional groups (Freifelder, 1982; Toyran *et al*., 2004; Toyran *et al*., 2006; Cakmak 2006). The reduction in the area of this band, which is the more profound in EDL muscle ($p<0.05$), suggests a decrease in the protein and glycogen content in simvastatin treatment. This reduction could have been resulted from the lack of the contribution from glycogen OH absorption (Melin *et al*., 2000, Cakmak *et al*., 2006). This decrease is as same as in the area of the band located at 1044 cm^{-1} (Lyman *et al.*, 1999; Rigas *et al.*, 1990; Cakmak *et al.*, 2003, Cakmak *et al*., 2006). By histological staining method, Smith *et al* (1991) also showed a decrease in the glycogen level of type II fibers (EDL muscle) as result of statin treatment, which further support our findings.

As it can be seen from Figures 3.4 , 3.8 and 3.12, the C-H region (3050-2800 cm^{-1}) is populated by absorptions arising from the vibrations of olefinic=CH, -CH_2 and -CH_3 groups, most of which originate from lipids (Severcan *et al*., 2000; Severcan *et al*., 2003, Cakmak *et al*., 2006). The area of the CH_3, the CH_2 asymmetric and the CH_2 symmetric stretching bands which are all due to lipid acyl chains, decreased in all three muscles, however, the most profoundly in EDL muscle($p<0.05$). This suggests a reduction in the amount of lipids and a change in the composition of the acyl chains. This result was also supported by the decrease in the area of the CH_2 bending (mainly lipids) at 1452 cm^{-1} and the COO^- symmetric stretching (fatty acids) at 1392 cm^{-1} (Severcan *et al*., 2000; Severcan *et al*., 2003). This prevalent decrease in lipid content may be due to an increase in skeletal muscle lipolysis or utilization of lipid sources because of statin treatment. Sato *et al*. (1991) have found that the activity of lipoprotein lipase increased in statin treated rat thigh muscle. The increase in

the activity of this enzyme shows an increase in the utilization of lipids as an energy source which might imply decrease in the area of lipid bands. On the other hand, by histological staining method, it has been shown that extensive lipid-filled vacuoles and lipid droplet accumulated in human muscle biopsies as a result of statin treatment (Phillips *et al*., 2002). In addition, by gas–liquid chromatography-mass spectrometry, Paiva *et al*. (2005) showed that the level of cholesterol and campesterol increased in human muscle tissue due to 80 mg/d simvastatin treatment. The lipid accumulation may be related to an increase in the receptor mediated uptake of cholesterol because the inhibition of cholesterol synthesis could lead to reduced synthesis of cholesterol in the muscle cells and the intake of cholesterol and other lipids from circulation increases in muscle tissue (Paiva *et al*., 2005). It has been reported that more and larger lipid droplets was observed in muscles of statin treated MCK-LPL mice than those in muscles of untreated mice and statin treated wild-type mice. The muscle cholesterol content in wild-type mice was also reported to be unchanged with statin treatment (Yokoyama *et al* 2007). However, it has been shown that the level of sarcolemmal lipids and mRNAs for membrane lipid associated proteins were unaffected by statin treatment (Draeger *et al*., 2006). As a result, there are some contradictory results about the effects of statin treatment on lipid composition of skeletal muscle. Our finding has shown a decrease in lipid content which contradicts with some of the studies stated above. These contradictory results may be due to the differences in the application dosage of statin.It is known that the adverse effects of statin are dose dependent. In the studies stated above low dose of statin approximately 1 mg/kg was applied but in our study high dose of statin about 50 mg/kg was administered.

The olefinic band (3010 cm^{-1}) arising from the CH stretching mode of the HC=CH groups, can be used as a measure of unsaturation in the acyl chains (Takahashi *et al.*, 1991, Liu *et al.*, 2002; Severcan *et al.*, 2005). As seen from Table 3.4, the area of this band decreased in all simvastatin treated muscle

types, but the most profoundly for EDL muscle ($p<0.01$), indicating a decrease in the population of unsaturation in acyl chains of lipid molecules. This loss of unsaturation may be due to an increase in lipid peroxidation (Sills *et al*., 1994; Kinder *et al*., 1997). Simvastatin inhibits ubiquinone synthesis which also serves as antioxidant in both mitochondria and lipid membranes. A decrease in its synthesis may induce decreased free radical scavenging indicating an increase in the amount of ROS (Reactive Oxygen Species). Hence, lipid peroxidation was increased in simvastatin treated skeletal muscles due to the increased production of ROS (Baker and Tarnopolsky, 2001). It was reported that after stopping statin therapy, the level of 8-epi-PGF2a in serum, plasma and urine decreased, which is indicator of a significant in-vivo oxidation injury, supporting our result (Sinzinger *et al*., 2000). In addition, it has been shown that statin treatment decreased plasmologens, which is associated with protection against oxidative damage. The decrease in the level of plasmologens may be functionally linked to an increase in oxidative stress i.e. ROS (Laaksonen *et al*., 2006) which also supports our result.

In addition to the decrease observed in the area of olefinic band, there was a frequency shift to higher values for the olefinic band in EDL muscle ($p<0.05$). In the previous studies, the frequency shift to lower values was reported as to be an indication of an increase in the order of the system (Mantsch, 1984; Lopez-Garcia *et al.*, 1993; Bizeau *et al.*, 2000; Severcan *et al*., 2003). In our study the shift to higher values was observed in olefinic =CH stretching band representing the disordering of the unsaturated lipids in membranes of skeletal muscle tissue but more profoundly for EDL muscle. This disordering effect result from the increase in the dehydration effect which was also seen at C=O stretching band located at 1741 cm^{-1} as a result of simvastatin treatment.

The frequency shifting of the CH_2 stretching vibrations can be used as a marker for the detection of lipid order (Liu *et al*. 2002; Mantsch, 1984; Severcan *et al*. 1997). In our study the frequency of the CH_2 asymmetric stretching band

shifted to lower values in simvastatin tretaed groups of three muscle types, but the shifting was the most profound in EDL muscle ($p<0.05$). This shifting demonstrates an increase in the order of the system, which indicates an increase in the number of trans conformers resulting in more rigid membrane structure. A possible explanation for the membrane rigidity is the presence of free radicals, and consequently the lipid peroxidation, which modifies lipid composition of the membrane. After oxidative stress, a decrease in the membrane unsaturated/saturated fatty acid ratio is detected with the formation of cross-linked lipid–lipid and lipid–protein moieties (Curtis *et al*., 1984; Levin *et al*., 1990; Niranjan and Krishnakantha, 2000). The altered unsaturated/saturated fatty acid ratio of membrane phospholipids evidently result in an increase in rigidity of membrane. Membrane lipid order parameter is required for the correct functioning ion channels. Therefore a more ordered membrane structure may alter the function of ion channels. It has been reported that statins impaired some membrane channels such as Na^+/K^+ ATPase, Na^+/Ca^{2+}, Na^+/Ca^{2+}ATPase pump and Na^+ channel (Nakahara *et al*, 1994; Pierno *et al*., 1995; Awayda *et al* 2004).

Bandwidths of the same bands also give information about the dynamics of the system (Mantsch, 1984, Schultz and Naumann, 1991; Lopez-Garcia *et al*., 1993; Severcan *et al*., 2003; Severcan *et al.*, 2005). The dramatic increase of the bandwidth of the CH_2 asymmetric stretching band suggested an increase in the lipid fluidity for all the treated muscle samples but this increase is the most dramatic for EDL muscles ($p<0.01$) (Levin *et al*., 1990; Severcan *et al*., 1999, Toyran and Severcan, 2003; Korkmaz and Severcan, 2005). It is known that cholesterol level in membrane affects its fluidity. A decrease in cholesterol level might increase membrane fluidity (Vevera *et al*., 2005). It has been reported that statin affect skeletal muscle membrane fluidity through changes in cholesterol content (Baker and Tarnopolsky, 2001; Wortmann, 2002).

As seen from Table 3.10, the area of the C=O stretching vibration band (1741 cm $^{-1}$) which is due to the cholesterol esters and triglycerides diminishes in all muscles types but significantly for EDL muscle ($p<0.05$), implying a relative decrease in the concentration of ester groups belonging to triglycerides and cholesterol esters. This was also confirmed by the decline in the area of the CO–O–C asymmetric stretching (1170 cm $^{-1}$) (Nara *et al*., 2002; Voortman *et al*., 2002). In addition, the dramatic shifting of the 1741 cm $^{-1}$ band to higher frequency values in simvastatin treated muscle types (Table 3.9) indicates a difference in packing of ester groups within the tissue (Jackson *et al*., 1998) and decrease in the strength of the existing hydrogen bonds of the glycerol skeleton closer to the head groups or decrease in the number of hydrogen bonds i.e. dehydration (Korkmaz *et al*, 2005). The dehydration effect of simvastatin may result from the variation of dipole interaction between drug and lipid .The difference in packing may result from the decrase in the amount of unsaturated lipids which was more profound for EDL muscle ($p<0.01$) (Cakmak *et al*., 2006; Nara *et al*., 2002). This was further confirmed by the decrease in the area of the olefinic CH stretching absorption at 3015 cm^{-1}. It has been reported that statin treatment reduces the total cholesterol content of the human skeletal muscle cells while no change was observed in the triglyceride amount of the human skeletal muscle cells (Yamazaki *et al*., 2006). In addition, Yokoyama *et al*. (2007) showed that muscle cholesterol content was unchanged with statin treatment. On the other hand, an increase in the level of cholesterol in human muscle has been shown as a result of 80 mg/g simvastatin treatment (Paiva *et al*., 2005).

As it is clearly seen in Table 3.10, a decrease in the area of Amide I and Amide II bands was observed bands for all three muscles, but most profoundly for EDL muscle ($p<0.01$), indicating a decrease in total protein content of skeletal muscle after simvastatin treatment especially in fast contracting glycolytic muscle. This result was also supported by the decrease in amide A band (at 3330 cm $^{-1}$), amide B band (at 3072 cm $^{-1}$) and CH_3 symmetric stretching band

(at 2876 cm $^{-1}$) which are also due to proteins. A possible explanation is that the decrease in the serum levels of lipids and fatty acids triggers muscle to use amino acids from proteins as an energy source. It has been suggested that extreme protein degradation will damage the muscle if the situation is so hard and this causes the formation of acute myopathy and rhambdomyolisis (Motijima *et al*., 1998, Tchapda ., 2005). Another explanation is that inhibition of mevalonate pathway by statins leads to the suppression of the prenylated (farnesylated or geranylated) small GTP proteins, such as Rho, Ras or Rac, which promote cell maintenance and cell survival and this leads to the apoptosis (Kaufmann *et al*., 2006). Moreover, Urso *et al*. (2005) showed that statin causes an increase in the number of genes involved in protein catabolism in the muscle which supports our finding.

The bandwidth of amide I band decrased significantly for EDL muscle ($p<0.05$) (Table 3.11). In adddition, the frequency of the amide I and amide II bands shifted to higher values in all muscles but slightly higher for EDL muscle ($p<0.01$) (Table 3.10). This result was also consistent with the shifts of the frequencies of amide A band (at 3330 cm $^{-1}$), and amide B band (at 3072 cm $^{-1}$).These indicate conformational changes in tissue proteins (Haris and Severcan, 1999; Jackson *et al*., 1999). It was previously described that biochemical and/or genetic abnormalities of proteins or genes involved in skeletal muscle energy metabolism in more than 50 % of patients is associated with statin-associated myopathy, supporting the changes in the synthesis and conformation of tissue proteins induced by statins (Vladutiu *et al*., 2006). In addition, it was reported a change in the action of protein folding in muscle as a result of statin treatment with exercise (Urso *et al*.,2005) which confirms statin induced structural changes in tissue proteins.

The band at 1392 cm^{-1} is due to the COO^- symmetric stretching vibrations of amino acid side chains and fatty acids (Jackson *et al.*, 1998; Cakmak *et al.*, 2003). The decrease in the area of this band indicates a decrease in the content

of amino acids and fatty acids, which is consistent with the other finding of our study stated above.

One of the important factors affecting the membrane structure and dynamics is the amount of proteins and lipids in the membranes (Szalontai *et al*., 2000). A precise lipid-to-protein ratio can be derived from the FTIR spectrum by calculating the ratio of the areas of the bands arising from lipids and proteins. The increase of this ratio especially in treated EDL muscle suggests that there was a much pronounced decrease in protein content when compared to the decrease in lipid content after simvastatin treatment (Table 3.10). Urso *et al.* (2005) stated that statin treatment with exercise considerably affected the Ubiquitin Proteasome Pathway which is tightly regulated and responsible for the recognition and degradation of the majority of proteins in skeletal muscle, which confirms our result.

The band located at 1344 cm^{-1} originates from the C-N and the C-C stretching and the N-H bending vibrations of collagen (Camacho *et al*., 2001; Gough *et al*., 2003; West *et al*., 2004). The 1365-1300 cm^{-1} spectral region contains bands assigned to plane-bending hydroxyl modes in saccharides (Cael *et al*., 1973; Carpenter and Crowe, 1989). Therefore, there may be contributions from saccharide molecules to this band. As seen from Table 3.9 and Figures 3.5, 3.9 and 3.13, a decrease was observed in the area of the amide III band located at 1343 cm^{-1} originating from the C-N and the C-C stretching and the N-H bending vibrations of collagen in all three muscles but the most profoundly for EDL muscle ($p<0.01$) (Camacho *et al.,* 2001; Gough et al., 2003; West *et al.,* 2004). This indicates a decrease in the amount of collagen in simvastatin treated muscles. It has been reported that pravastatin inhibited type IV collagen secretion in fetal calf serum due to suppression of mevalonate pathway products which plays a critical role in the proliferation of mammalian cells (Nishimura *et al* 1999). Moreover, Rombouts *et al* (2003) showed that simvastatin suppressed the collagen synthesis and cellular proliferation in hepatic satellite cells which also supports our results.

The PO_2 asymmetric and symmetric stretching bands located at 1239 cm^{-1} and 1080 cm^{-1} respectively, originating from the phosphate-stretching vibrations of nucleic acids and phospholipid head groups (Lyman *et al.,* 2001; Banyay *et al.*, 2003). These phosphate-stretching vibrations at 1300-1000 cm^{-1} monitor alterations in the quantity, conformational state, and the degree and position of phosphorylation of the nucleic acids in DNA, RNA and head-groups of the phospholipids (Mendelsohn and Mantsch, 1986; Dovbeshko *et al*, 2000; Kneipp *et al*, 2000). The frequency of the PO_2 asymmetric stretching mode is at 1240-1260 cm^{-1} when PO_2^- groups are completely non-hydrogen-bonded, and approximately at 1220 cm^{-1} when PO_2^- groups are completely hydrogen bonded (Rigas *et al.*, 1990; Wong *et al.*, 1991). So as the hydrogen bonding decreases, the frequency values shift to higher values in PO_2 asymmetric stretching vibration. In the absorbtion spectra of the skeletal muscle, in the region of the PO_2 asymmetric stretching band two bands were observed located at 1261 cm^{-1} and 1236 cm^{-1}. The band located at 1261 cm^{-1} is due to non-hydrogen-bonded PO_2^- groups and the band located at 1236 cm^{-1} is due to more hydrogen-bonded PO_2^- groups. The areas of these bands decreased more dramatically for EDL muscle (1261 cm^{-1} $p<0.01$, 1236 cm^{-1} $p<0.05$) as in comparison to the other two muscles as shown in Table 3.9. These results implied a decrease in the relative content of the nucleic acids in the treated tissues especially in EDL muscle (Ci *et al.,* 1999). As seen from Table 3.10, the frequencies of these bands shifted to higher values in EDL muscles whilst it shifted to lower values in DIA and SOL muscles. The shifts to higher values in the frequencies of these bands indicate dehydration around the PO_2^- functional groups of the nucleic acids and phospholipids while the shifts to lower values in the frequencies of these bands implies an increase in the hydration of the nucleic acid and phospholipids in membrane structures. The dehydration effect of simvastatin was also shown in the FTIR study of DPPC and DMPC multilamellar liposomes both gel and liquid-crystalline phases in the presence of simvastatin (Kocak et al 2007). All together these results suggest a change in DNA and RNA conformation. The decrease in the amount of nucleic acids

results from statin induced nuclear condensation and fragmentation through the activation of caspase 3 enzymes and it was also in agreement with other studies (Kubota *et al*., 2004). Schick *et al* (2007) reported that high dose simvastatin treatment lowered both mitochondrial and cellular DNA content in skeletal muscle.

The peak area ratio of the bands at 1080 cm^{-1} (phosphate symmetric stretching-nucleic acid) and 1540 cm^{-1} (amide II-protein) is often used to illustrate the change in the DNA and protein content of the cells (Mourant *et al*., 2003). A decrease in both protein and DNA content was observed in all muscles but the most profoundly for EDL muscle ($p<0.05$). The increase in this ratio implies protein content decreases more when compared with the DNA content (Table 3.12). This results supports that statin affects Ubiquitin Proteasome Pathway which is tightly regulated and responsible for the recognition and degradation of the majority of proteins in skeletal muscle.

The spectral region between 995-970 cm^{-1} is assigned to the ribose-phosphate main chain vibrations of RNA (Banyay *et al.*, 2003). The absorption bands originating from CC structure of the DNA backbone was assigned at 970-950 cm^{-1} (Banyay *et al.*, 2003). The band centered at 976 cm^{-1} is generally assigned to symmetric stretching mode of dianionic phosphate monoester of nucleic acids (Ci *et al.*, 1999; Chiriboga *et al.*, 2000; Çakmak *et al.*, 2003) and ribose-phosphate main chain vibrations of the RNA backbone (Banyay *et al.*, 2003; Tsuboi *et al.*, 1969). A decrease in the area of this band was observed in simvastatin treated muscle types which was more profound for EDL muscle ($p<0.05$), indicating a decrease in the nucleic acid, especially RNA content. This decrease suggests that the RNA production, therefore the protein synthesis decreases in simvastatin treated EDL muscle. This result supports the decrease in protein content mentioned earlier. The decrease in protein synthesis might have been caused by alterations in expression of nucleic acids which may be a result of any structural changes in nucleic acid structures.

The band centered at 929 cm^{-1} results from Z type of DNA (Banyay *et al.*, 2003; Liquier and Taillandier, 1996). A decrease in the area of this band which was more profound for EDL ($p<0.05$) implies a decrease in the area of DNA. Moreover, the frequency of this band shifted to higher values for EDL while it shifted to lower values for DIA and SOL. These results were consistent with the band centered at 873 cm^{-1} originating from the vibrations of N-type sugars in the sugar phosphate backbone of nucleic acids, both DNA and RNA. This shows simvastatin affects DNA structure oppositely in these muscles which were first to be reported in this current study. This effect may be due to the changes in fiber composition of EDL, DIA and SOL muscles. These results support statin induced DNA degradation and structural alterations in DNA.

There are many histological and electrophysiological studies on the effects of statins on the skeletal muscle fibers (England *et al*.1995; Schaefer *et al*., 2004, Draeger *et al*., 2006, Pierno *et al*., 1995, 1999, 2006; Gray *et al*., 2000; Liantonio et al., 2007; Inonue et al., 2003). It has been proposed that fast twitch muscle fibers are most sensitive to these drugs while slow twitch fibers are resistant to them. Moreover, it was reported that with the prolonged administration, all fiber types were ultimately affected. Our current study clearly showed that EDL muscle, which is composed of a high content of type II fibers, was more severely affected from statin treatment while SOL muscle which has high proportion of Type I fibers , was least affected from this drug in all the spectral parameters stated above.

During statin therapy, to detect statin induced mtyotoxicities, generally the level of serum creatine kinase enzyme level is measured. These myotoxicities are characterized by elevation in the level of Creatine Kinase in serum. However, there are many reports suggesting that the level of this enzyme was normal although patients suffer from myopathy which is one of the myotoxic effects of statin (Troseid *et al*., 2005; Philips *et al*., 2002). The adverse effects of statins on muscle are important for statin treated patients because these

drugs may cause even death due to the rhambdomyolisis. Therefore, ATR-FTIR and FTIR spectroscopy could be effective and useful tools to detect statin induced myotoxicities in muscle biopsies from statin treated patients in a very short time.

CHAPTER 5

CONCLUSION

The results of the present work indicated that significant alterations occurred in EDL, DIA and SOL skeletal muscle tissues after simvastatin treatment.

The detailed examination of the ATR-FTIR and FTIR spectra revealed the following observations:

There was a considerable decrease in both lipid and protein content of skeletal muscles, and these decreases were more easily observed for EDL muscle. It was also demonstrated for the first time in this study that the decrease in protein content was more remarkable when compared with the decrease in lipid content. The decrease in protein content suggested that protein degradation was increased or the synthesis of them was decreased in simvastatin treated muscles and this degradation changes from fast twitch to slow twitch fibers. While, the decrease in lipid content showed that lipolysis was increased which was reported in this current study for the first time.

Glycogen level was lower in simvastatin treated muscles, especially in EDL muscles.

In simvastatin treatment, muscle membrane lipids were more ordered when compared to control membranes, and this increase in order was the most pronounced in EDL muscle. The amount of unsaturated lipids decreased in treated tissues indicating the increased lipid peroxidation. Lipid peroxidation was found to be higher in EDL muscles. On the other hand, the disordering effect of simvastatin was observed for unsaturated lipids in EDL muscle.

Simvastatin treatment caused a decrease in the content of nucleic acids, especially RNA, and phospholipids in the membrane structures of skeletal muscles. It also caused a change in DNA and RNA conformation, possibly by alterations in the effect of hydrogen bonding in the DNA and RNA backbones.

The disordering effect of simvastatin for unsaturated lipids, change in DNA and RNA conformation, increase or decrease in hydrogen bonding of the DNA and RNA backbones were investigated for the first time in the present study.

In conclusion, in all of the spectral parameters investigated EDL muscle, which is composed of a high content of type II fibers, was found to be more severely affected from simvastatin treatment. This study was first to demonstrate the effect of simvastatin on the whole macromolecular content of skeletal muscle tissues, simultaneously. Moreover, it gives new insights to pathological studies for the detection of statin induced muscle degradation during the treatment of hypercholesterolemia.

REFERENCES

Akkas S.B., Inci S., Zorlu F.,(2007). "Melatonin Affects The Order, Dynamics And Hydration Of Brain Membrane Lipids". *Journal of Molecular Structure,* 834: 207-215

Alberts B., Johnson A., Raff M., Roberts K., Walter P., Lewis J., (2002). Molecular Biology of the Cell: Fourth Edition, New York: Garland Science.

Almuti K., Rimawi R., Spevack D., Ostfeld R.J. (2006). Effects of statins beyond lipid lowering: Potential for clinical benefits*". International Journal of Cardiology*, 109 (1):7-15.

Ariano M.A., Armstrong R.B., Edgerton V.R., (1973). "Hindlimb muscle fiber populations of five animals", *Journal of Histochemistry and Cytochemistry*, 21:51–55.

Awayda M.S., Shao W., Guo F., Zeidel M., Hill W. G. (2004) "ENaC membrane interactions: regulation of channel activity by membrane order". *Journal of General Physiology*,123,709-727.

Baker S. K., Tarnopolsky M. A.,(2001). "Statin myopathies: pathophysiologic and clinical Perspectives" *Clinical and Investigative Medicine*, 24(5):258-72.

Bakker-Arkema R.G., Davidson M.H., Goldstein R.J., Davignon J., Isaacsohn J.L., Weiss S.R., Keilson L.M., Brown W.V., Miller V.T., Shurzinske L.J., Black D.M., (1996). "Efficacy and safety of a new HMG-CoA reductase inhibitor, atorvastatin, in patients with hypertriglyceridemia". *JAMA*. 275(2):128-33.

Banyay M., Sarkar M., Graslund, A.,(2003). "A library of IR bands of nucleic acids in solution", *Biophysical Chemistry*, 104: 477–488.

Berthier C., and S. Blaineau (1997). "Supramolecular organization of the subsarcolemmal cytoskeleton of adult skeletal muscle fibres. A review." *Biology of the Cell*, 89(7):413-34.

Bittman R., (1997). "Cholesterol : its functions and metabolism in biology and medicine" New York : Plenum Press, c1997.

Bizeau M.E., Salano J.M., and Jeffrey, R.,(2000). "Menhaden oil feeding increases lypolysis without changing plasma membrane order in isolated rat adipocytes", *Nutrition Research*, 20(11): 1633-1644.

Bozkurt O., Bilgin M. D., Severcan F., (2007). "The effect of diabetes mellitus on rat skeletal extensor digitorum longus muscle tissue: An FTIR study". *Spectroscopy An Internatonal Journa,.* Volume 21, Number 3 pp. 151 - 160 .

Braun JEA., and Severson DL., (1992). "Regulation of the synthesis, processing and translocation of lipoprotein lipase". *Biochemical Journal* 287: 337-347.

Brown A.S., Bakker-Arkema R.G., Yellen L., Henley R.W. Jr., Guthrie R., Campbell C.F., Koren M.,Woo W., McLain R., Black D.M., (1998). "Treating patients with documented atherosclerosis to National Cholesterol Education Program-recommended low-density-lipoprotein cholesterol goals with atorvastatin, fluvastatin, lovastatin and simvastatin*". Journal of The American College of Cardiology*, 32(3):665- 672.

Brown M.S., Goldstein J.L., (2004). " Lowering plasma cholesterol by raising LDL receptors*". Atherosclerosis Supplements*, 5(3):57-9.

Cakmak G., Togan I., Uguz C., Severcan F., (2003). "FT-IR spectroscopic analysis of rainbow trout liver exposed to nonylphenol*". Applied Spectroscopy*, 57:835–841.

Cakmak, G., Togan, I., Severcan F., (2006). "17β-Estradiol induced compositional, structural and functional changes in rainbow trout liver, revealed by FT-IR spectroscopy: A comparative study with nonylphenol". *Aquatic Toxicology*, 77: 53–63.

Cael J.J., Koenig J.L., Blackwell J., (1973). "Infrared and raman spectroscopy of carbohydrates. 3. Raman spectra of the polymorphic forms of amylase", *Carbohydrate Research*, 29(1):123-34.

Camacho N.P., West P., Torzilli P.A., Mendelsohn R., (2001). "FTIR microscopic imaging of collagen and proteoglycan in bovine cartilage". *Biopolymers (Biospectroscopy),* 62: 1–8.

Carpenter J.F., Crowe J.H., (1989). "An infrared spectroscopic study of the interactions of carbohydrates with dried proteins". *Biochemistry*, 28(9):3916-22.

Chiriboga L., Yee H., Diem M., (2000). "Infrared spectroscopy of human cells and tissues. Part VI: A comparative study of histopathology and infrared microspectroscopy of normal, cirrhotic, and cancerous liver tissue". *Applied Spectroscopy*, 54: 1-8.

Ci X. Y., Gao T. Y., Feng J. and Guo Z. Q., (1999). "Fourier transform infrared characterization of human breast tissue: Implications for breast cancer diagnosis". *Applied Spectroscopy*, 53:312-315.

Corsini A., Bellosta S., Baetta R., Fumagalli R., Paoletti R., Bernini F., (1999). "New insights into pharmacofynamic and pharmacokinetic properties of statins". *Pharmacology and Therapeutics*, 84: 413-28.

Colthup N. B., Daly L. H. and Wiberley S. E., (1990). Introduction to infrared and raman spectroscopy, New York: Academic Press.

Cziraky M. J.,. Willey V. J., McKenney J.M., Kamat S. A., Fisher M. D., Guyton J. R., Jacobson T. A., Davidson M. H., (2006). "Statin Safety: An Assessment Using an Administrative Claims Database". *The American Journal of Cardiology*, 97(8), Supplement 1:S61-S68

Curtis M.T., Gilfor D., Farber J.L., (1984). "Lipid peroxidation increases the molecular order of microsomal membranes". *Archives of Biochemistry And Biophysics*, 235:644–649.

Del Zoppo G.J., The role of platelets in ischemic stroke*, Neurology* 51 (1998) (Suppl. 3), pp. S9–S14.

Delp M.D., Duan C., (1996). "Composition and size of type I, IIA, IID/X, and IIB fibers and citrate synthase activity of rat muscle". *Journal of Applied Physiology,* 80(1):261- 270.

Diem M., Boydston-White S., Chiriboga L., (1999). "Infrared spectroscopy of cells and tissues: shining light onto a novel subject*". Applied Spectroscopy*, 53: 148A-161A.

Diem M., (1993). Introduction to modern vibrational spectroscopy, John Wiley & Sons, USA.

Dirks A.J., Jones K.M., (2006). "Statin-induced apoptosis and skeletal myopathy" *American Journal of Physiology Cell Physiology,* 291:C1208-C1212.

Dogan A., Ergen K., Budak F., Sevecan F.,(2007). "Evaluation of disseminated candidiasis on an experimental animal model: A Fourier transform infrared study". *Applied Spectroscopy*, 61 (2): 199-203

Dovbeshko G. I., Gridina N. Y., Kruglova E. B. and Pashchuk, O. P., (2000). "FTIR spectroscopy studies of nucleic acid damage", *Talanta*, 53: 233-246.

Draeger A., Monastyrskaya K., Mohaupt M., H Hoppeler., 1 H Savolainen, 3 C Allemann1 and EB Babiychuk1 Statin therapy induces ultrastructural damage in skeletal muscle in patients without myalgia. *Journal of Pathology,* 2006; 210: 94–102.
Dubowitz V., (2006). "Muscle Biopsy" .Elsevier Science.

Garcia M.J., Reinoso R.F., Navarro S.A., Prous J.R., (2003). "Clinical pharmacokinetics of statins". *Methods and Findings in Experimental and Clinical Pharmacology*, 25(6):457-81

England J.D., Walsh J.C., Stewart P., Boyd I., Rohan A., Halmagyi G.M., (1995). "Mitochondrial myopathy developing on treatment with the HMG CoA reductase inhibitors--simvastatin and pravastatin". *Australian & New Zealand Journal of Medicine,* 25(4):374-5.

Evans M., Rees A., (2002A). "Effects of HMG-CoA reductase inhibitors on skeletal muscle: areall statins the same?". *Drug Safety*, 25(9):649-63.

Evans M, Rees A., (2002B). "The myotoxicity of statins*". Current Opinion in Lipidology,* 13(4):415-20.

Fassbender K., Stroick M. and Bertsch T.,(2002). " Effects of statins on human cerebral cholesterol metabolism and secretion of Alzheimer amyloid peptide". *Neurology,* 59:257–1258.

Freifelder, D., (1982). Physical Chemistry. Applications to biochemistry and molecular biology, Freeman, W. H. (Ed), New York.

Garrett W.E., Mumma M., Lucaveche C.L., (1983). "Ultrastructural differences in human skeletal muscle fiber types". *Orthopedic Clinics of North America*, 14(2):413-425.

Garip S., Bozoglu F., Severcan F.,(2007). "Differentiation of mesophilic and thermophilic bacteria with Fourier transform infrared spectroscopy" *Applied Spectroscopy,* 61 (2):186-192.

Ginsberg H.N., Le N.A., Short M.P., Ramakrishnan R., Desnick R.J., (1987). "Suppression of apolipoprotein B production during treatment of cholesteryl ester storage disease with lovastatin. Implications for regulation of apolipoprotein B synthesis". *Journal of Clinical Investigation*, 80(6):1692-7.

Goldstein JL, Brown MS., (1990). Regulation of the mevalonate pathway. *Nature*,343(6257):425-30.

Gough K.M., Zelinski D., Wiens R., Rak M., Dixon I.M., (2003). "Fourier transform infrared evaluation of microscopic scarring in the cardiomyopathic heart: effect of chronic AT1 suppression". *Analytical Biochemistry*, 15;316(2):232-42.

Gorgulu S.T., Dogan M., Severcan F.,(2007). “The characterization and differentiation of higher plants by Fourier transform infrared spectroscopy”. *Applied Spectroscopy,* 61 (3):300-308.

Gray D.F., Bundgaard H, Hansen P.S., Buhagiar K.A., Mihailidou A.S., Jessup W., (2000). “HMG CoA reductase inhibition reduces sarcolemmal Na(+)-K(+) pump density”. *Cardiovascular Research*, 47:329-35.

Grdadolnik J., (2002). “ATR-FTIR Spectroscopy: Its Advantages and Limitations. *Acta Chimica Slovenica*, 2002, 49:631−642.

Greisheimer E.M. and Wiedeman M.P., (1972). Physiology and anatomy, 9th Ed., J.B. Lippincott Company, Washington.

Griffiths, P. R., and de Haseth, J. A., (1986). In: Fourier Transform Infrared Spectrometry. Wiley, New York.

Grundy S.M., (1998). “Consensus statement: Role of therapy with "statins" in patients withhypertriglyceridemia”. *American Journal of Cardiology,* 81(4A):1B-6B.

Günzler H., GremlichH. U., (2002) “IR spectroscopy : an introduction” Wiley-VCH.

Haris P. I. and Severcan F., (1999). “FTIR spectroscopic characterization of protein structure in aqueous and non-aqueous media”, *Journal of Molecular Catalysis B: Enzymatic*, 7:207-221.

Harvey R.A., Champe P.A., Biochemistry: 3rd Edition, Baltimore: Lippincott Wiliams and Wilkins, 2005, pp. 222-223.

Inoue R., Tanabe M., Kono1 K., Maruyama1 K., Ikemoto1 T., Endo M., (2003). “Ca2+-Releasing Effect of Cerivastatin on the Sarcoplasmic Reticulum of Mouse and Rat Skeletal Muscle Fibers”. *Journal of Pharmacological Science* 93, 279 – 288.

Istvan E.S., Deisenhofer J. (2000). “The structure of the catalytic portion of human HMG-CoA reductase”. *Biochimica Biophysica Acta*, 1529(1-3):9-18.

Istvan E.S., Palnitkar M., Buchanan S.K., Deisenhofer (2000). "Crystal structure of the catalytic portion of human HMG-CoA reductase: insights into regulation of activity and catalysis". *EMBO Journal* 19(5):819-30.

Jackson M., Ramjiawan B., Hewko M., and Mantsch H. H., (1998). "Infrared microscopic functional group mapping and spectral clustering analysis of hypercholesterolomic rabbit liver". *Cellular and. Molecular Biology*, 44(1): 89-98.

Jamin N., Dumas P., Moncuit J., Fridman W., Teillaud J., Carr L. G., and Williams G. P., (1998). "Highly resolved chemical imaging of living cells by using synchrotron infrared microspectroscopy". *Applied Biological Sciences*, 95(9): 4837-4840.

Kanbara K., Sakai A., Watanabe M., Furuya E., Shimada M.,(1997). "Distribution of fiber types determined by in situ hybridization of myosin heavy chain mRNA and enzyme histochemistry in rat skeletal muscles". *Cellular and Moleular Biology* (Noisy-le-grand), 43(3):319-27.

Kaufmann P., Török M., Zahno A., Waldhauser KM., Brecht K., Krähenbühl S. (2006). "Toxicity of statins on rat skeletal muscle mitochondria". *Cellular and Molecular Life Science,* 63:2415-25.

Kilarski W., Sjostrom M., (1990). "Systematic distribution of muscle fibre types in the rat and rabbit diaphragm: a morphometric and ultrastructural analysis". *Journal of Anatomy* , 168:13-30.

Kinder R., Ziegler C., Wessels J.M., (1997). "γ-Irradiation and UV-C light-induced lipid peroxidation: A Fourier transform-infrared absorption spectroscopic study". *International. Journal of Radiation Biology*, 71(5):561-571.

Kiortsis D.N., Filippatos T.D., Mikhailidis D.P., Elisaf M.S. and Liberopoulos E.N., (2006). "Statin-associated adverse effects beyond muscle and liver toxicity". *Atherosclerosis*, In Press.

Kneipp J., Lasch P., Baldauf E., Beekes M., and Naumann D., (2000). "Detection of pathological molecular alterations in scrapie-infected hamster brain by Fourier transform infrared (FT-IR) spectroscopy". *Biochimica et Biophysica Acta,* 1501:189-199.

Korkmaz F., and Severcan F., (2005). "Effect of progesterone on DPPC membrane: Evidence for lateral phase separation and inverse action in lipid dynamics". *Archives in. Biochemistry and Biophysics*, 440:141–147.

Kubota T., Fujisaki K., Itoh Y., Yano T., Sendo T., Oishi R., (2004). "Apoptotic injury in cultured human hepatocytes induced by HMG-CoA reductase inhibitors". *Biochemical Pharmacology*, 67:2175–2186.

Kwak B., Mulhaupt F., Myit S. and Mach F., (2000). "Statins as a newly recognized type of immunomodulator". *Nature Medicine* ,6 :1399–1402.

Laaksonen R, Katajamaa M, Päivä H, Sysi-Aho M, Saarinen L., Junni P., Lütjohann D., Smet J., Coster RV., Seppänen-Laakso T., Lehtimäki T., Soini J., Oresic M.,(2006). "A systems biology strategy reveals biological pathways and plasma biomarker candidates for potentially toxic statin induced changes in muscle".*PLoS ONE* 1:e97.

Laufs U. and Liao J. K., (2003). "Isoprenoid metabolism and the pleiotropic effects of statins" . *Current Atherosclerosis Reports,* 5,(5):372-378.

de Lemos J. A., Blazing M. A.,,. Wiviott S. D., Lewis E. F., Keith A. A. White F. H. D., Rouleau J. L., Pedersen T.R., Gardner L. H., Mukherjee R., Ramsey K. E., Palmisano J., Bilheimer D.W., Pfeffer M. A. Califf R. M.; Braunwald E., (2004). "Early Intensive vs a Delayed Conservative Simvastatin Strategy in Patients With Acute Coronary Syndromes: Phase Z of the A to Z Trial". *Journal of the American Medical Association*, 292:1307 - 1316.

Levin G., Cogan U., Levy Y., Mokady S., (1990). "Riboflavin deficiency and the function and fluidity of rat erythrocyte membranes". *Journal of Nutrition,* 120:857–861.

Liantonio A., Giannuzzi V., Cippone V., Camerino G. M., Pierno S. Camerino D. C., (2007). "Fluvastatin and Atorvastatin Affect Calcium Homeostasis of Rat Skeletal Muscle Fibers". *Journal of Pharmacology and Experimental Therapeutics*, 321: 626-634.

Lieber, R. L., (2002). "Skeletal muscle structure, function & plasticity : the physiological basis of rehabilitation". Philadelphia : Lippincott Williams & Wilkins.

Liquier J. and Taillandier, E., (1996). Infrared spectroscopy of nucleic acids, Infrared Spectroscopy of Biomolecules, Wiley-Liss, Inc., USA, 131-158, 1996.

Liu K.Z., Bose R., Mantsch H.H., (2002). "Infrared spectroscopic study of diabetic platelets". *Vibrational Spectroscopy*, 28:131–136.

Locatelli S., Lutjohann D., Schmidt H.H., Otto C., Beisiegel U. and von Bergmann K., (2002). "Reduction of plasma 24S-hydroxycholesterol (cerebrosterol) levels using high-dosage simvastatin in patients with hypercholesterolemia: evidence that simvastatin affects cholesterol metabolism in the human brain". *Archives of Neurology* 59:213–216.

Lopez-Garcia, F., Villian J., and Gomez-Fernandez J.C., (1993). "Infrared spectroscopic studies of the interaction of diacylglycerols with phosphatidylcerol, phosphatidylserin in the presence of calcium". *Biochimica et Biophysica Acta*, 1169:264-272.

Lyman D.J., Murray–Wijelath J., Ambrad–Chalela E., Wijelath, E.S., (2001). "Vascular graft healing. ii. ftir analysis of polyester graft samples from implanted bi-grafts". *Journal of Biomedical Materials Research* (Appl. Biomater.), 58:221–237.

Lyman D.J., and Murray-Wijelath J., (1999). "Vacular graft healing: I.FTIR analysis of a implant model for studying the healing of a vascular graft". *Journal of Biomedical Materials Research* (Appl. Biomater.), 48:172-186.

Manoharan R., Baraga J.J., Rava R.P., Dasari R.R., Fitzmaurice M. and Feld M.S., (1993). "Biochemical analysis and mapping of atherosclerotic human artery using FTIR microspectroscopy". *Atherosclerosis*, 103:181-193.

McArdle W.D., Katch F.I., Katch V.L., (2001). Exercise Physiology, Energy, Nutrition and Human Performance, 5th Ed., Lippincott Williams and Wilkins, Washington.

Mcfarlane S. I., Muniyappa R., Francisco R., Sowers J. R., (2002). "Pleiotropic Effects Of Statins: Lipid Reduction and Beyond". *Journal of Clinical Endocrinology and. Metabolism*, 87(4):1451-1458.

Mantsch H.H., (1984). "Biological application of Fourier Transform Infrared Spectroscopy: A study of phase transitions in biomembranes". *Journal of Molecular Strucutre,* 113:201-212.

Martini H.F., Ober W.C., (2005). Anatomy and Physiology. Benjamin Cummings.

Matzno S., Yasuda S., Juman S., (2005). "Statin-induced apoptosis linked with membrane farnesylated Ras small G protein depletion, rather than geranylated Rho protein". *Journal of Pharmacy and Pharmacology*, 57:1475–84.

Masters B.A., Palmoski M.J., Flint O.P., Gregg R.E., Wang-Iverson D., Durham S.K. (1995). "In vitro myotoxicity of the 3-hydroxy-3-methylglutaryl coenzyme A reductase inhibitors, pravastatin, lovastatin, and simvastatin, using neonatal rat skeletal myocytes". *Toxicology and Applied Pharmacology* ,131(1):163-74.

Melin A., Perromat A., and Deleris G., (2000). "Pharmacologic Application of Fourier Transform IR Spectroscopy: In vivo Toxicity of Carbon tetrachloride on rat liver*". Biopolymers (Biospectroscopy),* 57:160-168.

Mendelsohn R. and Mantsch H. H., (1986). Fourier transform infrared studies of lipid-protein interaction, Progress in Protein-Lipid Interactions, Volume 2, Elsevier Science Publishers, Netherlands, 103-147.

Motojima K., Passilly P., Peters J.M., Gonzalez F.J., Latruffe N., (1998). "Expression of putative fatty acid transporter genes are regulated by peroxisome proliferator-activated receptor alpha and gamma activators in a tissue- and inducer-specific manner". *Journal of Biological Chemistry*, 273(27):16710-4.

Mourant J. R., Yamada Y. R., Carpenter S., Dominique L. R., Freyer J. P. (2003). "FTIR Spectroscopy demonstrates biochemical differences in mammalian cell cultures at different growth stages*"*. *Biophysical Journal*, 85(3):1938-47.

Nakahara K., Yada T., Kuriyama M., Osame M., (1994), "Cytosolic Ca2+ increase and cell damage in L6 rat myoblasts by HMG-CoA reductase inhibitors". *Biochemical and Biophysical Research Communications*, 202: 1579–1585.

Nara M., Okazaki M., Kagi H., (2002). "Infrared study of human serum verylow-density and low-density lipoproteins. Implication of esterified lipid

C=O stretching bands for characterizing lipoproteins". *Chemistry and Physics of. Lipids*, 117:1–6.

Niranjan T.G., Krishnakantha T.P., (2000). "Membrane changes in rat erythrocyte ghosts on ghee feeding". *Molecular and Cellular Biochemistry*, 204:57–63.

Nishimura M., Tanaka T., Yasuda T., Kurakata S., Kitagawa M., Yamada K., Saito Y., Hirai A.,(1999). "Effect of pravastatin on type IV collagen secretion and mesangial cell proliferation". *Kidney International Supplement,* 71:S97-100.

Okumura N., Hashida-Okumura A., Kita K., Matsubae M., Matsubara T., Takao T., Nagai K., (2005). "Proteomic analysis of slow- and fast-twitch skeletal muscles*", Proteomics*, 5: 2896–2906.

Olds R. J., (1988). A colour atlas of the rat :dissection guide. Wolfe Medical Pub. London.

Päivä H., Thelen KM., Van Coster R., Smet J., De Paepe B., Mattila KM., Laakso J., Lehtimäki T., von Bergmann K., Lütjohann D., Laaksonen R.,(2005). "High-dose statins and skeletal muscle metabolism in humans: a randomized, controlled trial". *Clinical Pharmacology and Therapeutics* , 78(1):60-68.

Paul DP., and Gahtan V., (2003). "Noncholesterol-Lowering Effects of Statins" Vascular *and Endovascular Surgery,* 37(5):301-313.

Pedersen T.R., Berg K. and Cook T.J., (1996). "Safety and tolerability of cholesterol lowering with simvastatin during 5 years in Scandinavian simvastatin survival study". *Archives of Internal Medicine,* 156 (1996), 2085–2092.

Phillips P.S., Haas R.H., Bannykh S., Hathaway S., Gray N.L., Kimura B.J., Vladutiu G.D., England J.D., (2002). "Statin-associated myopathy with normal creatine kinase levels". *Annals of Internal Medicine*, 137(7):581-5.

Pierno S., De Luca A., Tricarico D., Ferrannini E., ConteT., D'Alo G., (1992). "Experimental evaluation of the effects of pravastatin on electrophysiological parameters of rat skeletal muscle*". Pharmacological Toxicology,* 71:325-9.

Pierno S., De Luca A., Tricarico D., Roselli A., Natuzzi F., Ferrannini E., (1995). "Potential risk of myopathy by HMG-CoA reductase inhibitors: a comparison of pravastatin and simvastatin effects on membrane electrical properties of rat skeletal muscle fibers". *Journal of Pharmacology and Experimental Therapeutics,* 275:1490-6.

Pierno S., De Luca A., Liantonio A., Camerino C., Conte Camerino D. (1999) "Effects of HMG-CoA reductase inhibitors on excitation-contraction coupling of rat skeletal muscle". *European Journal of Pharmacology*;364:43-8.

Pierno S., Didonna M. P., Cippone V., Luca A. D., Pisoni M., Frigeri A., Nicchia G. P., Svelto M., Chiesa G., Sirtori C., Scanziani E., Rizzo C., Vito D. D. Camerino D. C., (2006). "Effects of chronic treatment with statins and fenofibrate on rat skeletal muscle: a biochemical, histological and electrophysiological study". *British Journal of Pharmacology,* 149: 909-919.

Popesko P., Rajtová V., Horák J., translated by I. Temcáková, Phil ., (2002). A colour atlas of the anatomy of small laboratory animals. Kosice. Saunders.

Rana F.R., Sultany, C.M. and Blazyk J., (1990). "Interactions between Salmonella typhimurium lipopolysaccharide and the antimicrobial peptide, magainin 2 amide". *FEBS Letters*, 261, 2:464-467.

Rigas B., Morgellot S., Goldman I.S., Wong P.T.T., (1990). "Human colorectal cancers display abnormal Fourier-transform infrared spectra". *Proceedings of the National Academy of Sciences*, 87: 8140-8144.

Roche V. F., (2005). "Antihyperlipidemic Statins: A Self-Contained, Clinically Relevant Medicinal Chemistry Lesson". *American Journal of Pharmaceutical Education*, 69(4): 546-560.

Rombouts K., Kisanga E., Hellemans K., Wielant A., Schuppan D., Geerts A., (2003). "Effect of HMG-CoA reductase inhibitors on proliferation and protein synthesis by rat hepatic stellate cells". *Journal of Hepatology*, 38(5):564-72.

Rosenson RS. (2004). "Current overview of statin-induced myopathy". *American Journal of Medicine,* 116: 408–416.

Sacks M., Pfeffer M.A., and Moye L.A., (1996). "The effect of pravastatin on coronary events after myocardial infarction in patients with average cholesterol levels. Cholesterol and recurrent events trial investigators," *New England Journal of Medicine*., 335:1001–1009.

Sato A., Watanabe K., Fukuzumi H., Hase K., Ishida F., Kamei T., (1991). "Effect of simvastatin (MK-733) on plasma triacylglycerol levels in rats". *Biochemical Pharmacology*, 41 (8):1163-1172.

Schachter M., (2005). "Chemical, pharmacokinetic and pharmacodynamic properties of statins: an update". *Fundamental & Clinical Pharmacology,* 19 (1):117-125.

Schaefer W. H., Lawrence J. W., Loughlin A. E., Stoffregen D. A., Mixson L. A., Dean D. C., Raab C. E., Yu N. X., Lankas G. R., and Frederick C. B., (2004) "Evaluation of ubiquinone concentration and mitochondrial function relative to cerivastatin-induced skeletal muscle myopathy in rats". *Toxicology and Appied Pharmacology* , 194: 10–23.

Schick B. A. , Laaksonen R., Frohlich J. J. , Päivä H., Lehtimäki T. , Humphries K. H., Côté H.C. F .(2007). "Decreased Skeletal Muscle Mitochondrial DNA in Patients Treated with High-Dose Simvastatin". *Clinical Pharmacology & Therapeutics*.81, 650–653.

Schultz, C. and Naumann, D., (1991). "In vivo study of the state of order of the membranes of Gram-negative bacteria by Fourier-transform infrared spectroscopy (FT-IR)", *FEBS Letters*, 294, 43-46.

Severcan, F., Gorgulu, G., Gorgulu, S.T., Guray, T., (2005). "Rapid monitoring of diabetes-induced lipid peroxidation by Fourier transform infrared spectroscopy: Evidence from rat liver microsomal membranes", *Analytical. Biochemistry*., 339: 36–40.

Severcan, F., Toyran, N., Kaptan, N. and Turan, B., (2000). "Fourier transform infrared study of diabetes on rat liver and heart tissues in the C-H region", *Talanta*, 53, 55-59.

Severcan, F., Kaptan, N., Turan, B., (2003). "Fourier transform infrared spectroscopic studies of diabetic rat heart crude membranes", *Spectroscopy*, 17: 569–577 569.

Severcan, F., (1997). "Vitamin E decreases the order of the phospholipid model membranes in the gel phase: An FTIR study". *Bioscience Reports*, 17: 231-235.

Sills, R.H., Moore, D.J. and Mendelsohn, R., (1994). "Erythrocyte peroxidation: quantitation by fourier transform infrared spectroscopy". *Analytical Biochemistry* 218: 118-123.

Shitara Y, Sugiyama Y., (2006). “Pharmacokinetic and pharmacodynamic alterations of 3-hydroxy-3-methylglutaryl coenzyme A (HMG-CoA) reductase inhibitors: drug-drug interactions and interindividual differences in transporter and metabolic enzyme functions”. *Pharmacology and Theraputics* 112(1):71-105.

Shier, D., Butler, J., Lewis, R., (1996). Hole’s human anatomy and phsiology, Wm. C. Brown Publishers, Dubuque

Sinzinger H.1; Lupattelli G.; Chehne F., (2000). “Increased lipid peroxidation in a patient with CK-elevation and muscle pain during statin therapy”. *Atherosclerosis*,153(1):255-256(2)

Sirvent P., Mercier J., Vassort G. Lacampagne A., (2005).”Simvastatin triggers mitochondria-induced Ca2+ signaling alteration in skeletal muscle”. *Biochemical and . Biophysical. Research. Communications*. 329 pp. 1067–1075

Smith P.F., Eydelloth R.S., Grossman S.J., Stubbs R.J., Schwartz M.S., Germershausen JI, Vyas KP, Kari PH, MacDonald JS., (1991). “HMG-CoA reductase inhibitor-induced myopathy in the rat: cyclosporine A interaction and mechanism studies”. *Journal of Pharmacolgy and Experimental Therapeutics*, 257:1225-1235

Steele, D., (1971). The Interpretation of Vibrational Spectra, William Clowes & Sons Lim., Great Britain.

Storey B. K.,(2004). “Functional metabolism :regulation and adaptation” Hoboken, N.J.: John Wiley & Sons, c2004.

Stuart, B., (1997). Biological Applications of Infrared Spectroscopy. John Wiley and Sons, Ltd., England.

Stuart, B. (2004). In: Infrared Spectroscopy, Fundamentals and Applications. John Wiley & Sons, Ltd.

Szalontai, B., Nishiyama, Y., Gombos, Z., and Murata, N., (2000). "Membrane dynamics as seen by Fourier Transform Infrared Spectroscopy in a cyanobacterium, synechocystis PCC 6803. The effects of lipid unsaturation and the protein-to-lipid ratio", *Biochimica et. Biophysica. Acta,* 1509; 409-419.

Taillandier, E., and Liquier, J., (1992). "Infrared spectroscopy of DNA", *Methods Enzymology*., 211:307–335.

Takahashi, H., French, S. M., and Wong, P. T. T., (1991). "Alterations in hepatic lipids and proteins by Chronic ethanol Intake: A high pressure fourier transform Infrared spectroscopic study on alcoholic liver disease in the rat alcohol".*Alcohol Clinical Experimental. Research*., 15(2): 219-223.

TchapdaN.L., (2005). "Mechanisms Of The 3- Hydroxyl-3-Methylglutaryl-Coenzyme A Reductase Inhibitor- Induced Myotoxicity In HumanSkeletal Muscle Cell Cultures" Kaiserslautern.

Toyran, N., Lasch, P., Naumann, D., Turan, B., Severcan, F., (2006). "Early alterations in myocardia and vessels of the diabetic rat heart: an FTIR microspectroscopic study", *Biochemical Journal.,* 397(3):427-36.

Toyran, N., and Severcan, F., (2003). "Competitive effect of vitamin D2 and Ca2+ on phospholipids model membranes: an FTIR study", *Chemistry and Physics of* . *Lipids*, 123:165-176.

Toyran N, Turan B, Severcan F. (2007) "Selenium alters the lipid content and protein profile of rat heart: an FTIR microspectroscopic study". *Archives in Biochemistry and Biophysics* .458(2):184-93.

Toyran, N., Zorlu, F., Dönmez, G., Öğe, K., Severcan, F., (2004). "Chronic hypoperfusion alters the content and structure of proteins and lipids of rat brain homogenates: A Fourier transform infrared spectroscopy study", *European Biophysical. Journal*., 33: 549–554.

Trøseid M, Henriksen OA, Lindal S., (2005). "Statin-associated myopathy with normal creatine kinase levels. Case report from a Norwegian family*".Acta Pathologica, Microbiologica, Et Immunologica Scandinavica*,113(9):635-7.

Tsuboi, M., (1969). "Application of infrared spectroscopy to structure studies of nucleic acids". *Applied Spectroscopy Reviews*, Dekker, New York, 45–90.

Urso M.L., Clarkson P.M., Hittel D., Hoffman E.P., Thompson P.D., (2005). "Changes in ubiquitin proteasome pathway gene expression in skeletal muscle with exercise and statins". *Arteriosclerosis Thrombosis and Vascular Biology.;* 25; 2560–2566.

Usui H., Shikata K. and Matsuda M.., (2003), "HMG-CoA reductase inhibitor ameliorates diabetic nephropathy by its pleiotropic effects in rats". *Nephrology DialysisTransplantation*18 :265–272.

Vega G.L. and Grundy S.M., (1998). "Effect of statins on metabolism of apo-B-containing lipoproteins in hypertriglyceridemic men". *American Journal of Cardiology*. 81(4A):36B-42B

Vevera J, Fisar Z, Kvasnicka T, Zdenek H, Starkova L, Ceska R, Papezova H (2005). "Cholesterol-lowering therapy evokes time-limited changes in serotonergic transmission". *Psychiatry Research* 133, 197–203.

Vigoraux, J.O. (1994). "The muscle Z band: lessons in stress management." Journal of Muscle Research and Cell Motility 15(3):237-55.

Vladutiu G.D., Simmons Z., Isackson P.J., Tarnopolsky M., Peltier W.L, Barboi A. C., Sripathi N., Wortmann R. L., Phillips P.S(2006). "Genetic risk factors associated with lipid-lowering drug-induced myopathies". *Muscle Nerve*. 34(2):153-62.

Voortman, G., Gerrits, J., Altavilla, M., Henning, M., Van Bergeijk, L., Hessels, J., (2002). "Quantitative determination of faecal fatty acids and triglycerides by Fourier transform infrared analysis with a sodium chloride transmission flow cell". *Clinical. Chemistry and . Laboratory. Medicine*., 40:795–798

Wang, J., Chi, C., Lin, S., and Chern, Y., (1997). "Conformational changes in gastric carcinoma cell membrane protein correlated to cell viability after treatment with adamantyl maleimide", *Anticancer Research,* 17: 3473-3478.

Wortmann R.L., (2002). “Lipid-lowering agents and myopathy”. *Current Opinion in Rheumatology* 2002; 14:643–647.

West, P.A., Bostrom, P.G., Torzilli, P.A., and Camacho, N.P., (2004). “Fourier Transform Infrared Spectral analysis of degenerative cartilage: an infrared fiber optic probe and imaging study”. *Applied Spectroscopy*, 58(4): 376-381.

Westwood F.R., Bigley A., Randall K., Marsden A.M., Scott R.C.,(2005). “Statin-induced muscle necrosis in the rat: distribution, development, and fibre selectivity”.*Toxicological Pathology*. 2005;33(2):246-57.

Wong, P.T.T., Wong, R.K., Caputo, T.A., Godwin, T.A., Rigas, B., (1991). “Infrared spectroscopy of exfoliated human cervical cells: Evidence of extensive structural changes during carcinogenesis*”, Proceedings of the National Academy of Sciences*., 88: 10988-10992.

Yamazaki H., Suzuki M., Aoki T., Morikawa S., Maejima T., Sato F.,Sawanobori K., Kitahara M., Kodama T., Saito Y., (2006) “Influence of 3-hydroxy-3-methylglutaryl Coenzyme A Reductase Inhibitors on Ubiquinone Levels in Rat Skeletal Muscle and Heart: Relationship to Cytotoxicity and Inhibitory Activity for Cholesterol Synthesis in Human Skeletal Muscle Cells” *Journal of Atherosclerosis Thrombosis*.13(6),295-30 .

Yilmaz O., Keser S., Tuzcu M., Çetintaş B., (2007).“Resveratrol (trans-3,4′,5-trihydroxystilbene) decreases lipid peroxidation level and protects antioxidant capacity in sera and erythrocytes of old female Wistar rats induced

by the kidney carcinogen potassium bromate”, *Environmental Toxicology and Pharmacology*, 24,(2), 79-85.

Yokoyama M., Seo T., Park T., Yagyu H. , Hu Y., Son N.H., Augustus A.S. , Vikramadithyan R.K. , Ramakrishnan R., Pulawa L. K., Eckel R.H., Goldberg

I.J. ,(2007). “Effects of lipoprotein lipase and statins on cholesterol uptake into heart and skeletal muscle” *Journal of Lipid Research.;* 48: 646-655.

Yono, K., Ohoshima, S., Shimuzu, Y., Moriguchi, T. and Katayama, H., (1996). “Evaluation of glycogen level in human lung carcinoma tissues by an infrared spectroscopic method”. *Cancer Letters,* 110:29-34.

Zhongsheng L., Fredericks P. M., lewellyn R.,Ward C. R. (2007). “Application of attenuated total reflectance micro-fourier transform infrared (atr-ftir) spectroscopy to the study of coal macerals: Examples from the Bowen basin, Australia. International”. *Journal of Coal Geology* 70(1-3):87-94.

http://goldbamboo.com/topic-t1183-a1-6Cholesterol.html